Instituto Tecnológico y de Estudios Superiores de Monterrey

Campus Monterrey

School of Engineering and Sciences

DEVELOPMENT OF BIOSENSORS FOR THE DETECTION OF CONTAMINANTS OF EMERGING CONCERN

A dissertation presented by

Marcela Herrera Domínguez

Submitted to the
School of Engineering and Sciences
in partial fulfillment of the requirements for the degree of

Doctor of Philosophy

In

Engineering Science

Major in Environmental Sciences

Monterrey Nuevo León, June 15th, 2023

To my parents, thanks for your unconditional support.
&
To Darwin, my reason for carrying on

Acknowledgements

I would first like to thank my thesis advisor, Dr. Nancy Ornelas, for all the support and guidance provided throughout the doctorate, for giving me all the necessary tools to do my work in the best possible way, thank you for your patience, for your time and for the support that went beyond the academic.

I thank Dr. Iris Aguilar, for her hard work during the publication process of the articles, for her valuable contributions and always accurate comments, thank you for your time and support.

To the members of my committee, Dr. Gesuri Morales, Dr. Eduardo Pisano, and especially to Dr. Raul Garcia for his collaboration in the completion of this thesis, because their help was an essential part in the development of this work. Thanks to everyone for always being available despite the distance, for being attentive to the research, for the advice and the time they dedicated to helping me.

To my parents, whom I love, and my dear siblings, for their unconditional support, for being my backup and because I know that I can count on you no matter the circumstances. For listening to me and advising me in bad times.

To my colleague and friend Angelica, with whom I shared these four years of doctoral studies, for the support and comfort given when things seemed difficult. Because we encouraged each other to move forward and give the best of ourselves.

To my dear friend Fabian, in whom I found a sincere friendship. I thank you for your company, for being with me in good times and bad times, for listening to me over and over again without invalidating me, for caring, for all the fun times we had, for the laughter and for bringing out that part of me that I enjoy; thank you for all your support, for being you and because with you I can be myself.

To the Tecnológico de Monterrey, for the financial support provided for my studies, for allowing me to be part of an academic community of excellence, and for the wonderful educational and personal development experience that the institution provided me.

To CONACYT, for the support for living I received throughout my PhD. degree.

DEVELOPMENT OF BIOSENSORS FOR THE DETECTION OF CONTAMINANTS OF EMERGING CONCERN

By

Marcela Herrera Domínguez

Abstract

In the present thesis work, two different biosensors are developed for use in the detection of contaminants of emerging concern in water. Specifically, the quantification of pharmacological compounds is desired since they are bioactive and have been shown to have harmful effects on aquatic organisms. The biosensors were developed using different approaches; one of them is an SPR-type optical biosensor that uses antibodies to perform the sensing, while the other is an enzyme-based electrochemical biosensor of the amperometric type. These biosensors were used for the detection of diclofenac and acetaminophen respectively, achieving detection limits that make them suitable for use in real samples.

The electrochemical biosensor has the advantage of being a simpler and easier to use design; however, the optical biosensor achieved a lower detection limit due to its high sensitivity and selectivity. Both biosensors provide valuable information in the development of biosensors for environmental monitoring.

LIST OF FIGURES

LIST OF TABLES

CONTENTS

CHAPTER I

1.1 Introduction

Contaminants of emerging concern (CEC) are compounds of several origins that have recently been detected in the environment; water, air and soil, and which have been shown to be toxic for living things. CEC, as their name indicates, are compounds that have already been cataloged as contaminants but have shown to have harmful effects that were previously unknown. These contaminants include a variety of household products such as detergents, insecticides, personal care products and pharmaceuticals, as well as industrial products such as flame retardants, varnishes, pesticides, and paints.

CEC are toxic, bioaccumulative, and persistent; they tend to accumulate in water bodies because wastewater treatment plants (WWTP) do not have the necessary technology for their removal. Because of this, their presence has been detected in all kinds of water, including surface water, groundwater and even drinking water [1]. The concentration of CEC in water are very low with ranges from ng/L to μg/L, making their detection a complicated task and, consequently, their regulation is limited; so far, only the European Union and the United States government have regulatory frameworks for the regulation of some of these pollutants that are considered to be of major importance [2,3].

The detection of this type of compounds is mainly performed by standard analytical techniques, such as gas chromatography (GC), liquid chromatography (LC) and high-performance liquid chromatography (HPLC) coupled most of the time to selective detectors such as mass spectrometer (MS) [4]. Although chromatographic techniques are accurate techniques to identify compounds at low concentrations, nonetheless their use as routine tests for the purpose of monitoring the discharge of CEC into water bodies is not viable, due to the fact that the analysis process involves rigorous sample preparation procedures, long analysis times, specialized equipment, high purity reagents and properly trained personnel; thus, making these techniques costly and time consuming. In addition, the use of solvents can represent a source of contamination. Consequently, there is an increasing need to develop other analytic methods that are efficient in detecting various compounds at low concentrations quickly, reliably and in situ.

Biosensors are devices that have proven to be a useful tool in the detection of various compounds. They have been most widely developed in the health area, but their use has been extended to the food and environmental areas [5–7]. Biosensors are highly sensitive devices that, with the right functionalization, can also become highly specific. Applying them for the quantification of CEC is feasible since they have demonstrated a great capacity to detect analytes at low concentration, reaching attomolar concentrations, even if dealing with small molecules [8,9]. Therefore, this thesis work is focused on developing biosensors that allow the specific detection of low molecular weight persistent organic compounds that can be used in environmental water samples.

1.1.1 Motivation

Waste from all personal care products and pharmaceuticals that are consumed, as well as inputs used in industry and pesticides for agriculture, reach water effluents and are concentrate in WWTP, which do not have the technology to degrade this type of pollutants that, until now, have been understudied. The European Union Water Framework Directive and the United States Environmental Protection Agency (USEPA) list priority pollutants to

be regulated, including drugs such as diclofenac and carbamazepine, as well as antibiotics such as chloramphenicol and pesticides such as atrazine [10,11].

CEC are found in trace concentrations in water, making their detection a complicated task, which currently, requires chromatographic techniques that, although accurate and reliable, are also complex and laborious, as well as costly. At present, the presence of CEC has been identified in wastewater, surface water, groundwater and even drinking water [12–14]. The lack of legislation regarding this type of contaminants is due to limited knowledge and the use of inappropriate analytical methods; therefore, practical and simple methodologies are required for routine analysis not only for drinking water purification plants but also for wastewater treatment plants.

Biosensors, with the appropriate bio-functionalization, are highly sensitive and selective devices that allow quantitative analysis with a level of confidence that is comparable with chromatographic techniques, as well as being fast and practical, which make them the appropriate systems for environmental monitoring. With the implementation of biosensors in the detection of this type of pollutants, it is expected to achieve, in the long term, the identification of pollutants presents in water, even in nanomolar concentrations.

1.1.2 Problem statement and context

The increase in the world population in turn implies an increase in the consumption of CEC and their accumulation in water bodies. Therefore, during the last decade, there has been a growing interest in studying their presence and the toxicological effects they may have. These investigations have shown that CEC are found not only in WWTP but are ubiquitously present in surface water throughout the world, as well as in drinking water and, to a lesser extent, in groundwater [12–14]. Long-term exposure to these compounds has negative consequences on the aquatic species and, in certain situations, can change the functionality of hormones and metabolism in humans and animals, including the feminization of fish due to contaminants that act as endocrine disruptors as well as the inhibition of the growth of algae and amphibians [1,15,16].

CEC are found in trace concentrations, so their detection requires the use of chromatographic techniques that make quantification a complicated task. In 2014 Kostich, Batt and Lazorchak [17] published an investigation in which they searched for the presence of drug contaminants in samples taken from treatment plants, in that article the authors mention that "due to the large number of sampling sites and chemical analytes, logistically it was too difficult and costly to collect and analyze blanks and duplicates from each location". Based on the above, it is evident that different analytical methods are required to detect this type of contaminants in water, which should be based on practical and simple methodologies that can be part of a routine analysis, allowing further regularization of their presence in water.

1.1.3 Solution overview

As mentioned above, the detection of CEC is currently mainly performed using instrumental analytical techniques such as GC, LC and HPLC, most of the time coupled to selective detectors such as MS. These techniques offer efficient detection and determination of CEC and their metabolites. For example, the USEPA currently recommends the GC-MS technique

for the analysis of pesticides and flame retardants in water samples such as atrazine, bromacil, chlorpyrifos, vinclozolin, among others [18]. Analytical methods based on these techniques employ highly sophisticated, time-consuming equipment and require intensive pretreatment of the samples to be analyzed. They involve, for example, extractions with toxic solvents, making these methods environmentally unfriendly. In addition, purification of the extracts is necessary, which requires highly trained personnel as well as specialized laboratories.

Therefore, in the present thesis, two types of biosensors were developed with the purpose of being used as a priority for the implementation of environmental monitoring methods. One of them is of electrochemical type and the other one is based in optical sensing. These have been coupled to different biological elements such as enzymes and antibodies, respectively. The indispensable characteristics with which the devices were built were reliability, operation robustness and simplicity in construction. They were also intended to be easy to operate, even by semi-skilled personnel. In parallel, these biosensors were developed using either enzymes or antibodies to detect the presence of drugs selectively and reversibly in water samples. The biosensors were conceived to be reusable and specific for the analytes of interest to be quantified.

1.2 Hypothesis

Through the development of selective electrochemical and SPR-based biosensors, it will be possible to carry out a quick, sensitive and in real time detection of drug-contaminants of emerging concern in water samples.

1.3 Objectives

1.3.1 General objective

To develop selective electrochemical and SPR-based biosensors in order to obtain analytical methods for detection of contaminants of emerging concern in water samples.

1.3.2 Specific objectives

1. To conduct theoretical research on surface plasmon resonance (SPR) and amperometric biosensors, as well as the state of the art of their applications in environmental water monitoring.
2. To establish the analytes of interest to be quantified by SPR and amperometric methods based on their particular characteristics.

For SPR biosensors

3. To synthesize the specific hapten-protein conjugate for the analyte of interest based on its characteristics.
4. To functionalize the gold-coated substrate in flow and standardize the method in terms of concentrations and incubation times at each step of the process.
5. To establish the optimal concentration of the antibody in the sample by affinity test.
6. To perform a calibration curve using synthetic samples and determine the analytical quality parameters in synthetic samples analyzed by the proposed methods based on biosensors coupled to SPR, such as linear ranges, limits of detection and limits of quantification.

7. To perform interference analysis by testing the affinity of the sensor to other molecules.

For amperometric biosensor

8. To obtain purified laccases from the culture of the fungus *Pycnoporus sanguineus*.
9. To synthesize molybdenum disulfide (MoS_2).
10. To optimize MoS_2 concentration for electrode functionalization.
11. To obtain preliminary testing of MoS_2-modified electrodes and different isoforms of native and commercial laccases.
12. To characterize the obtained electrodes with better amperage, voltage, and kinetic characteristics.
13. To perform a calibration curve for analyte quantification using MoS_2 and laccase modified electrodes.
14. To apply the developed methods based on amperometric biosensors on real water samples

CHAPTER II

2.1 Biosensors

Biosensors are analytical devices that combine a transducer with a biological element to generate measurable signals in response to a specific reaction between two elements. This reaction is proportional to the concentration of chemical components present in the sample. Biosensors primarily serve in the medical fields to detect diseases or conditions, but their use has been extended to the food industry [5], biotechnology [19] and environmental field [20].

Biosensors have three main components (1) the biological recognition elements; are generally a pair of molecules that have an affinity for each other and whose interaction can be exploited to obtain information of interest. At least one of these molecules must be biological to be considered a biosensor. The biological elements include enzymes, antibodies, genetic material, whole cells, among others. (2) A suitable transducer; a device that senses the physical changes produced by the reactions of biological elements and transforms them into a measurable signal; transducers can be mechanical, optical, electrochemical, piezoelectric, thermal, etc. And (3) a signal processor; usually a computer where the equipment is controlled, to observe the response behavior towards the samples and to obtain the data (see Figure 1). These elements can be combined with each other, so that a great variety of biosensor designs can be obtained.

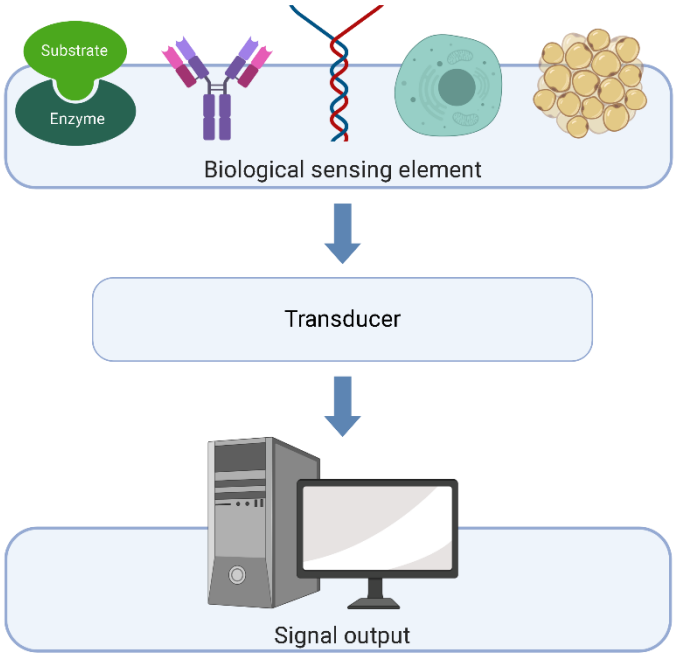

Figure 1. Diagram of the main elements of a biosensor.

These devices can offer high sensibility with minimum sample preparation, and detection can be carried out in real time, *in situ*, without the need to use chemical labels and in less time compared with chromatographic techniques [21]. Furthermore, with the right biological recognition element, biosensors can be highly specific.

Based on how biological recognition occurs, biosensors can be categorized in two groups: affinity and biocatalytic sensors [22]. Biocatalytic technology is user-friendly, economical, small, and relatively straightforward in design. Biocatalytic sensors use biological elements

such as enzymes, entire cells, or tissue [23]. Affinity sensors, on the other hand, employ the specific and powerful binding of biomolecules to a target analyte, such as antibodies, membrane receptors, or genetic material, to create a quantifiable signal [23]. In affinity biosensors, molecular recognition is essentially controlled by the complementary size and shape of the binding site to the target analyte. These sensors are extremely sensitive and selective due to the biomolecule's high affinity and specificity for its ligand [24].

Biosensors also can be classified according to their biological element into immunosensors, enzyme-based biosensors, aptasensors, etc. Or according to their transducer, they can be optical, mechanical, piezoelectrical, etc. biosensors. In this work, optical and electrochemical biosensors were designed, which themselves are divided into different categories. Likewise, enzymes and/or antibodies are used for their development. In the following subsections, the general concepts of the work will be discussed in detail.

2.1.1 Optical biosensors

These biosensors are those that take advantage of the optical phenomena of light to interact with biological elements to produce signals that are proportional to the concentrations of the analytes of interest [25]. Among the optical phenomena used in biosensing are reflection, refraction, fluorescence, resonance, surface plasmon resonance (SPR), interferometry, among others. Optical biosensors can be divided into those that are direct, in which the biological element responds directly to the transducer, for example the SPR type; and those that are indirect, which require a label to perform the measurement, for example those based on fluorescence [25].

Optical biosensors stand out because their signal is not compromised by electrical or magnetic interference, they provide more information about the sample, can detect different parameters and the sample can be read at different wavelengths simultaneously [26]. An SPR-based biosensor was developed herein and will be briefly described below.

SPR-based biosensors.

Surface Plasmon Resonance (SPR) is a phenomenon that occurs when the free electrons of a metal are excited by the electric field of incident light. Once the electrons are excited, they begin to oscillate collectively which in turn produces an evanescent wave. SPR is a useful phenomenon for monitoring changes in the refractive index because the evanescent wave is very sensitive to changes in the vicinity of the surface [27]. SPR biosensors are divided into two types, when the phenomenon occurs in metallic nanoparticles it is called Localized Surface Plasmon Resonance (LSPR) while when it is a metallic film it is simply called SPR [28].

SPR devices can be developed with different configurations, where the Kretschmann configuration is the most used. Kretschmann configuration consists of a prism that has a thin metallic film on one side while a polarized light passes through the other side. When the light reaches the metal, it acts as a mirror reflecting the light back to a photo detector. Generally, the metal film is made of gold as it is inert in the presence of other compounds. However, silver, copper, aluminum, and others can also be used.

The simplest way to make an SPR/LSPR biosensor is to have only a gold layer [29,30]. Nevertheless, recently the use of multilayers has been implemented, such is the case of graphene, this material has acquired interest for the development of SPR biosensors due to its optical and electrical properties. The incorporation of graphene to the SPR biosensors includes simple methodologies such as the addition of a layer of this material on the gold [31] or more complex arrangements such as the MoS_2/Al/MoS_2-graphene hybrid structure proposed by L. Wu *et al* [32] or the use of graphene doped with nickel nanoparticles that uses S.P. Ng *et al* [33].

One of the benefits of LSPR is that it allows experimenting with different types, materials and geometries in nanoparticles. The optical properties of the nanoparticles depend on their size and shape. Thus, playing with these properties, it can be improved the performance of the biosensor, for example, spherical and rod forms of nanoparticles have different optical properties and generate varying signal intensities [34]. The surface plasmon shifts from the visible to the near-infrared (NIR) region when the shape of nanoparticles is changed from spherical to rod. Gold nanostars with many branches and projecting tips, on the other hand, have the plasmon in the NIR wavelength. The high intensity of the nanostars in LSPR signals is proportional to the size of the tips and is a result of the hybridization of the central core and tips plasmon resonances [34]. The most reported is the use of spherical gold nanoparticles [35], but the use of triangular-shaped silver nanoparticles [36], gold nanorods [37] and gold nanostars [38] has also been tested.

2.1.2 Electrochemical biosensors

As the name implies, electrochemical biosensors are those whose biochemical reactions generate an electrical response. A typical electrochemical sensor is made up of a working electrode for sensing and a reference electrode that are separated by an electrolyte. For the majority of applications, a three-electrode setup is employed, with the reference linked to a high-input-impedance potentiostat and a counter electrode being used to complete the circuit for current flow [39]. These are divided into three types, (1) amperometric, those that generate a measurable current; (2) potentiometric, those that accumulate a measurable charge or potential; and (3) conductometric, those reactions that alter the conductive properties of the medium between the electrodes. Additionally, the monitoring of resistance (impedance) as well as reactance in the biosensor is gaining a place in biosensing [40].

Electrochemistry offers several advantages including very small sample volumes that can be used for measurement, minimal sample preparation, low cost, ease of use, miniaturization of portable systems and simplicity of construction [40,41]. In this thesis work, an amperometric type biosensor was developed, whose characteristics are specified in the following subsection.

Amperometric biosensors

Amperometric biosensors are a class of electrochemical biosensors in which biological recognition elements react to generate electroactive species on the sensing surface in such a way that a current is induced which can be measured and is related to the amount of an analyte in a sample [39]. In amperometry, the change in current due to electrochemical oxidation-reduction is measured over time while the potential between the working electrode and the reference electrode is kept constant. There are two ways to perform the analysis, one option

is to increase the potential step by step until the desired value is reached and then measure the current, or the potential is held at the desired value while the sample flows across the electrodes [40]. The current generated is proportional to the concentration of the electroactive species present in the sample. Since the oxidation or reduction potential used for detection is characteristic of the analyte species, amperometric biosensors offer greater selectivity [42].

Electrochemical biosensing systems consist of an electrochemical cell that can be either two- or three-electrode [43]. Three-electrode systems include a working (or indicator) electrode made of a chemically stable solid conductive material, such as platinum, gold or carbon; a reference electrode, which is usually made of metallic silver coated with a silver chloride layer; and an auxiliary platinum electrode. To maintain a known and constant potential at the reference electrode, it is usually placed separate from the redox reaction. The advantage of this system is that the current density passes through the auxiliary electrode, so the reference electrode maintains its potential throughout the measurement. A two-electrode cell has only the working and reference electrodes [44]. The reference electrode can carry the charge without any negative effects, as long as the current is low enough [41].

The incorporation of nanomaterials into electrochemical biosensors has been tested in recent years. The use of materials such as carbon nanoparticles and nanotubes, as well as graphene, have demonstrated improved response [45–47]. In addition, micromachining allows the fabrication of portable biosensing equipment for in situ detection, which is possible because miniaturizing the electrochemical detectors and the necessary control equipment is simple and can be done at low cost; also, reducing electrode dimensions can increase sensitivity. Given the small electrode dimensions the amount of sample required is minimal, which is a significant advantage when sample size is limited [48].

2.2 Biological sensing element

There are certain types of transmembrane proteins that bind to specific molecules called ligands. In addition to mediating physiological processes, receptors are natural targets for various toxins and drugs. The binding of the receptor to the ligand generates a specific cellular response and therefore they are used in bio-detection. In this kind of reactions, several types of proteins are involved, such as G proteins, enzymes, transcription factors and cellular receptors for antigen processing [49]. These types of biochemical reactions are highly specific, making them an excellent complement to the sensor transducers, obtaining a more sensitive and specific response for the detection of target analytes. The general aspects of the receptors used in this thesis are described below.

2.2.1 Enzymes

Enzymes are a type of protein that act as catalysts in chemical reactions in living organisms. One of their main characteristics is high substrate specificity, making them suitable as sensing elements in biosensors. Enzyme-catalyzed reactions produce changes in pH, temperature, molecular weight, charge, ions and absorption efficiency which results in measurable signals such as coloration or fluorescence that can be quantified by a proper instrument [50].

Enzymatic reactions can be carried out directly by promoting the bond between the substrate and the enzyme or indirectly by inhibiting enzymatic activity by blocking the active sites of

the enzyme with other compounds [51]. The final quantification is done by calculating the difference in enzymatic activity at the beginning and end of the reaction.

Enzymes are among the most widely used biomolecules in the development of biosensors. Among the advantages of using enzymes in this type of device is that their production is relatively simple and can be easily scaled up, which makes it possible to reduce costs. In addition, as enzymatic reactions are reversible, enzymatic biosensors can be reused thus maximizing their use. Nonetheless, these proteins are unstable, and their activity can be affected by temperature and pH changes or even denaturalize. These disadvantages can be reduced by immobilizing the enzymes on substrates or trapping them in polymer networks. However, despite being immobilized, enzymes tend to be unstable, so an important part of the research and development of enzyme biosensors is the performance of long-term stability and reproducibility studies [51].

From the above, it can be concluded that although enzymes have properties that make them optimal for use in biosensors and have great potential for large-scale production, their lack of stability makes their commercialization complicated. Another fact to highlight is that although in some cases these enzymes are commercial products, in other cases they are obtained from microorganisms, this being a favorable point since the production of enzymes from microorganisms allows obtaining biological material on a large scale and reducing costs.

2.2.2 Antibodies

Antibodies are a type of protein produced by the immune system to recognize and attack infections. When antibody-based reactions are carried out as part of an analytical method, they are called immunoassays. Antibodies are made up of globulin-type proteins which have a recognition site to react to the presence of a specific antigen. Moreover, a wide range of compounds can act as antigens, from macromolecules such as proteins, polysaccharides, polypeptides to simple molecules such as sugars, amino acids, phospholipids and drugs [52].

There are different formats of immunoassays, where competitive, inhibition and sandwich type are the most common (see Figure 2). Competitive immunoassays are characterized by using a labeled antigen and an unlabeled antigen, the antibody is supplied in a limiting amount so that both antigens compete to bind the antibody. It is called an inhibition immunoassay when the antibody is incubated with the unlabeled antigen as the limiting reagent and then interacts with the labeled antigen, which binds to the free antibody. Sandwich immunoassays consist of immobilizing an unlabeled antibody, then passing the sample containing the unlabeled antigen and finally passing a secondary antibody that is labeled [53]. Since the interactions between antigens and antibodies are highly specific, one can be used to quantify the other. The union of both parts produces a signal proportional to their concentration in the sample which is captured by the transducer.

The use of antibodies in the development of biosensors has as its main advantage the high affinity and specificity that an antibody has for its antigen. However, these properties can be affected during immobilization, having an impact on the performance of the biosensor [53]. Antibodies are produced by exposing some vertebrate organism to a foreign agent to induce an immune response. This process can take months, which is an obstacle to the development

and commercialization of immunosensors. It is now possible to produce recombinant antibodies by modifying the DNA of microorganisms [54]. Recombinant antibodies reduce production times and costs, but also makes it possible to manipulate the antibody to improve its affinity, specificity and stability characteristics, which cannot be controlled in traditional antibodies. In addition, recombinant antibodies can be immobilized on the substrate in a controlled manner, ensuring that they are deposited in the proper orientation and improving sensitivity [54]. In summary, the use of antibodies is one of the most viable options for biosensor development, and with continued research and innovation in antibody production, better immunosensors can be obtained at affordable costs.

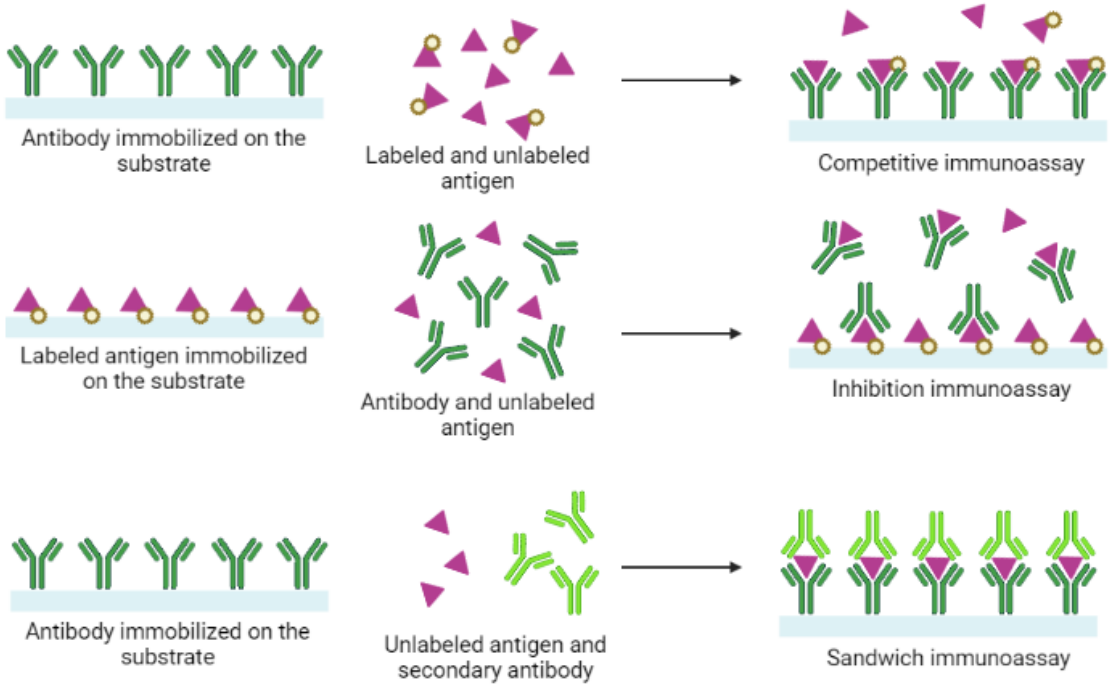

Figure 2. General elements of competitive, inhibition and sandwich immunoassay.

2.3 Contaminants of emerging concern

As mentioned above, CEC are a wide variety of chemical compounds that have been detected in the environment and originate from anthropogenic activities. These contaminants can be pharmaceuticals (veterinary and human), hygiene and personal care products, household products, hormones and steroids, industrial compounds, surfactants, flame retardants, agrochemicals, nanoparticles, microplastics, among others [55]. It has been demonstrated that most of them alter ecosystems, influence biochemical processes in the environment and deteriorate the health of species, causing carcinogenesis, mutagenesis, and endocrine alterations, which is why they are classified as of ecological interest and potentially dangerous.

Pharmaceuticals such as CEC are of special interest because they are compounds that are designed to interact with the biochemistry of the organism, therefore they can easily have a negative effect on marine species and humans [56,57]. This category of contaminants

includes antibiotics, synthetic hormones, analgesics and anti-inflammatory drugs, as well as specialized pharmaceuticals, antidepressants, antihypertensives, anticonvulsants, etc., in addition to metabolites and their transformation products [58]. Specifically, over-the-counter drugs such as acetaminophen (ACE) and diclofenac (DCF) have increased their presence in water bodies. That is why these were chosen as target analytes for the development of the biosensors presented in this thesis.

DCF, a non-steroidal anti-inflammatory drug, is one of the most extensively researched medications due to its potential toxicity to non-target species [59]. Diclofenac has been detected in wastewater and surface water in several countries. DCF has been shown to have diverse toxicological effects on aquatic organisms including bacteria and protozoa, crustaceans, mollusks, fish and algae [60]. Among the negative effects that have been demonstrated for DCF are that it causes oxidative stress in different species of fish and mollusks [61,62]; reproductive alterations in various species [63–65]; alterations in fish liver and kidney function [66–68]; and inhibits the growth of algae [64]. The exposure times in which these changes occur vary according to the species and the type of damage caused, occurring from 48 hours to 96 days [60].

ACE, also known as paracetamol, is widely used as an analgesic and antipyretic worldwide. It has also been detected in WWTP and surface water in concentrations up to 230 g/L all around the globe [69,70]; and its acute toxicity to aquatic organisms has been investigated [71]. Numerous studies have shown that ACE may interact with fish's endocrine systems, leading to aberrant embryonic development, growth, and detrimental effects on reproduction [72,73], as well as alteration in gill function [74]; moreover, it may have harmful effects on the kidney and liver [75,76].

CHAPTER III

3.1 Quantification of diclofenac by SPR immunosensor

In this chapter an SPR biosensor was developed that by means of an inhibition immunoassay can detect DCF at low concentrations. Briefly, in order for the antibody to have a better immunological response to DCF, the drug was bound to a carrier protein; in this case Bovine Serum Albumin (BSA). The DCF-BSA conjugate was subsequently immobilized on the surface of the sensor to interact with the antibodies present in the sample.

The work described in this chapter corresponds to an article entitled "Development of a surface plasmon resonance based immunosensor for diclofenac quantification in water" which was accepted by the journal Chemosphere and it is published with DOI: https://doi.org/10.1016/j.chemosphere.2023.139156

3.2 Methodology

3.2.1 DCF-BSA conjugate

The mixed anhydride method was used to couple DCF to BSA as a carrier protein [77]. Briefly, 0.08 mmol of DFC in its acid form were dissolved in 5 mL of 1,4-dioxane, and tributylamine and isobutyl chloroformate were added in equimolar amounts. The mixture was allowed to react for two hours at 4 °C. Then, 5 mL of BSA aqueous solution (pH 8.5) were dripped and stirred for 4 hours at room temperature to allow the DCF to react with the free amine groups and bind via an amide bond. Finally, the resulting mixture was purified by dialysis for three days using a 12-14 kDa membrane, lyophilized and stored at -20 °C.

3.2.2 DCF-BSA conjugate characterization

An AB Sciex 5800 MALDI-TOF mass spectrometer was used to characterize the DCF-BSA conjugate. To carry out the analysis, a 1:1 mixture of 5% trifluoroacetic acid (TFA) aqueous solution and acetonitrile (ACN) was prepared, and 10 mg mL^{-1} of α-cyano-3,4-hydroxycinnamic acid (CHCA) were added to the mixture to obtain the ionization matrix. Then, 2 µL of the respective conjugate and unmodified protein (200 µg mL^{-1} both) were deposited on the MALDI-TOF plate; once the samples were dry, 2 µL of the matrix were added over. Spectra were acquired in the positive reflector mode with a laser intensity between 4700-5400. Four replicates per sample were placed in the dish, and at least five shots were taken per sample.

3.2.3 Diclofenac quantification by SPR

SPR setup

The dual-channel NanoSPR 6-321 spectrometer was used for all conventional SPR measurements. The device used a GaAs semiconductor laser light source (λ = 670 nm), a manufacturer-supplied prism of high refractive index (n = 1.61 and a 30 µL flow cell. 50 nm gold layer SPR substrates previously modified with a self-assembled monolayer (SAM) of alkanethiols were inserted, and online analysis was conducted in an angular scanning mode with a 17-degree angular window that tracked the resonance angle every 5 s while simultaneously collecting the angular spectrum.

Sensor functionalization

SPR substrates were fabricated by e-beam deposition of a 2 nm chromium adhesion layer followed by a 50 nm gold layer onto precleaned BK7 glass slides. Before functionalization,

the sensors were rinsed with ethanol and dried under compressed air. The clean gold substrates were incubated overnight in a mixture of alkanethiols, 16-mercaptohexadecanoic acid and 11-mercaptoundecanol acid (1:10 molar ratio), to form a SAM on the surface. Then, one chemically modified sensor was placed in the SPR device and 0.01M PBS buffer was injected at a rate of 5 µL s^{-1} until the signal was stabilized. Subsequently, 80 µL of an EDC/NHS mixture were injected at a ratio of 0.3:0.1 M, and the mixture was incubated for 30 min. Next, 150 µL of the DCF-BSA conjugate at a concentration of 50 µg mL^{-1} were injected and incubated for 1.5 hours until the signal stabilized. Finally, 80 µL of a 1 M aqueous ethanolamine solution were injected for 20 min; Figure 3 shows a schematic of the functionalized sensor.

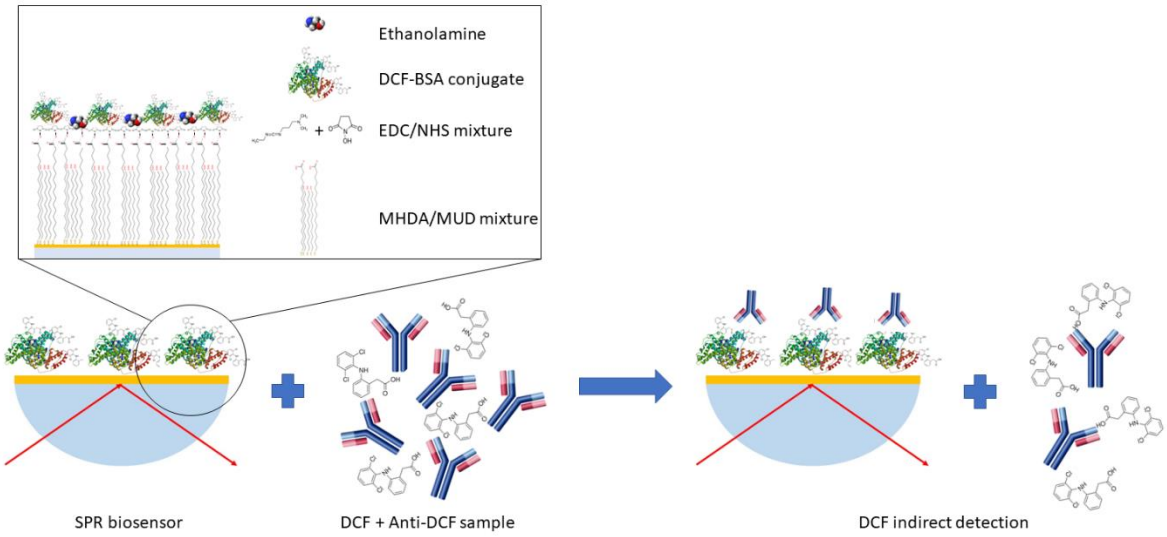

Figure 3. Schematic of the functionalized surface of the biosensor and the inhibition immunoassay for DCF detection.

Antibody affinity test

Prior to analyte quantification, a test was performed to verify the affinity of the anti-DCF for the conjugate. Anti-DCF was injected into a functionalized sensor at concentrations of 10, 20, 40, 60, 80 and 100 µg mL^{-1}. The injections were performed consecutively with PBS buffer re-equilibration steps between each measurement. These tests were performed in triplicate.

Specificity test

An interference test was performed to determine the specificity of the biosensor and to rule out its interaction with naproxen, ibuprofen, and ketorolac, three common anti-inflammatory drugs. The analytes were injected on the functionalized surface of the biosensor. The injections were consecutive, with a concentration of 15 µg L^{-1} in ultrapure water and an incubation time of 10 minutes per injection.

Inhibition assay for DCF detection

For this assay, 2, 7, 12, 17, 22, 27 and 32 µg L^{-1} of DCF in PBS were preincubated with 40 µg mL^{-1} of anti-DCF in a total volume of 100 µL for 30 min. During preincubation, the antibody is bound to the analyte until equilibrium of the reaction is reached. After preincubation, 80 µL were injected and allowed to flow continuously over the sensor surface

at a flow rate of 5 μL s^{-1} for 10 min and re-equilibrated with PBS buffer. Only antibodies with antigen-binding sites not occupied by analyte molecules are able to react with the functionalized sensor surface, as shown in Figure 1, resulting in a signal inversely related to the analyte concentration in the sample. Experiments were performed in triplicate. For data analysis, results were normalized in terms of the mean and standard deviation.

3.3 Results and discussion

3.3.1 MALDI-TOF Characterization

The MALDI-TOF mass/charge spectra (Figure 4) for pure BSA shows a sharp peak at m/z 65213.11 corresponding to the single charged protein. The peak at m/z 32830.17 comes from the doubly charged protein, the one at m/z 21853.89 is assigned to the triple charged protein and the one barely observed around m/z 44000.00 belongs to the triple charged protein dimer [78]. These same peaks are also observed in the mass/charge spectrum of the DCF-BSA conjugate. Pure BSA has a mass of 65213.11 Da and the DCF-BSA conjugate with a mass of 66535.31 Da.

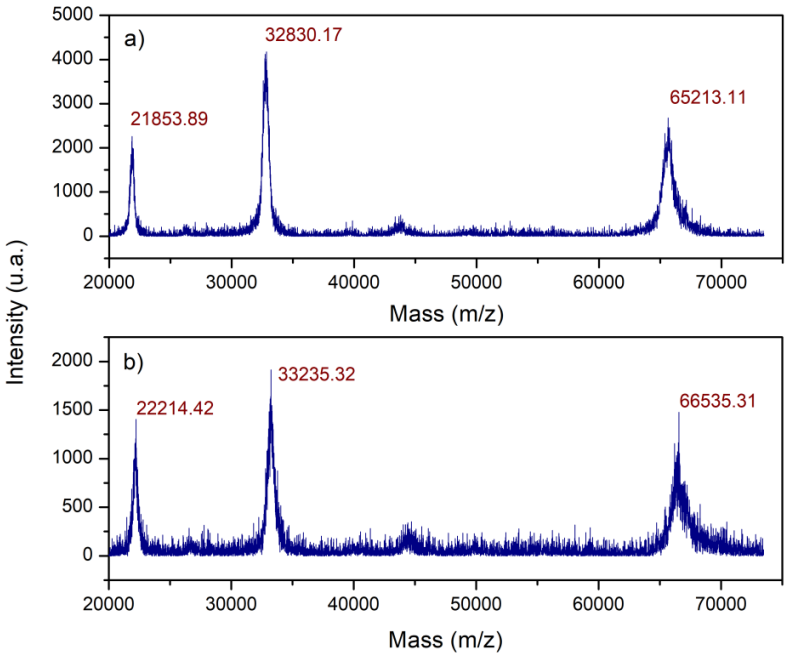

Figure 4. MALDI-TOF mass/charge spectrum of a) BSA and b) DCF-BSA conjugated.

3.3.2 Sensor functionalization

It is well known that the quality of the recognition element and the way it is immobilized onto the surface greatly impact the performance of an SPR biosensor. For the inhibition assay, the DCF-BSA conjugate was immobilized on the sensor surface, and to obtain a sufficiently high response, functionalization was carried out by activating the carboxyl groups. Initially, a half hour contact time between the DCF-BSA conjugate and the sensor was established. However, it was necessary to extend this step to reach saturation and stability. The ideal incubation time was determined as 1.5 hours; additional information regarding the conditions established for the immobilization of the DCf-BSA can be found in the supplementary information. Figure 5 (a) shows the sensogram in which a drop in the angle caused by the washing step, used to remove the molecules that were not covalently

bound, is observed after each functionalization stage. The change in the SPR angle before and after DCF-BSA conjugate injection ($\Delta\theta_{SPR}$) indicates an excellent immobilization due to the large increase in the angle. Finally, blocking with ethanolamine reduces non-specific binding of the analyte to the surface.

The % coverage can be estimated in terms of saturation; the change in angle after the total functionalization process (including hapten immobilization and ethanolamine blocking) is 0.194 degrees, where the change in angle corresponding to the deposition of conjugate is 0.18 degrees and the change by ethanolamine is 0.014 degrees. Considering that ethanolamine has the function of occupying any place where the conjugate has not adhered, it can be inferred that the conjugate occupies 92.7% of the surface.

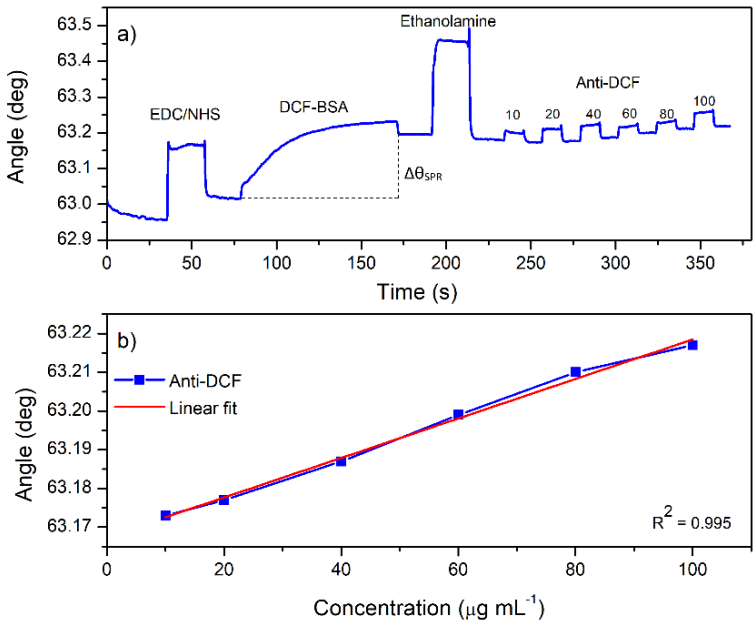

Figure 5. a) Sensogram of the functionalization steps and the subsequent calibration curve performed with anti-DCF and b) linear fit from the Anti-DCF affinity test.

In a similar published work in which a hapten-protein conjugate was used for the detection of 17-β estradiol, several injections of the conjugate were carried out for its immobilization (four injections of 10, 50, 100 and 150 μg mL^{-1}), taking a total of 1 hour to reach saturation [79]. The authors concluded that the same result could obtained in a single step by injecting the conjugate at 200 μg mL^{-1}. Hence, for future work it is proposed to increase the concentration of the conjugate and thus reduce the incubation time.

3.3.3 Antibody affinity test

To determine the affinity of the antibody towards the functionalized sensor, consecutive injections of Anti-DCF at different concentrations were performed. The objective of this test was to observe the behavior of the sensor with different concentrations of the antibody, as well as to assess possible sensor saturation after consecutive sample injections. A slight negative difference between the baseline before and after the first sample injection is observed in Figure 5 (a), which may be due to the removal of molecules that were unable to

covalently bind to the sensor surface. Subsequent injections confirmed that the antibody was indeed interacting and binding to the sensor.

As can be seen in the trend line, Figure 5 (b), the change in SPR angle increases on average from the 40 μg mL^{-1} injection onwards and then remains almost constant. Therefore, in order to visualize a positive difference in the SPR angle after each injection, a higher concentration of antibody (40 μg mL^{-1}) was employed to perform the competitive assay. Antibody response had a linear behavior, indicating a direct relationship between antibody concentration and changes in the SPR angle. Furthermore, despite the increased concentrations, the sensor does not seem to reach a point of total saturation up to this point. This indicates that the sensor can be used to read several consecutive samples. Measurements were performed in triplicate and results were consistent for every replicate, thus demonstrating reproducibility.

3.3.4 Biosensor specificity.

Figure 6 shows the results from the interference test, where the response to naproxen, ibuprofen and ketorolac is observed as a drop in the angle. This drop is attributed to a change of medium (from buffer to ultrapure water), and after the incubation and washing steps, the baseline returns to its original value for naproxen and ibuprofen, indicating there is no interaction with BSA. Only ketorolac produced a change in the SPR angle, with a shift of 0.0032 degrees, marked by the red line, this is because at the conditions at which the interferents were tested, the carboxyl group of ketorolac is more reactive towards BSA.

An insert was added in Figure 6 showing a fragment of the diclofenac detection curve; the angle shift for the lowest diclofenac concentration (2 μg L^{-1}) was 0.061 degrees, showing that the interference of ketorolac (15 μg L^{-1}) is about 5 %. However, it should be noted that, of the limited literature where ketorolac is analyzed in real samples, comparing for example the analysis in hospital water, the data indicate that there is a concentration of 0.47 μg L^{-1}, and 6.17 μg L^{-1} for diclofenac [80,81]. In general, regardless of the type of real sample analyzed, a lower incidence of ketorolac is found, hence interference by this pharmaceutical in real samples is expected to be insignificant.

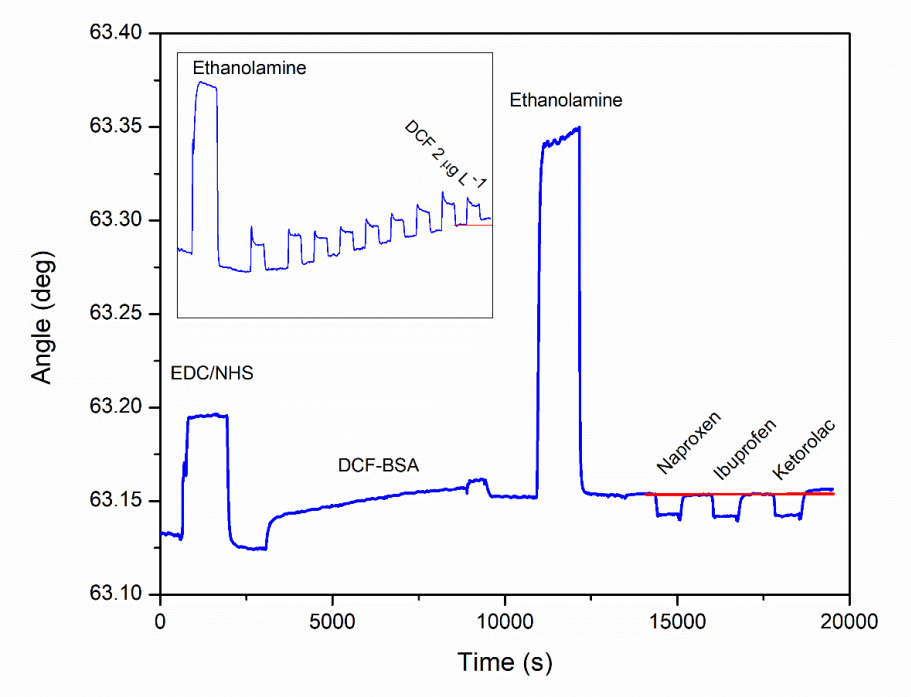

Figure 6. Interference test sensogram. Naproxen, ibuprofen, and ketorolac in ultrapure water were tested. Inset shows a section of the DCF detection curve.

3.3.5 Inhibition immunoassay

Due to the small size of DCF molecules, an indirect competitive (inhibition) assay was performed. Four repetitions of the assay were carried out, and results were normalized prior to data analysis. Figure 7 shows the obtained calibration curve after a fit using the sigmoidal Boltzman function [82] according to the Equation 1. Consequential to the fit used, an R2-value of 0.99 was obtained. For the calculation of LOD and LOQ, the 3SD and 10SD criteria were used, resulting in 3.15 µg L^{-1} and 10.52 µg L^{-1} respectively. The detection range is 2 to 32 µg L^{-1}, corresponding to the concentrations tested during the assay. Figure 4 shows the error bars, which represent the precision, the average precision being 1.96%. Finally, the sample analysis time is 10 min.

$$y = 9.06 + \frac{12.71 - 9.06}{1 + e^{\frac{x-21.12}{6.88}}}$$

Equation 1. Boltzman function used for fitting.

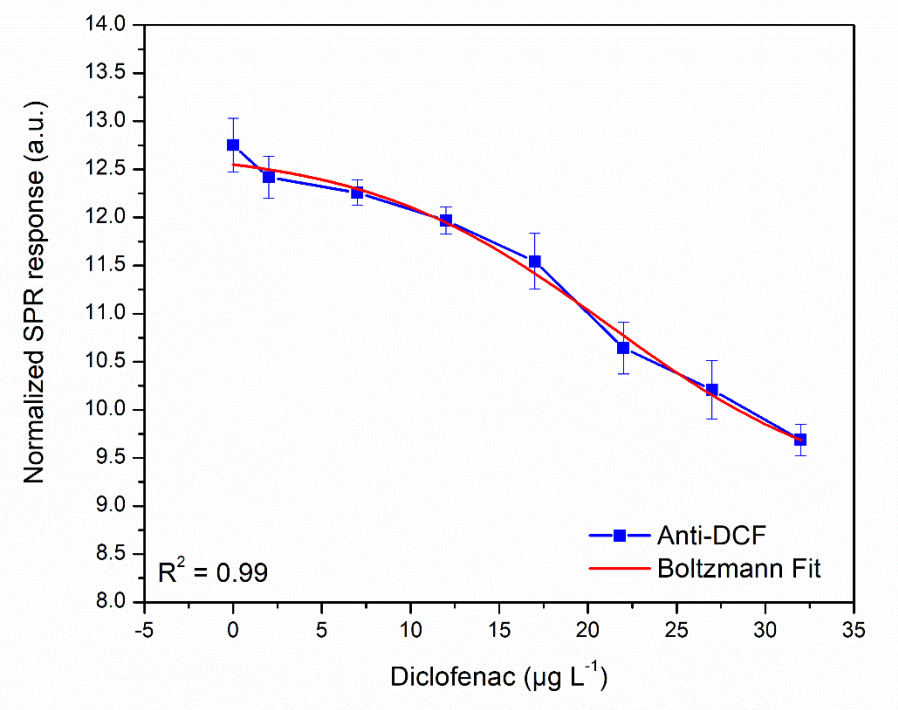

Figure 7. Calibration curve from the competitive assay for the detection of DCF.

Other biosensors have been previously developed for quantifying DCF, among these various electrochemical biosensors, as well as fluorescence and interferometric biosensors in the case of optical sensors. Table 1 shows the general information of the published works in comparison with this work. As can be seen, in terms of LOD, this biosensor offers similar results to the other SPR and QCM biosensors. However, it can also be seen that this biosensor achieved better performance in terms of analysis time and accuracy.

Table 1. Comparison between biosensors developed for DCF detection.

Biosensor type	**LOD µg L^{-1}**	**LOQ µg L^{-1}**	**Range µg L^{-1}**	**SD (%)**	**Analysis time**	**Sample tested**	**Reference**
SPR	3.15	10.52	2 – 32	1.96	10 min	Deionized water	**This work**
Interferometer	0.11	0.24	0.43 – 6.21	-	20 min	Milk	[83]
Photoelectrochemical	0.23	-	0.29 – 44.4	2.92	-	Lake water	[84]
Fluorescence	-	-	2961.4 – 14807.4	-	12 h	Wastewater	[85]
SPR (with nanostructures)	-	-	1 – 10	-	-	Deionized water	[86]
QCM	2.8	4.5	4.4 – 13.6	-	60 min	River water	[87]

To the best of our knowledge, only one work has addressed the use of an SPR immunosensor for DCF, in which a sensor with imprinted nanopillars was used [86]. In that work, DCF molecules were directly deposited on the sensor and an inhibition immunoassay was performed. The authors reported a detection range of 1 μg L^{-1} and 10 μg L^{-1}, and the LOD obtained herein (3.29 μg L^{-1}) is comparable to their results. The main differences between both works are (a) the immobilization strategy, i.e., pure DCF instead of a DCF hapten-protein conjugate, and (b) the use of nanostructured sensors based on nanopillars by Steinke et al., instead of a gold coated glass slide. The nanopillars intensify the SPR signal therefore eliminating the need for conjugating DCF to a bigger molecule, while in contrast in this work similar detection limits were reached without having to design complex nanostructures since the conjugate improves sensitivity. Having a biosensor whose configuration is simpler is highly advantageous in terms of accessibility, as it can reduce production time and costs and infrastructure requirements.

3.4 Conclusions

A DCF-BSA conjugate was developed for the detection of DCF. The conjugate was successfully synthesized, achieving binding of approximately 3 DCF molecules to each BSA molecule. The biosensor showed specificity towards DCF since other anti-inflammatory drugs such as ibuprofen and naproxen could not bind to the surface, only ketorolac showed affinity for the biosensor. However, interference by ketorolac is not significant since its concentrations in ambient water are minimal. The SPR biosensor fabricated using the DCF-BSA conjugate was able to detect DCF in concentrations of parts per billion, which are in the same order of magnitude than those quantified in wastewater, with a LOD of 3.15 μg L^{-1} and LOQ of 10.52 μg L^{-1}, the measurements were performed in a time of 10 min and with a SD of 1.96%, which improves the results of previous published works. Moreover, compared to the only other SPR biosensor built for the quantification of this molecule, detection limits and ranges were analogous considering the different approach used in each case (i.e., nanofabricated structures vs. a chemical-based method). An advantage of a chemical-based method is that there is little to no requirement for specialized infrastructure (e.g., clean rooms) or expensive top-down nanofabrication equipment, which can translate into higher accessibility.

CHAPTER IV

4.1 Detection of acetaminophen by enzyme based amperometric biosensor.

The work described in this chapter corresponds to an article entitled "Detection of Acetaminophen in Groundwater by Laccase-Based Amperometric Biosensors Using MoS_2 Modified Carbon Paper Electrodes" which is published in the journal Sensors with DOI: https://doi.org/10.3390/s23104633

Briefly, in this chapter an enzyme-based amperometric biosensor was developed; the design of the biosensor involves the use of laccases and molybdenum disulfide (MoS_2). For the optimization of the biosensor, three different types of laccase were tested, a commercial laccase from the fungus *Trametes versicolor* (TvL); and a laccase harvested and purified from a native strain of *Pycnoporus sanguineus*, from the latter two different isoforms were obtained and both were tested (Lac I and Lac II). Once the best response was obtained, the biosensor was tested for the detection of ACE in groundwater samples.

4.2 Methodology

4.2.1 Laccase Enzymes

A Laccase isoform (EC 1.10.3.2) from *P. sanguineus* CS43 (LacI and LacII) was obtained as described in our previous work [88]. Briefly, mycelia were recovered from a tomato medium supernatant after 10 days of culture by filtration (0.2 μm pore size). Then, the sample was concentrated by ultrafiltration with a tangential-flow filter (Membrane cut-off of 10 kDa, Sartorius Sartojet). The ultra-filtered sample was purified with a DEAE-cellulose ion exchange column eluted with a 20 to 300 mM phosphate buffer of pH 6.0 at a flow rate of 2 mL/min. Finally, laccase fractions were collected and concentrated. Commercially purified laccase from *T. versicolor* (EC 1.10.3.2) was kindly provided by Amano Enzyme Inc. (TvL). Laccase activity was determined as in a previous work [89], where the oxidation of 0.54 mM ABTS 50 mM citric/phosphate buffer of pH 4 was monitored by the increase in the absorbance at 420 nm. Total protein content was determined with the BCA reagents using bovine serum albumin (BSA) as standard and measured at 562 nm. Absorbance was measured using a Thermo 50 Scientific© Evolution 260 Bio UV-Visible Spectrophotometer (Thermo Fischer Scientific, Waltham, MA, USA). Measurements were triplicated. All solutions were prepared in MQ water. *P. sanguineus* CS43 fungal laccases were used as obtained from a freshly purified culture, and TvL was prepared according to previous work [89], where it was demonstrated to have an efficient electrochemical signal. Concentrations and/or enzymatic activities were not modified for the following experiments. Characterization of laccase enzymes is shown in Table 2.

Table 2. Enzymatic characterization of laccases from *P. sanguineus* CS43 and *Trametes versicolor*.

Sample	Conc. (mg/mL)	Activity (U/mL)	Specific Activity (U/mg)
TvL	1.32 ± 0.64	81.00 ± 30	61.50 ± 3.29
LacI	0.31 ± 0.48	33.87 ± 1.38	108.17 ± 7.35
LacII	0.48 ± 0.17	74.49 ± 0.97	155.11 ± 1.50

4.2.2 Synthesis of MoS_2 Nanostructured Material

The hydrothermal synthesis of MoS_2 was performed following the procedure reported by Najmaei et al. [90] with modifications. The modified synthesis is registered under patent MX-a-2017-016742 [91]. The first step consisted of the obtention of MoO_3 nanoribbons through the hydrothermal method: a dispersion of 2 mL of a saturated ammonium molybdate in HCl mixed by magnetic stirring for 30 min was then transferred to a Teflon-lined autoclave and left at 185 °C for 12 h. MoO_3 and sulfur powder were put into a tube furnace at 600 °C under nitrogen flow; afterward, the temperature was increased to 800 °C and was heated for 1 h. After the heating process, the furnace was left to cool down to room temperature under nitrogen flow. Then powder was stored for further use.

4.2.3 Immobilization of Laccase onto MoS_2 Modified Electrodes

Different solutions containing 0.5, 1, 2, and 5 mg/mL of MoS_2 were prepared and sonicated for 15 min. After a homogeneous solution was obtained, 10 µL of each solution was drop-casted onto the carbon paper (CP) electrode surface (0.25 cm^2) and left to dry at room temperature (CP-MoS_2). TBAB-Nafion polymer was used for enzyme immobilization according to the procedure previously reported [92,93]. Briefly, a solution of each purified enzyme (LacI, LacII, and TvL) was mixed with a solution of TBAB-Nafion to obtain a ratio of 3:1 (enzyme: TBAB-Nafion). Then, the solution was vortexed at 2000 rpm for 30 s. After a homogeneous solution was obtained, 10 µL was taken and drop-casted onto (a) pristine electrodes and (b) electrodes modified with MoS_2 to obtain the CP-Lac and CP-MoS_2-Lac working electrodes, respectively.

4.2.4 Electrochemical Measurements in the Optimization of Acetaminophen Detection

Voltametric and amperometric measurements were carried out on a CHI 611E Electrochemical Workstation (CH Instruments, Shanghai, China) with a conventional three-electrode system. Either carbon paper (CP) electrode or CP modified electrode was used as the working electrode, saturated calomel as the reference electrode (SCE), and a platinum mesh as the auxiliary electrode. All experiments were conducted at room temperature (~20 °C) in a beaker containing 5 mL of a 0.1 M citric acid/2 M KOH buffer (pH 4). The steady state amperometric response of working electrodes at different ACE concentrations was determined by successive additions of a 66.15 mM of ACE solution in MQ water. First, the working electrodes were equilibrated in 0.1 M citrate buffer at a constant potential of −0.1 V until a constant current was obtained, known as background current (I1). Then, aliquots of the ACE solution were added to the electrochemical cell and the obtained steady-state current response was recorded (I2). The obtained current difference ($\Delta I = I2 – I1$) was used to plot a calibration curve of ΔI vs. concentration of dopamine ([ACE]). All measurements were taken by triplicate.

4.2.5 Characterization Techniques

Raman spectra of modified electrodes were acquired using a Renishaw InVia spectrometer under ambient conditions with a 50× objective lens. Laser excitation was 633 nm using an Argon ion laser in the range of 100–1900 cm^{-1}. Laser power on the sample was set around 1.0 mW to avoid laser-induced heating. The modification of carbon paper electrodes with MoS_2 was verified with SEM micrographs. A Nova NanoSEM 200 (FEI Company, Hillsboro, OR, USA) Scanning Electron Microscope with an acceleration voltage of 15 kV in high vacuum conditions with a BSE detector with the capacity to acquire high

magnification images (>5000×) was used. Electrochemical impedance spectroscopic (EIS) measurements were carried out on a BioLogic SP-150 potentiostat with a conventional three-electrode system; the frequency range was between 100 kHz and 10 MHz, with the single sine amplitudes of 100 μA.

4.2.6 Application of Optimized Electrodes for the Detection of Acetaminophen in Groundwater Samples

To evaluate the practical effectiveness of the modified electrodes in a real environment, optimal working electrodes were used for the determination of ACE in groundwater. Groundwater samples were obtained from several aquifers located in the state of Nuevo Leon in northeastern Mexico. Sample pH varied between 6.77 and 7.88, indicating neutral to slightly alkaline water conditions within the studied area. Their concentration of major ions, Na^+, K^+, Ca^{2+}, Mg^{2+}, Cl^-, SO_4^{2-}, NO_3^-, and HCO_3^-, is related to water–rock interaction (lutites and limestones) [94]. The groundwater samples were pooled, and the pooled sample was preconditioned by adding 50mM citric acid and adjusting pH to 4 with KOH (2M). Electrochemical measurements were performed by successive injections of ACE into a 5 mL preconditioned groundwater sample.

4.3 Results and Discussion

4.3.1 Immobilization of Laccases onto MoS_2 Modified Electrodes

Michaelis–Menten kinetic parameters of the free and immobilized laccase enzymes on carbon paper electrodes modified with MoS_2 (CP-MoS_2-Lac) were determined using ABTS as a substrate. The values of the kinetic parameters shown in Table 3 were obtained by non-linear curve fitting of the reaction rate versus substrate concentration from the Michaelis–Menten equation. As observed, when laccases were subjected to the immobilization process, an increase in KMapp of 1.93 and 2.41 was obtained for TvL and LacI. Conversely, this effect was not observed when LacII (35.57 ± 4.79 μM) was immobilized, as no significant changes in its KMapp value were observed. The rise in KMapp is in general complemented by a decrease in affinity and may be a result of the enzyme's substrate diffusional restriction or the conformational changes caused by its entrapment in polymer micelles, which prevent substrate and laccase from interacting properly [95,96]. These findings indicate the existence and functioning of laccase enzymes after they were immobilized.

Table 3. Michaelis-Menten kinetic constants for both free and immobilized laccase enzymes on the carbon paper electrode surface.

Laccase	KMapp	
	Free	Immobilized
TvL	42.07 ± 3.136	123 ± 26.96
LacI	16.64 ± 2.548	58.68 ± 10.12
LacII	34.51 ± 5.857	35.57 ± 4.79

Bioelectrocatalytic activity was studied by cyclic voltammetry to corroborate the presence of immobilized laccase enzymes on the electrodes. Figure 8 shows the CVs taken at every film used in the construction of modified electrodes for ACE detection based on the immobilization of laccases onto CP-MoS_2 electrodes. CVs showed a quasi-reversible system with cathodic and anodic peaks at around 0.45 V and 0.55 V, respectively. Pristine CP

presented a reduction peak of 0.45 V and a maximum current of 20 µA; when CP was modified with MoS_2 (1 mg/mL), current decrease and shift in the reduction peak were observed.

Nonetheless, after adding laccase enzymes to CP-MoS_2 modified electrodes, it was possible to observe an increase in the current of the cathodic peak for three enzymes of around 30, 36, and 72 µA for LacI, LacII, and TvL respectively. Peak shifting and current increase in peak reduction for all bioelectrodes proved that laccases had been adsorbed on the surface of modified electrode, thus decreasing laccase biocatalytic activity while also causing a slower electron transfer due to the diffusion restriction attained by these layers.

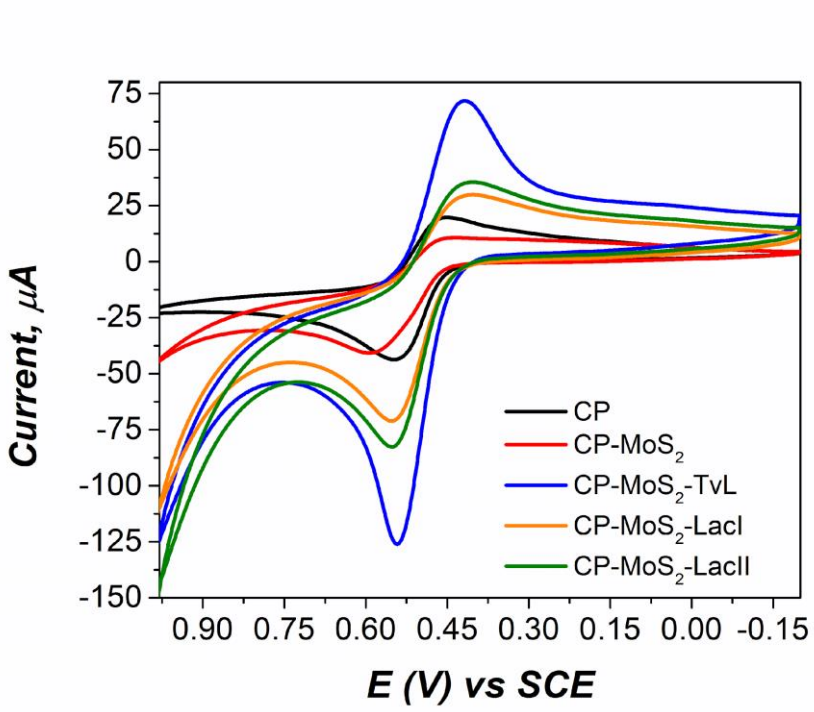

Figure 8. Cyclic voltammograms of electrodes in each immobilization step in a 0.5mM ACE solution in 0.1 M citrate buffer (pH 4) at a scan rate of 50 mV/s.

Laccase immobilization was also studied with Raman spectroscopy; this technique takes advantage of the fingerprint of specific molecules in a sample. Commonly, the analysis of enzymes (proteins) by Raman is based on bands associated with their peptide chains [97]. Figure 9 shows the Raman spectra of laccase-MoS_2 modified carbon paper electrodes in the range 500–1450 cm^{-1}; it was possible to observe characteristic peaks for CP, MoS_2, TBAB-Nafion, and laccases. Peaks at 1333 cm^{-1} correspond to disorder and defects in the carbon lattice (D-line) from the carbon paper [98]. For MoS_2, the signal at 645 cm^{-1} corresponds to a combination of the LA(M) frequency and the A1g mode, and the peak at around 820 cm^{-1} is due to the presence of a small amount of MoO_3 [99,100]. TBAB-Nafion (TB-Naf) presented several peaks in this region. The most prominent peaks at 732 and 1048 cm^{-1} correspond to CF_2 stretching and sulfonate (SO_3) symmetric stretch, respectively [101]. Most of the signals for laccase enzymes were overlapped by TBAB-Nafion polymer signals; this condition was expected since it is known that this polymer entraps enzymes through the

formation of a semi-permeable membrane that allows the diffusion of substrates and products [102]. Nonetheless, LacI and LacII presented a small peak at around 930 cm^{-1} probably for stretching of the γOH in the carboxylic groups in amino acids (glutamic acid and aspartic acid) [103]. TvL showed a more prominent peak at around 995 cm^{-1} probably due to the glycoproteic portion of laccase (C-O ribose); this higher signal may be associated with the fact that TvL was more concentrated than LacI and LacII [104,105].

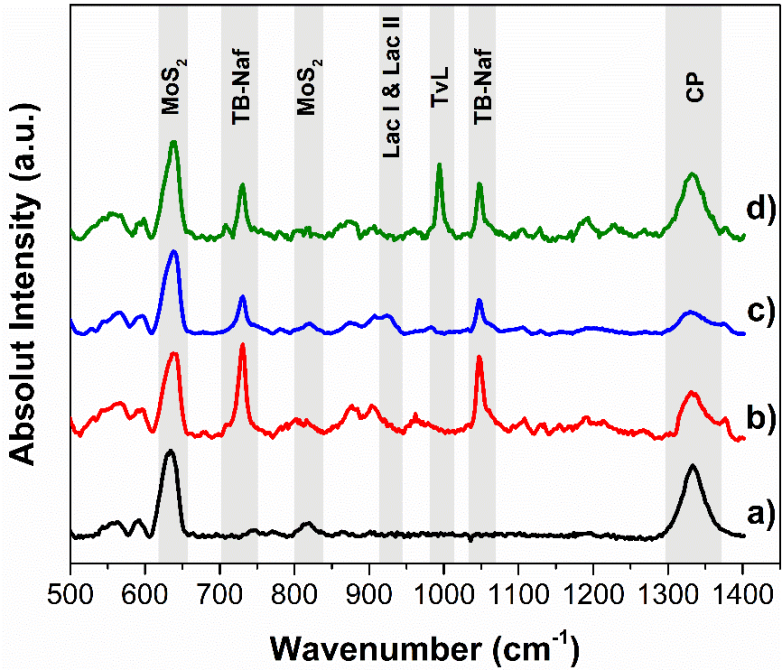

Figure 9. Raman spectra of a) CP-MoS_2, b) CP-MoS_2-LacI, c) CP-MoS_2-LacII, and d) CP-MoS_2-TvL.

The ACE molecule has a hydroxyl and amino derivative functional group; therefore, based on laccase reactivity, the presence of functional groups acting as electron-donating groups (EDG) such as hydroxyl (-OH) and amines (-NH_2) makes ACE susceptible to laccase attack [106]. The role of MoS_2 in this mechanism is the modification of the working electrode (carbon paper) to improve its conductive properties (transducer modifier), due to its features as a bandgap ranging from 1.2 to 1.8 eV, as well as higher adsorption capacity of ACEox [107–109]. Hence, according to this and CVs results, the proposed electron transfer mechanism for the developed CP-MoS_2-Lac biosensor is defined as follows: first, acetaminophen (ACEred) is oxidized enzymatically by laccases in the presence of oxygen to its respective N-acetyl-p-benzoquinoneimine form (ACEox), and then ACEox is electrochemically reduced back at the electrode surface to its ACEred form, which is reflected as an electrical current (Figure 10). For amperometric experiments, measurements were made at a potential of −0.1 V to ensure the electrochemical reduction of ACEox. Moreover, this potential avoids possible interference from MoS_2 precursors, specifically the remaining MoO_3. This low potential that was used was in accordance with previously reported studies [110,111].

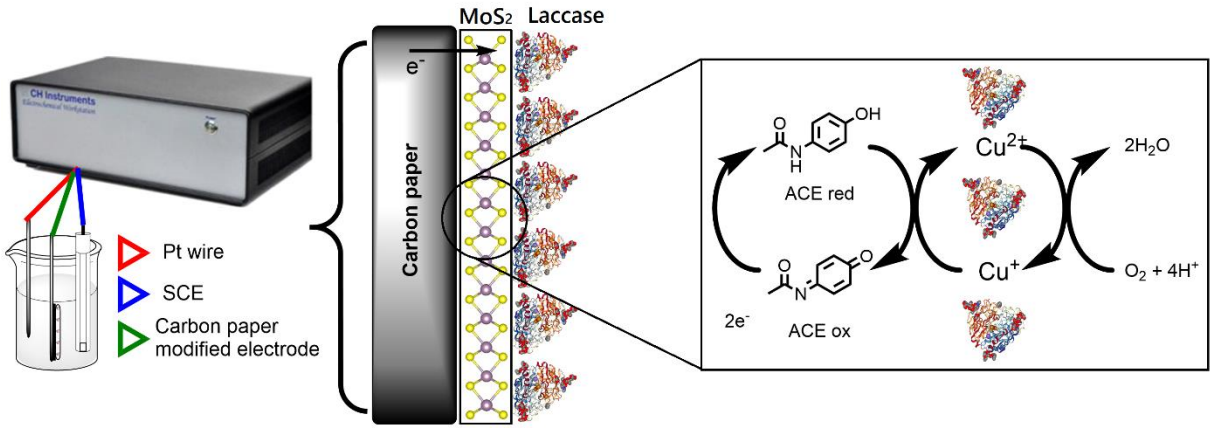

Figure 10. Electron transfer mechanism for our developed CP−MoS2 Lac bioelectrodes in the detection of acetaminophen.

4.3.2 Optimum MoS_2 Concentration for Laccase Bioelectrode Modification

All nonlinear regression of the Michaelis–Menten model was used to evaluate the apparent electrochemical enzymatic kinetics of the bioelectrodes toward the substrate. This model can be used to study the influence of factors such as temperature, pH, immobilization technique, and diffusion-limiting membranes on an enzymatic system [112,113]. In this sense, the following modified equation was used:

$$J = \frac{J_{max}[S]}{KM_{app} + [S]}$$

where J is the current density, KM_{app} is the apparent Michaelis constant which quantifies the enzymatic affinity for the substrate, and J_{max} is the maximum current density [114,115]. Since the recognition system of the proposed enzymatic bioelectrode depends on the enzymatic kinetics, ACE detection was evaluated under steady-state conditions to compare the apparent affinity of KM_{app} and J_{max} of ACE at the bioelectrodes. Consecutive injections of ACE into a stirred buffer solution measured at a potential of −0.1V were made. Representative amperometric curves for 1 mg/mL of MoS_2 modified electrodes (Figure 11) showed an evident electrocatalytic effect obtained after adding ACE into the system.

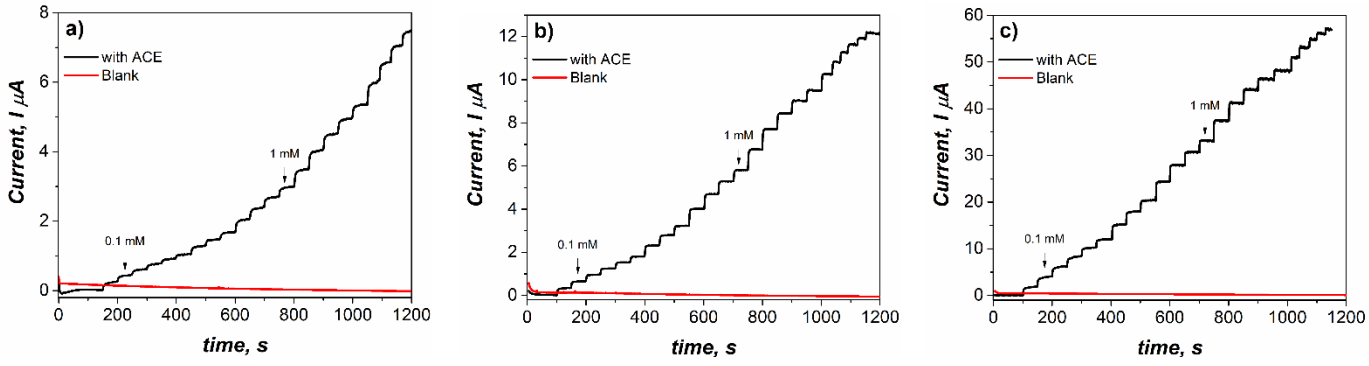

Figure 11. Amperometric i–t curves for the CP-MoS2-Lac modified electrodes with successive addition of ACE into 0.1 M citric acid/2M KOH pH 4 recorded at −0.1 V. For a) CP-MoS2-TvL, b) CP-MoS2-LacI, and c) CP-MoS2-LacII.

All the bioelectrodes demonstrated a Michaelis–Menten kinetic behavior, as can be seen in Figure 12. It is also possible to observe that modification of MoS_2 in a concentration of 0.5–5 mg/mL did not cause a noteworthy increase in the electrochemical detection of ACE when using LacI and TvL, where maximum current densities were around 45 µA/cm^2. On the other hand, for LacII, a significant increase in current density was observed using 1 and 2 mg/mL of MoS_2. The maximum current density for LacII was around 210 µA/cm^2 when using 1 mg/mL of MoS_2.

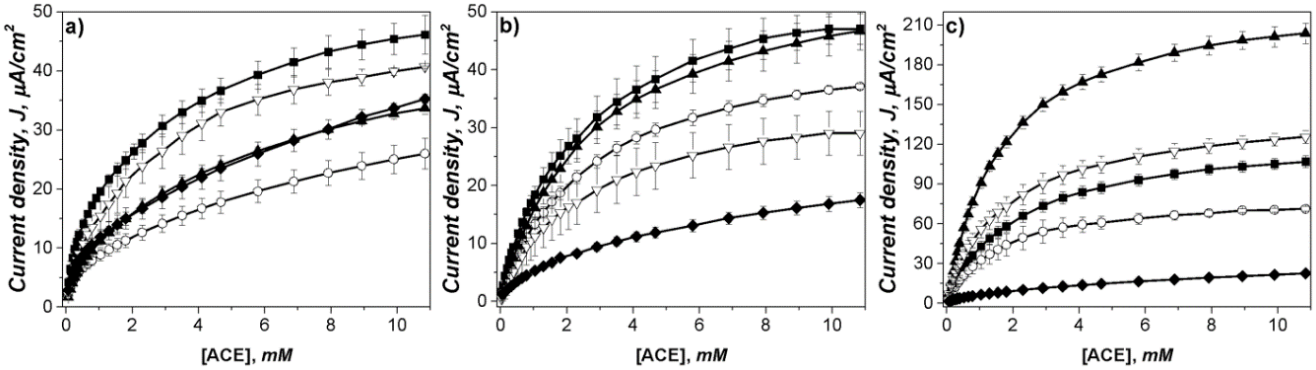

Figure 12. Apparent steady-state Michaelis–Menten kinetics of ACE for a) CP-MoS2-TvL, b) CP-MoS2-LacI, and c) CP-MoS2-LacII, determined in stirred citric acid/KOH (pH 4, 500 rpm) at an applied potential of −0.1 V vs. SCE. MoS2 concentrations were: 0 mg/mL (■), 0.5 mg/mL (○), 1 mg/mL (▲), 2 mg/mL (▽), and 5 mg/mL (♦). Error bars represent standard deviation (n = 3).

Values for KM_{app} and J_{max} from nonlinear regression of the Michaelis–Menten model are reported in Table 4. Usually, low KM values are associated with high affinity [116]; taking this into account, the results for LacI and TvL modified bioelectrodes confirm that MoS_2 did not have a significant effect on the concentrations that were studied. Contrarily, for LacII, lower KM_{app} and higher J_{max} were achieved when 1 and 2 mg/mL of MoS_2 were used. From these results, the MoS_2 concentration considered to be optimum for further uses was 1 mg/mL since low KM_{app} and the highest J_{max} were obtained.

Table 4. Apparent steady-state Michaelis–Menten kinetic values of LacI, LacII, and TvL MoS2 modified bioelectrodes for ACE, determined in stirred citric acid/KOH (pH 4, 50 mM, 500 rpm) at an applied potential of −0.1 V vs. SCE.

MoS_2	**TvL**		**LacI**		**LacII**	
Concentration	**KM_{app} (µM)**	**J_{max} (µA/cm^2)**	**KM_{app} (µM)**	**J_{max} (µA/cm^2)**	**KM_{app} (µM)**	**J_{max} (µA/cm^2)**
Unmodified						
-	1659 ± 250	51.11 ± 2.59	2164 ± 151	53.68 ± 1.43	1908 ± 77	129.3 ± 1.76
Modified with MoS_2						
0.5mg/mL	2613 ± 254	29.80 ± 1.09	2474 ± 65	45.39 ± 0.44	1501 ± 99	81.05 ± 1.68
1 mg/mL	2952 ± 155	41.03 ± 0.85	2702 ± 143	58.01 ± 1.17	1656 ± 37	234.7± 1.65
2 mg/mL	1791 ± 99	49.84 ± 0.91	2429 ± 232	34.34 ± 1.30	1604 ± 66	142.2± 1.81
5 mg/mL	2733 ± 253	40.33 ± 1.43	3535 ± 250	22.07 ± 0.65	4176 ± 331	29.54 ± 1.04

4.3.3 Characterization of Optimum MoS_2 Modified Electrodes

According to the above results, the electrode with the best efficiency in ACE determination was the one modified with MoS_2 at 1 mg/mL. SEM and electrochemical impedance spectroscopy (EIS) were carried out in order to study the electrode properties. SEM micrographs of CP and CP-MoS_2 modified with 1 mg/mL are shown in Figure 13. From Figure 13 a, it is possible to observe that CP is composed of carbon fibers with an average diameter of 6.72 ± 0.65 µm, and that no impurities were observed. When CP was modified with 1 mg/mL of MoS_2 (Figure 13 b), it was well distributed throughout the CP surface; uniform distribution was confirmed by EDS mapping (Figure 13 e,f). At high magnification (Figure 13 c), it is possible to observe that MoS_2 morphology resembles ribbons with an average length of 5 µm and an average width of 0.4 µm. Moreover, some nano-platelets grown over the surface (indicated with arrows in Figure 13 d) were observed, which can serve as electroactive sites that are more accessible for the substrate to experience reduction reactions. No visible gaps between the stacked MoS_2 ribbons were visible, suggesting that, as the concentration of ribbon increases, they tend to stack in an ordered manner, ensuring a good contact between adjacent ribbons and the surface of the electrode, which suggests that the electron transfer process is favored. EDS analysis (Figure 13 g) was performed to characterize the chemical composition of CP-MoS_2, confirming the existence of the element C, and Mo and S in a 1:2 ratio.

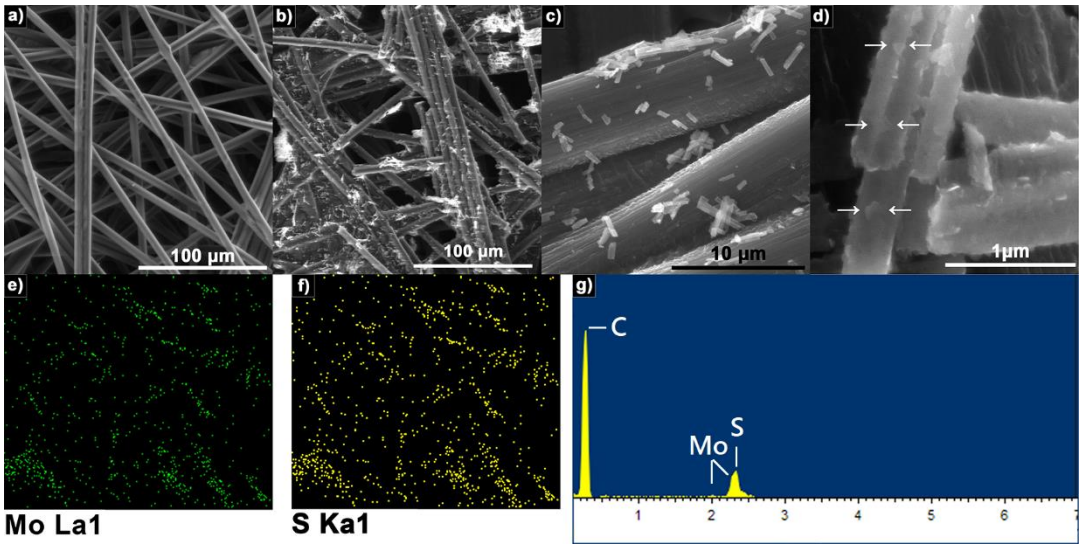

Figure 13. Representative SEM micrographs of electrodes: bare CP a) and CP modified with 1 mg/mL of MoS_2 b–d). EDS mapping of Mo and S elements distribution within CP e,f). EDS spectrum of MoS_2 onto CP g).

The Nyquist plot (Figure 14) shows the electrochemical impedance spectra (EIS) of CP, CP-MoS_2, CP-MoS_2-TvL, and CP-MoS_2-LacII. TvL was taken for comparison. All plots show the typical semicircle portion at high frequencies that correspond to an electron-transfer limited process with the transfer of electrons between the electrolyte and the electrode surface. Symbols represent the experimental data, and solid lines represent the fitted data to an equivalent circuit (inset Figure 14) to determine the charge transfer resistance (Rct) and double-layer capacitance (Cdl) at the interface of the developed electrodes. The basic Randles circuit was modified by an additional parallel RC circuit for a better fit. This additional circuit

was required possibly due to the higher roughness of CP [117]. It was possible to observe that CP unmodified by MoS_2 or laccase had an Rct of 61.21 ± 0.21 Ω. After that, when MoS_2 was added to the electrode, a slight decrease in Rct to 59.73 ± 0.73 was obtained; this result may be associated with the electrical conductivity given by MoS_2, promoting direct electron transfer reactions. When TvL was added, an Rct of 63.84 ± 0.62 was obtained, while, for LacII, an Rct to 61.34 ± 0.27 was observed. The hindered electron transfer shown for CP-MoS_2-TvL and CP-MoS_2-LacII may be due to the addition of laccase enzymes to the electrode [118]. Despite this increase in transfer-resistant charge compared to CP-MoS_2, LacII had a lower Rct compared to TvL.

The characterization of electrodes in optimal conditions showed that the use of MoS_2 as a CP modifier agent in the manufacture of bioelectrodes produces a positive effect, facilitating the transfer of electrons in the system.

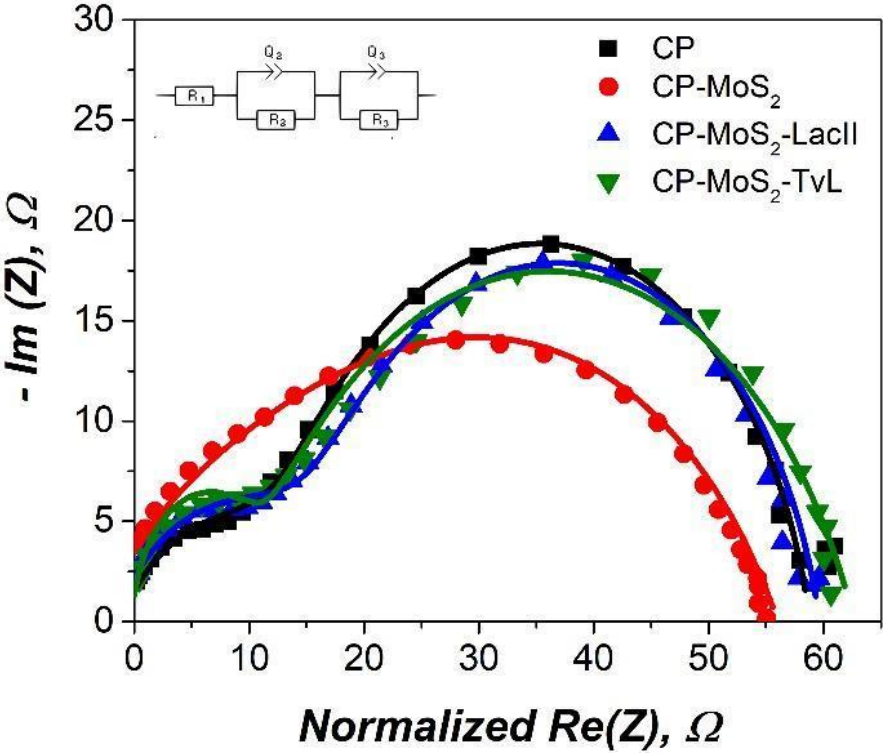

Figure 14. Representative Nyquist plots in each step of bioelectrode fabrication. Measured in citric acid/KOH buffer pH 4 using a frequency range between 100 kHz and 10 MHz, with single sine amplitudes of 100 μA.

4.3.4 Application of Modified Electrodes in the Detection of Acetaminophen

Based on enzymatic kinetics, by using the lower KM_{app} and higher J_{max} values, the optimal combination of enzyme/MoS_2 concentration for electrode modification was the one fabricated with LacII and a concentration of 1 mg/mL. Thus, further analyses were performed to determine the linear ranges and limits of detection for ACE. As stated before, commercially available TvL was used for comparison against native LacII. Figure 15 and Table 5 show the results for electrodes unmodified and modified with 1 mg/mL of MoS_2 and with LacII and TvL.

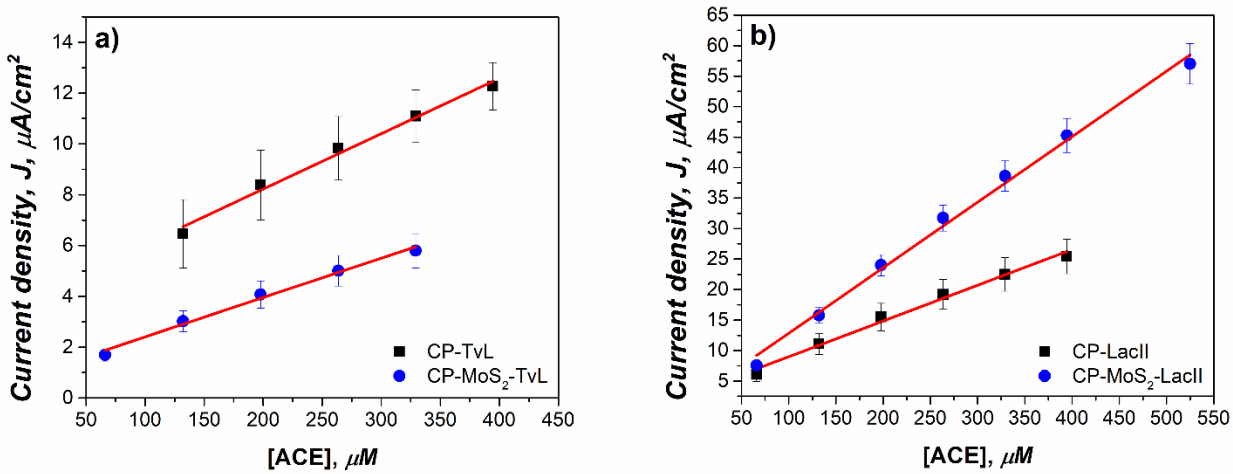

Figure 15. Calibration curves for ACE using the electrodes unmodified and modified with 1 mg/mL of MoS2 in citric acid/KOH buffer pH 4 for a) LacII, and b) TvL.

It was found that CP-MoS_2-LacII presented a broader linear range of 66–525 µM than TvL, which had a range of 66–329 µM, when both were used in electrodes modified with MoS_2. These results agree with the fact that the linear range of enzymatic biosensors is limited to substrate concentrations well below Km, where the reaction rate is diffusion-limited and grows almost linearly when substrate concentration increases [119]. The almost 2-fold improvement in sensitivity for the LacII electrode, which passed from 0.0586 to 0.1083 µA/µM cm^2, can be attributed to the presence of MoS_2 in the electrode. Consequently, a negative effect of sensitivity could be observed for TvL, which was reduced significantly from 0.0218 to 0.0155 µA/µM cm^2. The sensitivity values obtained may be associated with changes in enzymatic affinity after immobilization since, as shown above, TvL presented a lower affinity with a decreased sensitivity, whereas LacII affinity was not affected by immobilization process, and exhibited an increase in sensitivity.

Table 5. Linear range, sensitivities, and correlation coefficients obtained for the calibration curves of the modified electrodes in the determination of ACE.

Bioelectrode	Linear Range (µM)	Sensitivity (µA/µM cm^2)	R^2
CP-LacII	66–395	0.058	0.9901
CP-MoS_2-LacII	66–525	0.108	0.9948
CP-TvL	132–395	0.021	0.9901
CP-MoS_2-TvL	66–329	0.015	0.9901

The limits of detection (LOD) for CP-MoS_2-LacII and CP-MoS_2-TvL were determined by adding a 5 mM acetaminophen solution gradually until a statistically significant change response in current was observed. The obtained values for the modified electrodes were 0.2 µM for CP-MoS_2-LacII and of 2.00 µM for CP-MoS_2-TvL, which are among the lowest reported when compared with other oxidoreductase-based electrochemical biosensors for the detection of acetaminophen, as compared in Table 4. In addition, it is possible to observe that our developed bioelectrodes showed better sensitivity in the detection of ACE, reaching almost twice the value of those reported in Table 6. It is important to mention that the amperometric signals recorded for TvL were noisier than those recorded by the native LacII enzyme; this fact could translate into a much more reliable measurement.

Table 6. Analytical characteristics of some enzyme-based electrochemical biosensors reported for the determination of acetaminophen.

Electrode	Detection method	Sample	Linear range (µM)	Sensitivity (µA/µM cm^2)	LOD (µM)	Ref.
GCPE-PPO	Amp (−0.1V)	50 M phosphate buffer solution pH 7.4.	Up to70	0.015 µA/µM	7.8	[110]
GCE-HRP @ PAA-BIS	Amp (−0.1V)	50 mM sodium phosphate buffer pH 7.0 with 100 mM KCl	5.6–331.1	0.069	1.7	[111]
GCE-HRP-PPY SPE-HRP-PPY	Amp (−0.175 V)	0.2 mM H_2O_2 in phosphate buffer pH = 7.4	9.3–83.7 3.1–55.9	- -	6.5 1.52	[120]
GCE-nano PPY-HRP GCE-flat PPY-HRP	Amp (−0.2 V)	Phosphate buffer solution (pH 7.4)	5–60 5–300	0.050 0.002	0.1 4.1	[121]
GCE-clay-PEI-HRP	Amp (0 V)	100 mM phosphate buffer saline (pH 7.4)	5.25–49.5	0.013 µA/µM	0.63	[122]
SPE-CoPC/Tyr	CV	100 m M phosphate-buffer pH 6 /100 mM KCl	up to 40	−0.088	0.5	[123]
CPE-EP-PPO	DPV 10 mV/s	100 mM phosphate buffer (pH 6.0)	600–1150	-	5.0	[124]
CPE-PPO	DPV 10 mV/s	100 mM phosphate buffer pH 7.0	5–245	-	3.0	[125]
CP-LacII CP-TvL CP-MoS_2-LacII CP-MoS_2-TvL	Amp −0.1 V	100 mM citric acid / 2 M KOH buffer (pH 4)	66–395 132–395 66–525 66–329	0.058 0.021 0.108 0.015	- - 0.2 2.0	**Present study**
CP-MoS_2-LacII CP-MoS_2-TvL	Amp −0.1 V	Groundwater (50mM citric acid/2 M KOH)	1–155.1 29.82–155.1	0.017 0.005	0.50 24.88	**Present study**

*GCPE-: glassy carbon paste electrode. PPO: polyphenol oxidase. GCE: glassy carbon electrode. HRP horseradish peroxidase. PAA-BIS:—polyacrylamide—*N*,*N*-methylenebisacrylamide. PPY: polypyrrole. SPE: screen-printed electrode. PEI: polyethyleneimine. CoPC: polyvinyl alcohol photocrosslinkable polymer. Tyr: tyrosinase. CPE: carbon paste electrode. EP-PPO: eggplant polyphenol oxidase. MWCNT: multiwall carbon nanotubes. PANI: polyaniline. GA: glutaraldehyde. Amp: Amperometry. CAmp: Chronoamperometry. CV: Cyclic Voltammetry. DPV: Differential pulse voltammetry.

4.3.5 Application of Modified Electrodes in the Amperometric Detection of Acetaminophen in a Groundwater Sample from a City in Northeastern Mexico

With the aim of confirming the validity and feasibility of the biosensor for detecting ACE in groundwater, an aliquot of groundwater was preconditioned by adding citric acid to reach a concentration of 50 mM, then adjusting pH to 4 with KOH. Then, successive injections of ACE were made to a 5 mL preconditioned groundwater sample. The detection of ACE was studied by increasing concentration up to around 150 µM to determine the linear range, sensitivity, and LOD in this water sample used as a model of environmental importance.

Figure 16 and Table 7 summarize the application of 1 mg/mL modified electrodes with TvL and LacII in the detection of ACE in groundwater; this study was performed up to a concentration of around 150 µM, where typical CECs are found [70,126].

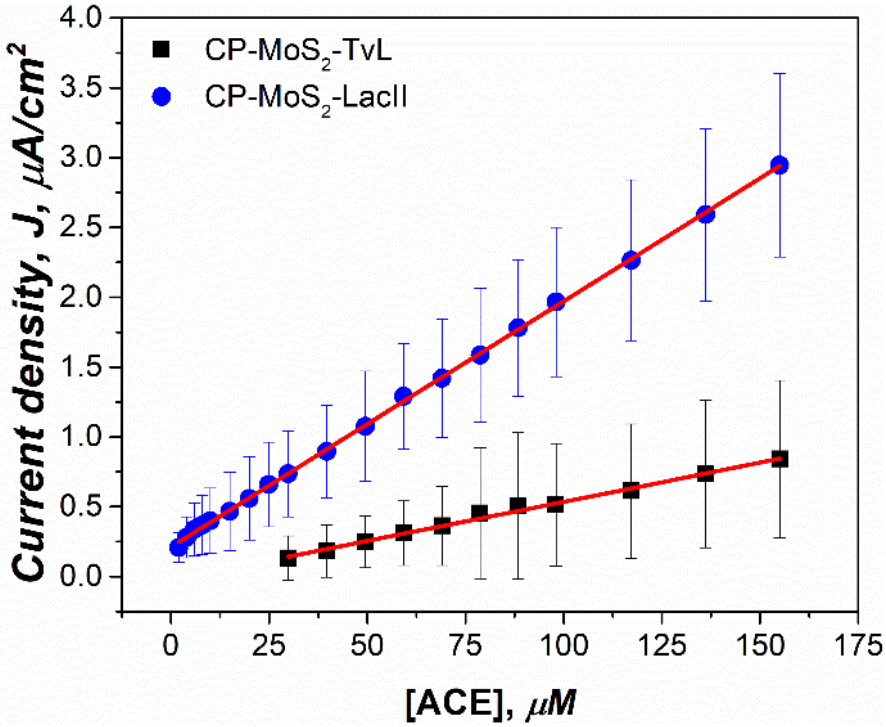

Figure 16. Calibration curves for ACE using the electrodes modified with 1 mg/mL of MoS2 for LacII and TvL, both in groundwater (5 mL) pre-conditioned with 0.05 M citric acid and adjusted to pH 4 con 2M KOH.

LacII presented a wider linear range from 1 to 155 µM compared to TvL, which had a linear range of 29.82–155 µM. In terms of linearity, LacII also presented a better R^2 value of 0.9992 than the TvL (0.9933). As is also shown in Table 6, LOD for Lac II was lower than that for TvL, which was an expected result since, on the one hand, it is known that Lac II has presented an enhanced resistance to common inhibitors such as major ions Na^+, K^+, Ca^{2+}, Mg^{2+}, Cl^-, SO_4^{2-}, NO^{3-}, which are normally found in groundwater, and, on the other hand, LacII did not show significant affinity change after the immobilization process. Furthermore, the sensitivity of LacII was shown to be around 3-fold higher when compared to TvL, confirming that the native laccase enzyme is a better candidate for use in practical applications for ACE detection in water samples of environmental importance such as groundwater.

Table 7. Linear range, sensitivities, and correlation coefficients obtained for the calibration curves for the modified electrodes in the determination of ACE in groundwater samples.

Electrode	Linear Range (µM)	Linear Range (µg/L)	Sensitivity (nA/µMcm^2)	R^2	LOD (µM)	LOD (µg/L)
CP–MoS_2 – Lac	1–155	151.13–23,436.1	17.7	0.9992	0.50	75.57
CP–MoS_2 – TvL	29.82–155	4507.84–23,436.1	5.6	0.9933	24.88	3760.27

From these results, it was possible to observe that the use of native laccase LacII for the fabrication of a modified electrode in the development of a laccase-based electrochemical biosensor can be a powerful element for the determination of any noticeable increase in the guidance value for ACE of 200 µg/L, which can be an indicator of pollution by this drug. Moreover, laccase-based amperometric biosensors have the advantage of being of easy usage, fast, and with good performance and selectivity, which may be convenient for the detection of these emerging pollutants [127].

4.4 Conclusions

The use of MoS_2 as a two-dimensional material for the modification of carbon paper electrodes coupled with the immobilization of laccase enzymes allowed the development of a novel bioelectrode for use in the development of a laccase-based amperometric biosensor. The resulting bioelectrode showed good analytical performance in the determination of ACE in citric acid buffer, providing a sensitivity of 108.3 nA/µM*cm^2 and an LOD of 0.2 µM, which are among the lower values reported for this oxidoreductase-based biosensor. It was also demonstrated that MoS_2 allowed an increase in sensitivity. Furthermore, the difference in the nature of laccase enzymes was investigated, presenting a very important effect for the development of novel bioelectrodes; hence, it is of utmost importance to investigate enzymes with improved detection yields. For example, of the two isoforms of the laccase enzyme from the white-rot fungi, *Pycnoporus sanguineus* CS43 (LacI and LacII) and the commercial laccase (*Trametes versicolor*), better results were achieved for LacII native laccase.

The bioelectrode application in the determination of ACE in groundwater samples was successfully carried out, with LacII showing a good performance against naturally found inhibitors (major ions). This achieved an LOD of 0.5 µM and a linear range of 1–98.04 µM equivalent to 151.13–14,819.9 µg/L. The properties of this developed bioelectrode can be effectively used to develop a monitor tool for any significant increase in guidance values emitted by environmental organisms defined at 200 µg/L to study water pollution by this pharmaceutical.

CHAPTER V

5.1 General Conclusions

The electrochemical biosensor is easier to manufacture, because being of the catalytic type does not require the formation of a conjugate for the quantification of small molecules, which proves the advantage it has in terms of ease of manufacture and miniaturization capacity. On the other hand, the SPR biosensor, due to its configuration and components, makes it difficult to design a portable device. In addition, the design of the SPR biosensor turned out to be slightly more complex due to the use of the DCF-BSA conjugate. Since it is an affinity biosensor, the response generated by the antibody is strongly influenced by the quality of the antigen present; in this sense, the synthesis of the conjugate is a delicate process that must be carried out under the appropriate conditions.

In terms of sensing, the detection limits achieved were 3.15 $\mu g\ L^{-1}$ for DCF by SPR and 75.57 $\mu g\ L^{-1}$ for ACE in amperometry. Both biosensors achieved detection of pharmaceuticals at concentrations low enough to be used in real samples; however, it is evident that SPR is better in terms of sensitivity. The immunoassay proved to have a high specificity, which is also an advantage in the detection of this type of contaminants.

Both works provide new findings in the application of these analytical techniques for environmental water samples. They demonstrate that it is worthwhile to continue research in this area, designing new biosensors that are increasingly sensitive, simple and portable, so that CEC can be quantified quickly and reliably.

5.2 Future work

For future work we propose the development of specific SPR biosensors for the detection of carbamazepine (CBZ) and diazepam (DZP). CBZ is an anticonvulsant drug used in the treatment of epilepsy and for bipolar disorder as a mood stabilizer, it is one of the most frequently found drugs in water samples, so its detection is important [128]. On the other hand, DZP has anxiolytic, myorelaxant, anticonvulsant and sedative properties; it stands out for being one of the most prescribed anxiolytics, therefore its detection is also relevant [129]. Both drugs have been shown to be toxic to aquatic organisms, having effects on the development of crustaceans and fish [130–132]. Of the two, CBZ has been shown to have more toxicological effects both acutely and chronically, causing malformations and a decrease in the reproduction of certain fishes, as well as causing oxidative stress, liver and gill damage, and damage to the aquatic biofilm [64,128,132,133].

For the development of biosensors, the methodology proposed is similar to the one presented here, with the difference that prior to the synthesis of the hapten-protein conjugate, the pharmaceutical molecule requires a previous modification, as described below.

1. Preparation of immunogen

Since the molecules, both CBZ and DZP, do not have a carboxyl functional group in its structure it is first necessary to modify them to obtain the conjugate. For CBZ a reaction is performed using iminostilbene as a precursor, along with triglycine which provides the carboxyl functional group needed for protein conjugation; In the case of DZP, 3-hemisuccinate is used [134,135].

2. Synthesis and purification of hapten-protein conjugates
For preparing the haptens conjugated with BSA, the mixed anhydride method is used, which consists of two steps. First, the hapten, containing a carboxyl group, is treated with isobutyl chloroformate in the presence of tributylamine. This results in the formation of a mixed anhydride to which the protein is added. Then, the hapten reacts with the free amine groups and they are linked through an amide bond [77].

3. Sensor functionalization in continuous flow mode.
Functionalization of the sensor is carried out under continuous flow, which is achieved by attaching a microfluidic system to the SPR arrangement. Once the sensor is clean, a self-assembled layer of anchor molecules, specifically alkanethiols, is deposited on the surface. The sensor is then placed in the SPR device, and the following solutions are sequentially injected into the system: (1) a solution that forms the immobilization matrix, (2) the hapten-protein conjugate and (3) an ethanolamine solution that occupies the spaces still available in the sensor so the sample interacts only with the immobilized hapten.

4. Calibration curve using synthetic samples.
Synthetic samples will be prepared by using ultrapure water spiked with the respective analyte at different known concentrations. Once SPR set up has been calibrated and optimized at a fixed incidence-angle; synthetic samples previously incubated with the specific antibody at a fixed concentration will be analyzed in continuous flow mode. The detection process occurs when the sample flow interacts with the immunosensor settled in the SPR system; in this case, the free antibody will bind to the immunogenic conjugate on the surface of the sensor. In consequence the amount of the analyte will be estimated in inverse proportion to the antigen-antibody bonds. Calibration curves for each target analyte will be carried out in order to obtain analytical parameters such as linear ranges, sensitivity, detection and quantification limits, among others.

5. Measurement of real samples.
The measurement of real samples is carried out following the procedure described for the calibration curve, but the sample is prepared by mixing the antibody with a problem solution containing the target analyte.

Bibliography

1. Pérez Solsona, S.; Pérez-Alvarez, I.; Gómez-Oliván, L.M.; Islas-Flores, H.; SanJuan-Reyes, N.; Sánchez-Aceves, L.; Galar-Martínez, M.; López De Alda, M.; Barceló, D. Determination of Metals and Pharmaceutical Compounds Released in Hospital Wastewater from Toluca, Mexico, and Evaluation of Their Toxic Impact. *Environ. Pollut.* 2018, *240*, 330–341, doi:10.1016/j.envpol.2018.04.116.

2. US EPA Contaminants of Emerging Concern Including Pharmaceuticals and Personal Care Products Available online: https://www.epa.gov/wqc/contaminants-emerging-concern-including-pharmaceuticals-and-personal-care-products (accessed on 14 May 2023).

3. European Commission Surface Water. Protecting EU Surface Waters from Chemical Pollution Available online: https://environment.ec.europa.eu/topics/water/surface-water_en (accessed on 14 May 2023).

4. Richardson, S.D.; Ternes, T.A. Water Analysis: Emerging Contaminants and Current Issues. *Anal. Chem.* 2018, *90*, 398–428, doi:10.1021/acs.analchem.7b04577.

5. Monosik, R.; Stredansky, M.; Tkac, J.; Sturdik, E. Application of Enzyme Biosensors in Analysis of Food and Beverages. *Food Anal. Methods* 2012, *5*, 40–53, doi:10.1007/s12161-011-9222-4.

6. Erdem, A.; Senturk, H.; Yildiz, E. Recent Progress on Biosensors Developed for Detecting Environmental Pollutants. In *Biosensors: Fundamentals, Emerging Technologies, and Applications*; CRC Press, 2022; pp. 213–231 ISBN 9781000612622.

7. Nehra, M.; Kanika; Dilbaghi, N.; Kumar, R.; Kumar, S. Trends in Point-of-Care Optical Biosensors for Antibiotics Detection in Aqueous Media. *Mater. Lett.* 2022, *308*, 131235, doi:10.1016/j.matlet.2021.131235.

8. Bekmurzayeva, A.; Ashikbayeva, Z.; Assylbekova, N.; Myrkhiyeva, Z.; Dauletova, A.; Ayupova, T.; Shaimerdenova, M.; Tosi, D. Ultra-Wide, Attomolar-Level Limit Detection of CD44 Biomarker with a Silanized Optical Fiber Biosensor. *Biosens. Bioelectron.* 2022, *208*, 114217, doi:10.1016/J.BIOS.2022.114217.

9. Verdian, A.; Khoshbin, Z.; Chen, C.H.; Hu, Q. Attomolar Analyte Sensing Technique for Detection of Pb2+ and Hg2+ Ions Based on Liquid Crystal. *Talanta* 2023, *253*, 124042, doi:10.1016/J.TALANTA.2022.124042.

10. Rivera-Jaimes, J.A.; López de Alda, M.; Aceña, J.; Melgoza-Alemán, R.M.; Postigo, C.; Barceló, D. Study of Pharmaceuticals in Surface and Wastewater from Cuernavaca, Morelos, Mexico: Occurrence and Environmental Risk Assessment. *Sci. Total Environ.* 2017, *613–614*, 1263–1274, doi:10.1016/j.scitotenv.2017.09.134.

11. Chinnaiyan, P.; Thampi, S.G.; Kumar, M.; Mini, K.M. Pharmaceutical Products as

Emerging Contaminant in Water: Relevance for Developing Nations and Identification of Critical Compounds for Indian Environment. *Environ. Monit. Assess.* 2018, *190*, doi:10.1007/s10661-018-6672-9.

12. K'oreje, K.O.; Vergeynst, L.; Ombaka, D.; De Wispelaere, P.; Okoth, M.; Van Langenhove, H.; Demeestere, K. Occurrence Patterns of Pharmaceutical Residues in Wastewater, Surface Water and Groundwater of Nairobi and Kisumu City, Kenya. *Chemosphere* 2016, *149*, 238–244, doi:10.1016/j.chemosphere.2016.01.095.

13. Gibson, R.; Durán-Álvarez, J.C.; Estrada, K.L.; Chávez, A.; Jiménez Cisneros, B. Accumulation and Leaching Potential of Some Pharmaceuticals and Potential Endocrine Disruptors in Soils Irrigated with Wastewater in the Tula Valley, Mexico. *Chemosphere* 2010, *81*, 1437–1445, doi:10.1016/j.chemosphere.2010.09.006.

14. Baz-Lomba, J.A.; Salvatore, S.; Gracia-Lor, E.; Bade, R.; Castiglioni, S.; Castrignanò, E.; Causanilles, A.; Hernandez, F.; Kasprzyk-Hordern, B.; Kinyua, J.; et al. Comparison of Pharmaceutical, Illicit Drug, Alcohol, Nicotine and Caffeine Levels in Wastewater with Sale, Seizure and Consumption Data for 8 European Cities. *BMC Public Health* 2016, *16*, 1–11, doi:10.1186/s12889-016-3686-5.

15. Santos, L.H.M.L.M.; Araújo, A.N.; Fachini, A.; Pena, A.; Delerue-Matos, C.; Montenegro, M.C.B.S.M. Ecotoxicological Aspects Related to the Presence of Pharmaceuticals in the Aquatic Environment. *J. Hazard. Mater.* 2010, *175*, 45–95, doi:10.1016/j.jhazmat.2009.10.100.

16. Björkblom, C.; Högfors, E.; Salste, L.; Bergelin, E.; Olsson, P.; Katsiadaki, I.; Wiklund, T. Estrogenic and Androgenic Effects of Municipal Wastewater Effluent On ... *Environ. Toxicol. Chem.* 2009, *28*, 1063–1071.

17. Kostich, M.S.; Batt, A.L.; Lazorchak, J.M. Concentrations of Prioritized Pharmaceuticals in Effluents from 50 Large Wastewater Treatment Plants in the US and Implications for Risk Estimation. *Environ. Pollut.* 2014, *184*, 354–359, doi:10.1016/j.envpol.2013.09.013.

18. U. S. ENVIRONMENTAL PROTECTION AGENCY METHOD 527 DETERMINATION OF SELECTED PESTICIDES AND FLAME RETARDANTS IN DRINKING WATER BY SOLID PHASE EXTRACTION AND CAPILLARY COLUMN GAS CHROMATOGRAPHY/ MASS SPECTROMETRY (GC/MS) 2005, 1–44.

19. Mohsin, M.; Ahmad, A. Genetically-Encoded Nanosensor for Quantitative Monitoring of Methionine in Bacterial and Yeast Cells. *Biosens. Bioelectron.* 2014, *59*, 358–364, doi:10.1016/j.bios.2014.03.066.

20. Gao, H.; Generelli, S.; Heitger, F. Online Monitoring the Water Contaminations with Optical Biosensor. *Proceedings* 2017, *1*, 522, doi:10.3390/proceedings1040522.

21. Rodriguez-Mozaz, S.; Lopez de Alda, M.J.; Barceló, D. Advantages and Limitations

of On-Line Solid Phase Extraction Coupled to Liquid Chromatography-Mass Spectrometry Technologies versus Biosensors for Monitoring of Emerging Contaminants in Water. *J. Chromatogr. A* 2007, *1152*, 97–115.

22. Xu, F.; Zhen, G.; Yu, F.; Kuennemann, E.; Textor, M.; Knoll, W. Combined Affinity and Catalytic Biosensor: In Situ Enzymatic Activity Monitoring of Surface-Bound Enzymes. *J. Am. Chem. Soc.* 2005, *127*, 13084–13085, doi:10.1021/ja050818q.

23. van der Lelie, D.; Corbisier, P.; Baeyens, W.; Wuertz, S.; Diels, L.; Mergeay, M. The Use of Biosensors for Environmental Monitoring. *Res. Microbiol.* 1994, *145*, 67–74, doi:10.1016/0923-2508(94)90073-6.

24. Turner, A.P.F. Biosensors - Sense and Sensitivity. *Science (80-.).* 2000, *290*, 1315–1317.

25. Damborský, P.; Švitel, J.; Katrlík, J. Optical Biosensors. *Essays Biochem.* 2016, *60*, 91–100, doi:10.1042/EBC20150010.

26. Tereshchenko, A.; Bechelany, M.; Viter, R.; Khranovskyy, V.; Smyntyna, V.; Starodub, N.; Yakimova, R. Optical Biosensors Based on ZnO Nanostructures: Advantages and Perspectives. A Review. *Sensors Actuators, B Chem.* 2016, *229*, 664–677, doi:10.1016/j.snb.2016.01.099.

27. Islam, M.S.; Kouzani, A.Z.; Dai, X.J.; Michalski, W.P.; Gholamhosseini, H. Comparison of Performance Parameters for Conventional and Localized Surface Plasmon Resonance Graphene Biosensors. *Proc. Annu. Int. Conf. IEEE Eng. Med. Biol. Soc. EMBS* 2011, 1851–1854, doi:10.1109/IEMBS.2011.6090526.

28. Estevez, M.C.; Otte, M.A.; Sepulveda, B.; Lechuga, L.M. Trends and Challenges of Refractometric Nanoplasmonic Biosensors: A Review. *Anal. Chim. Acta* 2014, *806*, 55–73, doi:10.1016/j.aca.2013.10.048.

29. Thakur, A.; Qiu, G.; NG, S.P.; Guan, J.; Yue, J.; Lee, Y.; Wu, C.M.L. Direct Detection of Two Different Tumor-Derived Extracellular Vesicles by SAM-AuNIs LSPR Biosensor. *Biosens. Bioelectron.* 2017, *94*, 400–407, doi:10.1016/j.bios.2017.03.036.

30. Morales-Luna, G.; Herrera-Domínguez, M.; Pisano, E.; Balderas-Elizalde, A.; Hernandez-Aranda, R.I.; Ornelas-Soto, N. Plasmonic Biosensor Based on an Effective Medium Theory as a Simple Tool to Predict and Analyze Refractive Index Changes. *Opt. Laser Technol.* 2020, *131*, doi:10.1016/j.optlastec.2020.106332.

31. Hossain, M.B.; Rana, M.M. DNA Hybridization Detection Based on Resonance Frequency Readout in Graphene on Au SPR Biosensor. *J. Sensors* 2016, *2016*, doi:10.1155/2016/6070742.

32. Wu, L.; Jia, Y.; Jiang, L.; Guo, J.; Dai, X.; Xiang, Y.; Fan, D. Sensitivity Improved SPR Biosensor Based on the MoS2/Graphene-Aluminum Hybrid Structure. *J. Light. Technol.* 2017, *35*, 82–87, doi:10.1109/JLT.2016.2624982.

33. Ng, S.P.; Qiu, G.; Ding, N.; Lu, X.; Wu, C.M.L. Label-Free Detection of 3-Nitro-L-Tyrosine with Nickel-Doped Graphene Localized Surface Plasmon Resonance Biosensor. *Biosens. Bioelectron.* 2017, *89*, 468–476, doi:10.1016/j.bios.2016.04.017.

34. Fathi, F.; Rashidi, M.R.; Omidi, Y. Ultra-Sensitive Detection by Metal Nanoparticles-Mediated Enhanced SPR Biosensors. *Talanta* 2019, *192*, 118–127.

35. Jin, Y.; Wong, K.H.; Granville, A.M. Developing Localized Surface Plasmon Resonance Biosensor Chips and Fiber Optics via Direct Surface Modification of PMMA Optical Waveguides. *Colloids Surfaces A Physicochem. Eng. Asp.* 2016, *492*, 100–109, doi:10.1016/j.colsurfa.2015.11.025.

36. Zhao, Q.; Duan, R.; Yuan, J.; Quan, Y.; Yang, H.; Xi, M. A Reusable Localized Surface Plasmon Resonance Biosensor for Quantitative Detection of Serum Squamous Cell Carcinoma Antigen in Cervical Cancer Patients Based on Silver Nanoparticles Array. *Int. J. Nanomedicine* 2014, *9*, 1097–1104, doi:10.2147/IJN.S58499.

37. Cottat, M.; Thioune, N.; Gabudean, A.M.; Lidgi-Guigui, N.; Focsan, M.; Astilean, S.; Lamy de la Chapelle, M. Localized Surface Plasmon Resonance (LSPR) Biosensor for the Protein Detection. *Plasmonics* 2013, *8*, 699–704, doi:10.1007/s11468-012-9460-3.

38. Kim, S.; Lee, H.J. Gold Nanostar Enhanced Surface Plasmon Resonance Detection of an Antibiotic at Attomolar Concentrations via an Aptamer-Antibody Sandwich Assay. *Anal. Chem.* 2017, *89*, 6624–6630, doi:10.1021/acs.analchem.7b00779.

39. Hammond, J.L.; Formisano, N.; Estrela, P.; Carrara, S.; Tkac, J. Electrochemical Biosensors and Nanobiosensors. *Essays Biochem.* 2016, *60*, 69–80, doi:10.1042/EBC20150008.

40. Grieshaber, D.; MacKenzie, R.; Vörös, J.; Reimhult, E. Electrochemical Biosensors - Sensor Principles and Architectures. *Sensors* 2008, *8*, 1400–1458, doi:10.3390/s80314000.

41. Ronkainen, N.J.; Halsall, H.B.; Heineman, W.R. Electrochemical Biosensors. *Chem. Soc. Rev.* 2010, *39*, 1747–1763, doi:10.1039/b714449k.

42. Eggins, B. *Chemical Sensors and Biosensors*; John Wiley & sons, LTD: West Sussex, England, 2007; ISBN 9780470511305.

43. Pohanka, M.; Skládal, P. Electrochemical Biosensors - Principles and Applications. *J. Appl. Biomed.* 2008, *6*, 57–64, doi:10.32725/jab.2008.008.

44. Zhang, S.; Wright, G.; Yang, Y. Materials and Techniques for Electrochemical Biosensor Design and Construction. *Biosens. Bioelectron.* 2000, *15*, 273–282, doi:10.1016/S0956-5663(00)00076-2.

45. Kour, R.; Arya, S.; Young, S.-J.; Gupta, V.; Bandhoria, P.; Khosla, A. Review—

Recent Advances in Carbon Nanomaterials as Electrochemical Biosensors. *J. Electrochem. Soc.* 2020, *167*, 037555, doi:10.1149/1945-7111/ab6bc4.

46. Rivas, G.A.; Rubianes, M.D.; Rodríguez, M.C.; Ferreyra, N.F.; Luque, G.L.; Pedano, M.L.; Miscoria, S.A.; Parrado, C. Carbon Nanotubes for Electrochemical Biosensing. *Talanta* 2007, *74*, 291–307, doi:10.1016/j.talanta.2007.10.013.

47. Ge, S.; Yan, M.; Lu, J.; Zhang, M.; Yu, F.; Yu, J.; Song, X.; Yu, S. Electrochemical Biosensor Based on Graphene Oxide-Au Nanoclusters Composites for l-Cysteine Analysis. *Biosens. Bioelectron.* 2012, *31*, 49–54, doi:10.1016/j.bios.2011.09.038.

48. Zhang, W.; Wang, R.; Luo, F.; Wang, P.; Lin, Z. Miniaturized Electrochemical Sensors and Their Point-of-Care Applications. *Chinese Chem. Lett.* 2020, *31*, 589–600, doi:10.1016/j.cclet.2019.09.022.

49. Chambers, J.P.; Arulanandam, B.P.; Matta, L.L.; Weis, A.; Valdes, J.J. Biosensor Recognition Elements. *Curr. Issues Mol. Biol. 2008, Vol. 10, Pages 1-12* 2008, *10*, 1–12, doi:10.21775/CIMB.010.001.

50. Sarkar, A.; Sarkar, K.D.; Amrutha, V.; Dutta, K. An Overview of Enzyme-Based Biosensors for Environmental Monitoring. In *Tools, Techniques and Protocols for Monitoring Environmental Contaminants*; Elsevier, 2019; pp. 307–329 ISBN 9780128146798.

51. Zhu, Y.C.; Mei, L.P.; Ruan, Y.F.; Zhang, N.; Zhao, W.W.; Xu, J.J.; Chen, H.Y. Enzyme-Based Biosensors and Their Applications. In *Biomass, Biofuels, Biochemicals: Advances in Enzyme Technology*; Elsevier B.V., 2019; pp. 201–223 ISBN 9780444641144.

52. Miyai, K. Classification of Immunoassay. In *Principles and Practice of Immunoassay*; Palgrave Macmillan UK, 1991; pp. 246–264.

53. Wu, J.; Ju, H.X. Clinical Immunoassays and Immunosensing. *Compr. Sampl. Sample Prep.* 2012, *3*, 143–167, doi:10.1016/B978-0-12-381373-2.00071-5.

54. Zeng, X.; Shen, Z.; Mernaugh, R. Recombinant Antibodies and Their Use in Biosensors. *Anal. Bioanal. Chem.* 2012, *402*, 3027–3038, doi:10.1007/s00216-011-5569-z.

55. Parida, V.K.; Saidulu, D.; Majumder, A.; Srivastava, A.; Gupta, B.; Gupta, A.K. Emerging Contaminants in Wastewater: A Critical Review on Occurrence, Existing Legislations, Risk Assessment, and Sustainable Treatment Alternatives. *J. Environ. Chem. Eng.* 2021, *9*, 105966.

56. Comerton, A.M.; Andrews, R.C.; Bagley, D.M. Practical Overview of Analytical Methods for Endocrine-Disrupting Compounds, Pharmaceuticals and Personal Care Products in Water and Wastewater. *Philos. Trans. R. Soc. A Math. Phys. Eng. Sci.* 2009, *367*, 3923–3939, doi:10.1098/rsta.2009.0111.

57. Küster, A.; Adler, N. Pharmaceuticals in the Environment: Scientific Evidence of Risks and Its Regulation. *Philos. Trans. R. Soc. B Biol. Sci.* 2014, *369*.

58. Biel-Maeso, M.; Baena-Nogueras, R.M.; Corada-Fernández, C.; Lara-Martín, P.A. Occurrence, Distribution and Environmental Risk of Pharmaceutically Active Compounds (PhACs) in Coastal and Ocean Waters from the Gulf of Cadiz (SW Spain). *Sci. Total Environ.* 2018, *612*, 649–659, doi:10.1016/j.scitotenv.2017.08.279.

59. Al-Rajab, A.J.; Sabourin, L.; Lapen, D.R.; Topp, E. The Non-Steroidal Anti-Inflammatory Drug Diclofenac Is Readily Biodegradable in Agricultural Soils. *Sci. Total Environ.* 2010, *409*, 78–82, doi:10.1016/j.scitotenv.2010.09.020.

60. Acuña, V.; Ginebreda, A.; Mor, J.R.; Petrovic, M.; Sabater, S.; Sumpter, J.; Barceló, D. Balancing the Health Benefits and Environmental Risks of Pharmaceuticals: Diclofenac as an Example. *Environ. Int.* 2015, *85*, 327–333, doi:10.1016/j.envint.2015.09.023.

61. Schmidt, W.; O'Rourke, K.; Hernan, R.; Quinn, B. Effects of the Pharmaceuticals Gemfibrozil and Diclofenac on the Marine Mussel (Mytilus Spp.) and Their Comparison with Standardized Toxicity Tests. *Mar. Pollut. Bull.* 2011, *62*, 1389–1395, doi:10.1016/j.marpolbul.2011.04.043.

62. De Felice, B.; Copia, L.; Guida, M. Gene Expression Profiling in Zebrafish Embryos Exposed to Diclofenac, an Environmental Toxicant. *Mol. Biol. Rep.* 2012, *39*, 2119–2128, doi:10.1007/s11033-011-0959-z.

63. Hong, H.N.; Kim, H.N.; Park, K.S.; Lee, S.K.; Gu, M.B. Analysis of the Effects Diclofenac Has on Japanese Medaka (Oryzias Latipes) Using Real-Time PCR. *Chemosphere* 2007, *67*, 2115–2121, doi:10.1016/j.chemosphere.2006.12.090.

64. Ferrari, B.; Paxéus, N.; Giudice, R. Lo; Pollio, A.; Garric, J. Ecotoxicological Impact of Pharmaceuticals Found in Treated Wastewaters: Study of Carbamazepine, Clofibric Acid, and Diclofenac. *Ecotoxicol. Environ. Saf.* 2003, *55*, 359–370, doi:10.1016/S0147-6513(02)00082-9.

65. Dietrich, S.; Ploessl, F.; Bracher, F.; Laforsch, C. Single and Combined Toxicity of Pharmaceuticals at Environmentally Relevant Concentrations in Daphnia Magna – A Multigenerational Study. *Chemosphere* 2010, *79*, 60–66, doi:10.1016/J.CHEMOSPHERE.2009.12.069.

66. Schwaiger, J.; Ferling, H.; Mallow, U.; Wintermayr, H.; Negele, R.D. Toxic Effects of the Non-Steroidal Anti-Inflammatory Drug Diclofenac. Part I: Histopathological Alterations and Bioaccumulation in Rainbow Trout. *Aquat. Toxicol.* 2004, *68*, 141–150, doi:10.1016/j.aquatox.2004.03.014.

67. Triebskorn, R.; Casper, H.; Scheil, V.; Schwaiger, J. Ultrastructural Effects of Pharmaceuticals (Carbamazepine, Clofibric Acid, Metoprolol, Diclofenac) in Rainbow Trout (Oncorhynchus Mykiss) and Common Carp (Cyprinus Carpio). In

Proceedings of the Analytical and Bioanalytical Chemistry; Springer, February 10 2007; Vol. 387, pp. 1405–1416.

68. Triebskorn, R.; Casper, H.; Heyd, A.; Eikemper, R.; Köhler, H.R.; Schwaiger, J. Toxic Effects of the Non-Steroidal Anti-Inflammatory Drug Diclofenac: Part II. Cytological Effects in Liver, Kidney, Gills and Intestine of Rainbow Trout (Oncorhynchus Mykiss). *Aquat. Toxicol.* 2004, *68*, 151–166, doi:10.1016/j.aquatox.2004.03.015.

69. Togola, A.; Budzinski, H. Multi-Residue Analysis of Pharmaceutical Compounds in Aqueous Samples. *J. Chromatogr. A* 2008, *1177*, 150–158, doi:10.1016/j.chroma.2007.10.105.

70. aus der Beek, T.; Weber, F.A.; Bergmann, A.; Hickmann, S.; Ebert, I.; Hein, A.; Küster, A. Pharmaceuticals in the Environment-Global Occurrences and Perspectives. *Environ. Toxicol. Chem.* 2016, *35*, 823–835, doi:10.1002/etc.3339.

71. Kim, Y.; Choi, K.; Jung, J.; Park, S.; Kim, P.G.; Park, J. Aquatic Toxicity of Acetaminophen, Carbamazepine, Cimetidine, Diltiazem and Six Major Sulfonamides, and Their Potential Ecological Risks in Korea. *Environ. Int.* 2007, *33*, 370–375, doi:10.1016/j.envint.2006.11.017.

72. Erhunmwunse, N.O.; Tongo, I.; Ezemonye, L.I. Acute Effects of Acetaminophen on the Developmental, Swimming Performance and Cardiovascular Activities of the African Catfish Embryos/Larvae (Clarias Gariepinus). *Ecotoxicol. Environ. Saf.* 2021, *208*, 111482, doi:10.1016/j.ecoenv.2020.111482.

73. Parolini, M.; Binelli, A.; Cogni, D.; Provini, A. Multi-Biomarker Approach for the Evaluation of the Cyto-Genotoxicity of Paracetamol on the Zebra Mussel (Dreissena Polymorpha). *Chemosphere* 2010, *79*, 489–498, doi:10.1016/j.chemosphere.2010.02.053.

74. Solé, M.; Shaw, J.P.; Frickers, P.E.; Readman, J.W.; Hutchinson, T.H. Effects on Feeding Rate and Biomarker Responses of Marine Mussels Experimentally Exposed to Propranolol and Acetaminophen. In Proceedings of the Analytical and Bioanalytical Chemistry; Springer, October 18 2010; Vol. 396, pp. 649–656.

75. Montaseri, H.; Forbes, P.B.C. Analytical Techniques for the Determination of Acetaminophen: A Review. *TrAC - Trends Anal. Chem.* 2018, *108*, 122–134, doi:10.1016/j.trac.2018.08.023.

76. Anthérieu, S.; Le Guillou, D.; Coulouarn, C.; Begriche, K.; Trak-Smayra, V.; Martinais, S.; Porceddu, M.; Robin, M.-A.; Fromenty, B. Chronic Exposure to Low Doses of Pharmaceuticals Disturbs the Hepatic Expression of Circadian Genes in Lean and Obese Mice. *Toxicol. Appl. Pharmacol.* 2014, *276*, 63–72, doi:10.1016/J.TAAP.2014.01.019.

77. Gendloff, E.H.; Casale, W.L.; Ram, B.P.; Tai, J.H.; Pestka, J.J.; Hart, L.P. Hapten-Protein Conjugates Prepared by the Mixed Anhydride Method. Cross-Reactive

Antibodies in Heterologous Antisera. *J. Immunol. Methods* 1986, *92*, 15–20, doi:10.1016/0022-1759(86)90497-7.

78. Kamath, V.P.; Diedrich, P.; Hindsgaul, O. *Use of Diethyl Squarate for the Coupling of Oligosaccharide Amines to Carrier Proteins and Characterization of the Resulting Neoglycoproteins by MALDI-TOF Mass Spectrometry**; 1996; Vol. 13;.

79. Kumbhat, S.; Gehlot, R.; Sharma, K.; Singh, U.; Joshi, V. Surface Plasmon Resonance Based Indirect Immunoassay for Detection of 17β-Estradiol. *J. Pharm. Biomed. Anal.* 2019, *163*, 211–216, doi:10.1016/j.jpba.2018.10.015.

80. Calderón, A.; Meraz, M.; Tomasini, A. Pharmaceuticals Present in Urban and Hospital Wastewaters in Mexico City. *J. Water Chem. Technol.* 2019, *41*, 105–112, doi:10.3103/s1063455x19020073.

81. Oliveira, T.S.; Murphy, M.; Mendola, N.; Wong, V.; Carlson, D.; Waring, L. Characterization of Pharmaceuticals and Personal Care Products in Hospital Effluent and Waste Water Influent/Effluent by Direct-Injection LC-MS-MS. *Sci. Total Environ.* 2015, *518–519*, 459–478, doi:10.1016/j.scitotenv.2015.02.104.

82. Xue, C.S.; Erika, G.; Jiří, H. Surface Plasmon Resonance Biosensor for the Ultrasensitive Detection of Bisphenol A. *Anal. Bioanal. Chem.* 2019, *411*, 5655–5658, doi:10.1007/s00216-019-01996-8.

83. Rau, S.; Hilbig, U.; Gauglitz, G. Label-Free Optical Biosensor for Detection and Quantification of the Non-Steroidal Anti-Inflammatory Drug Diclofenac in Milk without Any Sample Pretreatment. *Anal. Bioanal. Chem.* 2014, *406*, 3377–3386, doi:10.1007/s00216-014-7755-2.

84. Okoth, O.K.; Yan, K.; Feng, J.; Zhang, J. Label-Free Photoelectrochemical Aptasensing of Diclofenac Based on Gold Nanoparticles and Graphene-Doped CdS. *Sensors Actuators, B Chem.* 2018, *256*, 334–341, doi:10.1016/j.snb.2017.10.089.

85. Schirmer, C.; Posseckardt, J.; Schröder, M.; Gläser, M.; Howitz, S.; Scharff, W.; Mertig, M. Portable and Low-Cost Biosensor towards on-Site Detection of Diclofenac in Wastewater. *Talanta* 2019, *203*, 242–247, doi:10.1016/j.talanta.2019.05.058.

86. Steinke, N.; Döring, S.; Wuchrer, R.; Kroh, C.; Gerlach, G.; Härtling, T. Plasmonic Sensor for On-Site Detection of Diclofenac Molecules. *Sensors Actuators, B Chem.* 2019, *288*, 594–600, doi:10.1016/j.snb.2019.02.069.

87. Mazouzi, Y.; Miche, A.; Loiseau, A.; Beito, B.; Méthivier, C.; Knopp, D.; Salmain, M.; Boujday, S. Design and Analytical Performances of a Diclofenac Biosensor for Water Resources Monitoring. *ACS Sensors* 2021, *6*, 3485–3493, doi:10.1021/acssensors.1c01607.

88. Ramírez-Cavazos, L.I.; Junghanns, C.; Ornelas-Soto, N.; Cárdenas-Chávez, D.L.; Hernández-Luna, C.; Demarche, P.; Enaud, E.; García-Morales, R.; Agathos, S.N.;

Parra, R. Purification and Characterization of Two Thermostable Laccases from Pycnoporus Sanguineus and Potential Role in Degradation of Endocrine Disrupting Chemicals. *J. Mol. Catal. B Enzym.* 2014, *108*, 32–42, doi:10.1016/j.molcatb.2014.06.006.

89. Hickey, D.P.; Lim, K.; Cai, R.; Patterson, A.R.; Yuan, M.; Sahin, S.; Abdellaoui, S.; Minteer, S.D. Pyrene Hydrogel for Promoting Direct Bioelectrochemistry: ATP-Independent Electroenzymatic Reduction of N 2. *Chem. Sci.* 2018, *9*, 5172–5177, doi:10.1039/c8sc01638k.

90. Najmaei, S.; Liu, Z.; Zhou, W.; Zou, X.; Shi, G.; Lei, S.; Yakobson, B.I.; Idrobo, J.-C.; Ajayan, P.M.; Lou, J. Vapor Phase Growth and Grain Boundary Structure of Molybdenum Disulfide Atomic Layers Vapour Phase Growth and Grain Boundary Structure of Molybdenum Disulphide Atomic Layers SUPPLEMENTARY INFORMATION. *Nat. Mater.* 2013, *12*, 754–759, doi:10.1038/NMAT3673.

91. Dominguez-Rovira, M.A.; Garcia-Garcia, A.; Toxqui-Teran, A. MX-a-2017-016742 Metodo Para La Obtencion de Cintas de Disulfuro de Molibdeno En Fase Gaseosa, a Partir de La Sulfuracion de Trioxido de Molibdeno 2017.

92. Moore, C.M.; Akers, N.L.; Hill, A.D.; Johnson, Z.C.; Minteer, S.D. Improving the Environment for Immobilized Dehydrogenase Enzymes by Modifying Nafion with Tetraalkylammonium Bromides. *Biomacromolecules* 2004, *5*, 1241–1247, doi:10.1021/bm0345256.

93. Meredith, S.; Xu, S.; Meredith, M.T.; Minteer, S.D. Hydrophobic Salt-Modified Nafion for Enzyme Immobilization and Stabilization. *J. Vis. Exp.* 2012, e3949, doi:10.3791/3949.

94. Mora, A.; Mahlknecht, J.; Rosales-Lagarde, L.; Hernández-Antonio, A. Assessment of Major Ions and Trace Elements in Groundwater Supplied to the Monterrey Metropolitan Area, Nuevo León, Mexico. *Environ. Monit. Assess.* 2017, *189*, 394, doi:10.1007/s10661-017-6096-y.

95. Spinelli, D.; Fatarella, E.; Di Michele, A.; Pogni, R. Immobilization of Fungal (Trametes Versicolor) Laccase onto Amberlite IR-120 H Beads: Optimization and Characterization. *Process Biochem.* 2013, *48*, 218–223, doi:10.1016/j.procbio.2012.12.005.

96. Fatarella, E.; Spinelli, D.; Ruzzante, M.; Pogni, R. Nylon 6 Film and Nanofiber Carriers: Preparation and Laccase Immobilization Performance. *J. Mol. Catal. B Enzym.* 2014, *102*, 41–47, doi:10.1016/j.molcatb.2014.01.012.

97. Pereira, A.S.; Tavares, P.; Limão-Vieira, P. *Radiation in Bioanalysis*; 2019; ISBN 9783030282462.

98. Qian, X.; Wang, X.; Zhong, J.; Zhi, J.; Heng, F.; Zhang, Y.; Song, S. Effect of Fiber Microstructure Studied by Raman Spectroscopy upon the Mechanical Properties of

Carbon Fibers. *J. Raman Spectrosc.* 2019, *50*, 665–673, doi:10.1002/jrs.5569.

99. Castellanos-Gomez, A.; Barkelid, M.; Goossens, A.M.; Calado, V.E.; Van Der Zant, H.S.J.; Steele, G.A. Laser-Thinning of MoS 2: On Demand Generation of a Single-Layer Semiconductor. *Nano Lett.* 2012, *12*, 3187–3192, doi:10.1021/nl301164v.

100. Windom, B.C.; Sawyer, W.G.; Hahn, D.W. A Raman Spectroscopic Study of MoS 2 and MoO 3: Applications to Tribological Systems. *Tribol. Lett.* 2011, *42*, 301–310, doi:10.1007/s11249-011-9774-x.

101. Zeng, J.; Jean, D.I.; Ji, C.; Zou, S. In Situ Surface-Enhanced Raman Spectroscopic Studies of Nafion Adsorption on Au and Pt Electrodes. *Langmuir* 2012, *28*, 957–964, doi:10.1021/la2035455.

102. Cai, R.; Abdellaoui, S.; Kitt, J.P.; Irvine, C.; Harris, J.M.; Minteer, S.D.; Korzeniewski, C. Confocal Raman Microscopy for the Determination of Protein and Quaternary Ammonium Ion Loadings in Biocatalytic Membranes for Electrochemical Energy Conversion and Storage. *Anal. Chem.* 2017, *89*, 13290–13298, doi:10.1021/acs.analchem.7b03380.

103. Sumayya, A.; Yohannan Panicker, C.; Varghese, H.T.; Harikumar, B. Vibrational Spectroscopic Studies and AB Initio Calculations of L-Glutamic Acid 5-Amide. *Rasayan J. Chem.* 2008, *1*, 548–555.

104. Baker, M.J.; Hussain, S.R.; Lovergne, L.; Untereiner, V.; Hughes, C.; Lukaszewski, R.A.; Thiéfin, G.; Sockalingum, G.D. Developing and Understanding Biofluid Vibrational Spectroscopy: A Critical Review. *Chem. Soc. Rev.* 2016, *45*, 1803–1818, doi:10.1039/c5cs00585j.

105. Movasaghi, Z.; Rehman, S.; Rehman, I.U. Raman Spectroscopy of Biological Tissues. *Appl. Spectrosc. Rev.* 2007, *42*, 493–541, doi:10.1080/05704920701551530.

106. Yang, S.; Hai, F.I.; Nghiem, L.D.; Price, W.E.; Roddick, F.; Moreira, M.T.; Magram, S.F.; Yanga, S.; Faisal I. Hai; Long D. Nghiem; et al. Understanding the Factors Controlling the Removal of Trace Organic Contaminants by White-Rot Fungi and Their Lignin Modifying Enzymes: A Critical Review. *Bioresour. Technol.* 2013, *141*, 97–108, doi:10.1016/j.biortech.2013.01.173.

107. Donarelli, M.; Ottaviano, L. 2D Materials for Gas Sensing Applications: A Review on Graphene Oxide, MoS2, WS2 and Phosphorene. *Sensors 2018, Vol. 18, Page 3638* 2018, *18*, 3638, doi:10.3390/S18113638.

108. Saraf, M.; Natarajan, K.; Saini, A.K.; Mobin, S.M. Small Biomolecule Sensors Based on an Innovative MoS2–RGO Heterostructure Modified Electrode Platform: A Binder-Free Approach. *Dalt. Trans.* 2017, *46*, 15848–15858, doi:10.1039/C7DT03888G.

109. Barua, S.; Dutta, H.S.; Gogoi, S.; Devi, R.; Khan, R. Nanostructured MoS2-Based

Advanced Biosensors: A Review. *ACS Appl. Nano Mater.* 2018, *1*, 2–25, doi:10.1021/ACSANM.7B00157/ASSET/IMAGES/MEDIUM/AN-2017-00157D_0030.GIF.

110. Rodríguez, M.C.; Rivas, G.A. Glassy Carbon Paste Electrodes Modified with Polyphenol Oxidase: Analytical Applications. *Anal. Chim. Acta* 2002, *459*, 43–51, doi:10.1016/S0003-2670(02)00088-0.

111. González-Sánchez, M.I.; Rubio-Retama, J.; López-Cabarcos, E.; Valero, E. Development of an Acetaminophen Amperometric Biosensor Based on Peroxidase Entrapped in Polyacrylamide Microgels. *Biosens. Bioelectron.* 2011, *26*, 1883–1889, doi:10.1016/j.bios.2010.03.024.

112. Economou, A. Enzymatic Biosensors. In; 2013; pp. 123–160.

113. Janata, J. *Principles of Chemical Sensors*; Springer US, 2009; ISBN 9780387699301.

114. Mross, S.; Pierrat, S.; Zimmermann, T.; Kraft, M. Microfluidic Enzymatic Biosensing Systems: A Review. *Biosens. Bioelectron.* 2015, *70*, 376–391.

115. Milton, R.D.; Wu, F.; Lim, K.; Abdellaoui, S.; Hickey, D.P.; Minteer, S.D. Promiscuous Glucose Oxidase: Electrical Energy Conversion of Multiple Polysaccharides Spanning Starch and Dairy Milk. *ACS Catal.* 2015, *5*, 7218–7225, doi:10.1021/acscatal.5b01777.

116. Ranjbakhsh, E.; Bordbar, A.K.; Abbasi, M.; Khosropour, A.R.; Shams, E. Enhancement of Stability and Catalytic Activity of Immobilized Lipase on Silica-Coated Modified Magnetite Nanoparticles. *Chem. Eng. J.* 2012, *179*, 272–276, doi:10.1016/j.cej.2011.10.097.

117. De Lima Citolino, L.V.; Braunger, M.L.; Oliveira, V.J.R.; Olivati, C.A. Study of the Nanostructure Effect on Polyalkylthiophene Derivatives Films Using Impedance Spectroscopy. *Mater. Res.* 2017, *20*, 874–881, doi:10.1590/1980-5373-MR-2016-0670.

118. RoyChoudhury, S.; Umasankar, Y.; Hutcheson, J.D.; Lev-Tov, H.A.; Kirsner, R.S.; Bhansali, S. Uricase Based Enzymatic Biosensor for Non-Invasive Detection of Uric Acid by Entrapment in PVA-SbQ Polymer Matrix. *Electroanalysis* 2018, *30*, 2374–2385, doi:10.1002/elan.201800360.

119. Banica, F.-G. *Chemical Sensors and Biosensors : Fundamentals and Applications*; John Wiley & Sons Inc, 2012; ISBN 0470710667.

120. Cernat, A.; Tertis, M.; Griveau, S.; Bedioui, F.; Sandulescu, R. New Modified Electrodes with HRP Immobilized in Polymeric Films for Paracetamol Analysis. *Farmacia* 2012, *60*, 1–12.

121. Cernat, A.; Griveau, S.; Richard, C.; Bedioui, F.; Săndulescu, R. Horseradish

Peroxidase Nanopatterned Electrodes by Click Chemistry: Application to the Electrochemical Detection of Paracetamol. *Electroanalysis* 2013, *25*, 1369–1372, doi:10.1002/elan.201300030.

122. Maghear, A.; Cristea, C.; Marian, A.; Marian, I.O.; Săndulescu, R. A Novel Biosensor for Acetaminophen Detection with Romanian Clays and Conductive Polymeric Films. *Farmacia* 2013, *61*, 1–11.

123. Calas-Blanchard, C.; Istamboulié, G.; Bontoux, M.; Plantard, G.; Goetz, V.; Noguer, T. Biosensor-Based Real-Time Monitoring of Paracetamol Photocatalytic Degradation. *Chemosphere* 2015, *131*, 124–129, doi:10.1016/j.chemosphere.2015.03.019.

124. Garcia, L.F.; Benjamin, S.R.; Antunes, R.S.; Lopes, F.M.; Somerset, V.S.; Gil, E. de S. Solanum Melongena Polyphenol Oxidase Biosensor for the Electrochemical Analysis of Paracetamol. *Prep. Biochem. Biotechnol.* 2016, *46*, 850–855, doi:10.1080/10826068.2016.1155060.

125. Antunes, R.S.; Garcia, L.F.; Somerset, V.S.; Gil, E. de S.; Lopes, F.M. The Use of a Polyphenoloxidase Biosensor Obtained from the Fruit of Jurubeba (Solanum Paniculatum L.) in the Determination of Paracetamol and Other Phenolic Drugs. *Biosensors* 2018, *8*, 1–11, doi:10.3390/bios8020036.

126. Brack, W.; Dulio, V.; Slobodnik, J. The NORMAN Network and Its Activities on Emerging Environmental Substances with a Focus on Effect-Directed Analysis of Complex Environmental Contamination. *Environ. Sci. Eur.* 2012, *24*, 29, doi:10.1186/2190-4715-24-29.

127. Fernández-Fernández, M.; Sanromán, M.Á.; Moldes, D. Recent Developments and Applications of Immobilized Laccase. *Biotechnol. Adv.* 2013, *31*, 1808–1825.

128. van den Brandhof, E.J.; Montforts, M. Fish Embryo Toxicity of Carbamazepine, Diclofenac and Metoprolol. *Ecotoxicol. Environ. Saf.* 2010, *73*, 1862–1866, doi:10.1016/j.ecoenv.2010.08.031.

129. Nunes, B.; Carvalho, F.; Guilhermino, L. Acute Toxicity of Widely Used Pharmaceuticals in Aquatic Species: Gambusia Holbrooki, Artemia Parthenogenetica and Tetraselmis Chuii. *Ecotoxicol. Environ. Saf.* 2005, *61*, 413–419, doi:10.1016/j.ecoenv.2004.08.010.

130. Brausch, J.M.; Connors, K.A.; Brooks, B.W.; Rand, G.M. Human Pharmaceuticals in the Aquatic Environment: A Review of Recent Toxicological Studies and Considerations for Toxicity Testing. *Rev. Environ. Contam. Toxicol.* 2012, *218*, 1–99.

131. Jacob, R.S.; de Souza Santos, L.V.; D'Auriol, M.; Lebron, Y.A.R.; Moreira, V.R.; Lange, L.C. Diazepam, Metformin, Omeprazole and Simvastatin: A Full Discussion of Individual and Mixture Acute Toxicity. *Ecotoxicology* 2020, *29*, 1062–1071, doi:10.1007/s10646-020-02239-8.

132. Li, Z.H.; Zlabek, V.; Velisek, J.; Grabic, R.; Machova, J.; Kolarova, J.; Li, P.; Randak, T. Acute Toxicity of Carbamazepine to Juvenile Rainbow Trout (Oncorhynchus Mykiss): Effects on Antioxidant Responses, Hematological Parameters and Hepatic EROD. *Ecotoxicol. Environ. Saf.* 2011, *74*, 319–327, doi:10.1016/j.ecoenv.2010.09.008.

133. Chen, H.; Gu, X.; Zeng, Q.; Mao, Z. Acute and Chronic Toxicity of Carbamazepine on the Release of Chitobiase, Molting, and Reproduction in Daphnia Similis. *Int. J. Environ. Res. Public Health* 2019, *16*, 209, doi:10.3390/ijerph16020209.

134. Bahlmann, A.; Weller, M.G.; Panne, U.; Schneider, R.J. Monitoring Carbamazepine in Surface and Wastewaters by an Immunoassay Based on a Monoclonal Antibody. *Anal. Bioanal. Chem.* 2009, *395*, 1809–1820, doi:10.1007/s00216-009-2958-7.

135. Tomii, S.; Takatori, T. Production and Characterization of Antibodies Reactive with Diazepam. *Japanese J. Clin. Chem.* 1984, *13*, 281–285, doi:10.14921/jscc1971b.13.5_281.

Curriculum Vitae

Marcela Herrera-Domínguez

+52 6182035203
marchem0116@gmail.com

Education

2019–Present PhD, *Tecnológico de Monterrey*, **Monterrey-Mexico,** *Engineering science*.

2017–2019 Master's, *Tecnológico de Monterrey*, **Monterrey-Mexico,** *Engineering sciences*.

2012–2017 Bachelor's, *Instituto Tecnológico de Durango*, **Durango-Mexico,** *Biochemical engineering*.

Research stays

2018 Brookhaven National Laboratory, *Upton, NY*.

Characterization of lymphoma-type cancer cell lines was performed by SEM microscopy. Sample preparation was done by critical point drying. The clean room facilities were used.

2021 University of California, Riverside, *Riverside, CA*.

Work was carried out on the development of biosensors for the detection of pharmaceuticals.

Publications

***Discrimination of radiosensitive and radioresistant murine lymphoma cells by Raman spectroscopy and SERS*, *Iris Aguilar-Hernández, Diana L Cárdenas-Chavez, Tzarara López-Luke, Alejandra García-García, Marcela Herrera-Domínguez, Ed- uardo Pisano, Nancy Ornelas-Soto*, Biomedical Optics Express, (2020) 388-405.**

***Plasmonic biosensor based on an effective medium theory as a simple tool to predict and analyze refractive index changes*, *Gesuri Morales-Luna, Marcela Herrera-Domínguez, Eduardo Pisano, Alejandro Balderas-Elizalde, Raul I Hernandez-Aranda, Nancy Ornelas-Soto*, Optics & Laser Technology, (2020) 106332.**

***Optical Biosensors and Their Applications for the Detection of Water Pollutants*,** *Marcela Herrera-Domínguez*, ***Gesuri Morales-Luna, Jürgen Mahlknecht, Quan Cheng, Iris Aguilar-Hernández, Nancy Ornelas-Soto*, Biosensors, (2023).**

***Detection of Acetaminophen in Groundwater by Laccase-Based Amperometric Biosensors Using MoS2 Modified Carbon Paper Electrodes*,** *Marcela Herrera-Domínguez*, ***Koun Lim, Iris Aguilar-Hernández, Alejandra García-García, Shelley D Minteer, Nancy Ornelas-Soto, Raúl Garcia-Morales*, Sensors, (2023).**

***Development of a surface plasmon resonance based immunosensor for diclofenac quantification in water*, *Marcela Herrera-Domínguez, Alexander S Lambert, Gesuri Morales-Luna, Eduardo Pisano, Iris Aguilar-Hernandez, Jürgen Mahlknecht, Quan Cheng, Nancy Ornelas-Soto*, Chemosphere, (2023).**

This document was typed in using Microsoft Word by Marcela Herrera Domínguez

biosensors

MDPI

Review

Optical Biosensors and Their Applications for the Detection of Water Pollutants

Marcela Herrera-Domínguez [1], Gesuri Morales-Luna [2], Jürgen Mahlknecht [1], Quan Cheng [3], Iris Aguilar-Hernández [1,*] and Nancy Ornelas-Soto [1,*]

[1] Tecnológico de Monterrey, Escuela de Ingeniería y Ciencias, Ave. Eugenio Garza Sada 2501, Monterrey 64849, Mexico
[2] Departamento de Física y Matemáticas, Universidad Iberoamericana, Prolongación Paseo de la Reforma 880, Mexico City 01219, Mexico
[3] Department of Chemistry, University of California, Riverside, CA 92521, USA
* Correspondence: iaguilarh@tec.mx (I.A.-H.); ornel@tec.mx (N.O.-S.)

Abstract: The correct detection and quantification of pollutants in water is key to regulating their presence in the environment. Biosensors offer several advantages, such as minimal sample preparation, short measurement times, high specificity and sensibility and low detection limits. The purpose of this review is to explore the different types of optical biosensors, focusing on their biological elements and their principle of operation, as well as recent applications in the detection of pollutants in water. According to our literature review, 33% of the publications used fluorescence-based biosensors, followed by surface plasmon resonance (SPR) with 28%. So far, SPR biosensors have achieved the best results in terms of detection limits. Although less common (22%), interferometers and resonators (4%) are also highly promising due to the low detection limits that can be reached using these techniques. In terms of biological recognition elements, 43% of the published works focused on antibodies due to their high affinity and stability, although they could be replaced with molecularly imprinted polymers. This review offers a unique compilation of the most recent work in the specific area of optical biosensing for water monitoring, focusing on both the biological element and the transducer used, as well as the type of target contaminant. Recent technological advances are discussed.

Keywords: optical biosensors; water pollutants; water monitoring; interferometers; resonators; SPR biosensor; fiber optic biosensors; emerging contaminants; heavy metals in water; waterborne pathogens

Citation: Herrera-Domínguez, M.; Morales-Luna, G.; Mahlknecht, J.; Cheng, Q.; Aguilar-Hernández, I.; Ornelas-Soto, N. Optical Biosensors and Their Applications for the Detection of Water Pollutants. *Biosensors* **2023**, *13*, 370. https://doi.org/10.3390/bios13030370

Received: 31 January 2023
Revised: 1 March 2023
Accepted: 2 March 2023
Published: 10 March 2023

1. Introduction

Detecting pollutants in water bodies accurately is crucial for quantifying their impact and developing tailored strategies to reduce their effects. Due to the variable complexity of environmental water samples, as well as the low concentrations at which some pollutants are found, so far chromatographic techniques are the gold standard for analytical detection [1,2]. However, biosensors have positioned themselves as a good alternative to these classical techniques. According to Markets and Markets, in 2021 the biosensors market was valued at USD 25.5 billion and is projected to reach USD 36.7 billion by 2026 [3].

Currently, biosensors primarily serve in the medical fields and life sciences, but their use has been extended to the food industry [4], biotechnology [5] and environmental monitoring [6], the latter which will be discussed in depth in this review. Biosensors are analytical devices that use biological recognition elements connected to transducers to generate a signal in response to a specific reaction between two elements [7]. This reaction is proportional to the concentration of chemical components present in the sample. There are numerous approaches to develop a biosensor, but overall, a biosensor can be classified as electrochemical, piezoelectric, optical, mechanical, and thermal, depending on the type of transducer used.

Optical biosensors stand out because they can provide valuable information about a sample (e.g., kinetic behavior, concentration, molecular interaction, etc.) while avoiding electrical or magnetic interference [8]. Moreover, optical biosensors are highly sensitive and can detect analytes even at attomolar [9] and femtomolar [10] concentrations. Despite the aforementioned advantages, electrochemical biosensors are still the most commercialized type of portable biosensor, mostly because they are easier to miniaturize.

The main challenges for the development of portable commercial optical biosensors are (a) device miniaturization, (b) stability of the biological recognition element, and (c) device reusability. Nevertheless, there are successful benchtop commercial optical biosensors used for drug discovery, small molecule, and therapeutic screening, among which the Biacore system and its iterations have been in production since around 2004 [11]. These biosensors are not commonly for environmental applications, although research advances could bring breakthroughs in this area.

Recently, optical sensors and biosensors have been developed that take advantage of the optical elements of smartphones to capture signals and transform them into measurable values. For example, high-resolution cameras allow for data acquisition, while exposure lights provide the sources of light excitation [12]. Hence, the optical characteristics of an image, such as color, luminescence, pixel counts, reflected light, and scattered light can be processed to obtain relevant information [13]. Smartphone-based optical sensors and biosensors use colorimetric [14], fluorescence [15] or bright-field imaging [16] as their detection principle; due to the complexity of this data, tools such as machine learning and deep learning are used for processing [12]. Within the biosensors that have been developed with this technology, most of them have been used for disease diagnosis [17] and point-of-care analysis [15]. However, their working principles can also be extended to environmental monitoring. For example, a smartphone has been used to detect the fluorescence emitted by labeled antibodies to quantify bisphenol A in lake and tap water [18]. Although further research is still required for the development of portable and accessible biosensors using this technology, the progress achieved so far represents a breakthrough in the miniaturization of optical devices and their potential use for on-site water monitoring.

The aim of this literature review is to analyze the most recent works published on the specific topic of optical biosensors for the detection of pollutants in water, since information is needed on fast, simple and in situ methodologies that can be used even by users without highly specialized training to increase their awareness of the type and concentration of pollutants found in water bodies and incentivize regulatory measures.

At present, review articles have been published on optical biosensors, but these are mostly focused on biomedical sensing applications such as biomarkers, disease detection [17] and point-of-care analysis [13]. Similarly, although to a lesser extent, biosensors have been used in the food industry [2].

Unlike the few reviews that broadly focus on biosensing water pollutants [19–21], this paper purposely excludes other types of biosensors such as electrochemical, mechanical, piezoelectric, etc., and instead seeks to expand the information pertaining exclusively to optical biosensors published in the last decade. Optical biosensors are highly promising for environmental analysis because of their versatility in terms of configuration and types of target samples and the fact that optical devices stand out from other types of transducers because of their immunity to external signals [22].

This review discusses recent advances in the development and application of optical biosensors for the environmental monitoring of water samples (freshwater and wastewater), focusing on the detection of pesticides, pharmaceuticals, microorganisms, toxins and heavy metals. A brief description of the main types of biological detection elements is given, as well as a discussion of their advantages and limitations. Subsequently, the different types of optical transducers currently available and their working principle are described, including some of the progress made in their different configurations. Next, papers from the last decade on the subject of optical biosensors for water monitoring are presented. Works are detailed, with an emphasis on each of the elements that conform the biosensor (i.e.,

transducer and biological element), specific type of sample (e.g., freshwater, wastewater) and analytical parameters.

2. Methods

The literature review was conducted using the following databases: Pubmed, ScienceDirect and Scopus. The search was delimited to last decade and the following search terms were used: "optical biosensors", "environmental monitoring", "water samples", "resonators", "interferometer", "grating biosensors", "SPR", "refractometers", "fiber optic biosensors", "immunoassay", "pharmaceuticals in water", "emerging contaminants", "heavy metals", "waterborne pathogens", "DNA biosensors", and "whole cell biosensors". A total of 46 original research articles were considered for analysis. Once the articles were collected, they were classified according to the type of contaminant detected. For each article the type of transducer used, the biological element, the analyte of interest and the type of water sample in which it was tested was identified.

3. Main Optical Biosensor Components

3.1. Biological Recognition Element

3.1.1. Enzymes

Enzymes are among the most used biomolecules in the development of biosensors. A main advantaged offered by enzymes is that their production can be easily scaled up [23]. Nonetheless, enzymatic activity can be affected by temperature and pH changes, and they are susceptible to denaturization. These challenges can be solved by immobilizing enzymes on substrates or trapping them in polymer networks [23]. An important part of the research and development of enzyme biosensors is focused on long-term stability and reproducibility studies [24].

3.1.2. Antibodies

Antibodies are a type of protein produced by the immune system to recognize and attack infections. In a biosensor, the chemical interaction between an antigen and an antibody produces a signal proportional to their concentration in the sample, which is then captured by a transducer [25]. Antibodies can be produced for any type of target molecule, including molecules with low molecular weights [26]. However, the affinity and specificity of an antibody can be affected during immobilization, impacting the overall biosensor performance [27].

3.1.3. DNA

Biosensors with DNA or RNA as the biological recognition elements are called genosensors. Genosensors can have high selectivity to interact with their complementary polymerase chains, and the sensitivity of the biosensor is improved by increasing the chain length of the genetic material [28]. These biosensors can be used to detect fractions of DNA/RNA or other types of biomolecules or chemical compounds [29].

Nucleic chains can be prepared using polymerase chain reaction (PCR), which is simple and does not involve the use of hazardous material [30]. Genosensors are limited by the number of molecules with which the genetic material can interact. In addition, hybridization processes can take days, hampering their use in commercial and real-time monitoring settings [30]. Therefore, most genosensors are developed for clinical applications.

3.1.4. Other

Other biological elements used in the development of biosensors include tissues, whole cells, non-enzymatic proteins, and fatty acids.

As the name implies, whole-cell biosensors use the entire cell as a recognition element rather than isolated or purified components (e.g., enzymes, nucleic acids). Using the whole cell as a recognition element can decrease biosensor specificity and slows down the response time [31]. Still, they can interact with various types of target compounds and

are versatile when integrated into different device configurations [32]. For example, the non-enzymatic proteins ERα and ERβ estrogen have been used not only for the detection of their target hormones [33], but also to target endocrine disrupting compounds in water [34]. Other examples are the use of lectins from Concanavalin A for pathogen detection [35], and stearic acid as a recognition element for copper [36].

In recent decades, whole-cell bioreporters (WCBs) have emerged as a low cost, high specificity, high sensitivity, and rapid alternative to biological receptors. These are living microorganisms with chromosomes or plasmids that have a regulatory promoter and a promoterless reporter either naturally present in the cells or added by genetic modification [37]. The protein encoding the reporter gene produces detectable signals when the regulatory promoter is active or repressed by a particular chemical or environmental stress [37]. WCBs are divided into class I, II and III based on which parameters are detected and how they are transformed into a measurable signal: those that react specifically to a type of target compound by increasing the output signal (class I), those that react specifically to stress conditions by increasing the output signal (class II), and those that react specifically to compounds or stress by decreasing the output signal (class III) [38]. WBCs have been shown to have excellent suitability for use in biosensors for water monitoring. Class I are the most widely employed for the detection of contaminants in water, although Class II and III have also been used to a lesser extent [39].

Molecularly imprinted polymers (MIP) are synthetic receptors in which specific recognition sites are formed via synthesis with a target template [40]. The resulting MIP is therefore capable of selectively recognizing the target analyte in the template-derived sites. MIPs have been developed to overcome the stability limitations affecting enzymes, as well as the high cost of producing antibodies.

3.1.5. Comparison of Biological Elements for Optical Sensors Monitoring Water Quality

Table 1 compares the main biological recognition elements in terms of their affinity for an analyte, specificity, sensibility, stability, versatility, and cost.

Table 1. Comparison between different biological recognition elements.

Biological Element	Affinity	Specificity	Sensibility (LOD, ng L^{-1})	Stability	Versatility	Cost
Enzyme	High	Medium/high	12,000–1 × 10^{-4}	Medium/low	High	Low
Antibody	High	High	250–0.07 × 10^{-6}	High	High	High
DNA/RNA	Very High	Very high	4.14–4.4 × 10^{-3}	High	Low	Low
Cell	Medium	Medium	2900–0.5	High	Medium	Low
MIP	High	High	1900–0.08	High	High	Low

Enzymes were classified as medium to high specificity (Table 1) as some enzymes can react with molecules that have similar structures to their substrate, so their use can be expanded to more than one target molecule. In water monitoring, this medium/high specificity can be exploited for the simultaneous detection of more than one pollutant. For example, the enzymatic detection of pesticides has been performed via acetylcholinesterase [41,42], halogenated compounds have been detected using haloalkane dehalogenases [43,44] and acid phosphatase has been used for heavy metals [45]. Despite this, according to our literature review, enzymes represent only 12% of the biological material used in the development of optical biosensors for water quality.

According to the data collected in this review, 42% of biosensors use antibodies as their recognition element. Antibodies are the preferred recognition element used for the detection of emerging pollutants such as pesticides [46], pharmaceuticals [47], and miscellaneous organic compounds [48,49]. They have also been used for monitoring pathogenic microorganisms [50] and toxins [51].

In the case of genetic material, as is well known, nucleic bases bind only adenine-thymine and cytokine-guanine. The combinations of these base pairs make DNA the receptor with the highest affinity and selectivity. However, this also limits their versatility

and their potential applications in water quality. So far, DNA-based biosensors have been employed for the detection of pathogenic microorganisms and heavy metals in water, the latter of which is due to their mutagenic capacity on DNA. Genosensors have also been developed for detecting organic compounds such as bisphenol A [52], and Kim et al. developed a biosensor combining an aptamer with antibodies for the detection of tetracycline [53].

As for cells, being a complete system allows them to interact with more than one molecule, which detracts from their specificity but adds versatility. Cells have been shown to be able to detect different types of contaminants in water. So far, yeasts cells, microalgae and bacteria have contributed to the detection of pharmaceuticals [54], pesticides [55], and heavy metals in water [56].

MIPs can have high affinity and specificity and have the advantage of being more stable and having a low cost compared to natural receptors [57]. Their main uses in water quality biosensors are in the detection of emerging pollutants, mainly in pharmaceuticals, and MIPs have been shown to have detection limits close to those of antibodies [47,58]. Research and development of MIPs is emerging, but they could be a viable alternative for the mass production and commercialization of biosensors in the future.

In Table 1, sensitivity was considered as a function of the limit of detection (LOD). LOD ranges in terms of ng L^{-1} were obtained from the articles discussed in this review. It is important to note that for each biological element, these limits are variable and depend on the type of transducer employed in the biosensor. For example, in the case of enzymes, the reached upper limit (Table 1, 12,000 ng L^{-1}) corresponds to a fluorescence-based biosensor, while the lower limit is for a resonator (Table 1, 1×10^{-4} ng L^{-1}). This shows that both the biological element and the transducer have a direct impact on the final performance of the biosensor, so choosing the right components is critical.

3.2. Optical Transducer

3.2.1. Interferometer

Interferometry is based on the superposition of a pair of light beams with different optical paths (space or dielectric media acting as waveguides) to generate controlled interferences. Interferometry is able to determine changes in the thickness or refractive index of a surface; any change in the refractive index of the bulk or adsorption of a biocoating induces changes in the intensity or phase of the resulting signal [59]. The light beams must be coherent with each other; in other words, they must come from the same source, be monochromatic and have the same frequency. Because of the interference produced, there is a change in the intensity of the resulting light, which depends on the optical path of the beams [60]. The first configurations used in the development of interferometers were by Mach-Zehnder and Young. Other configurations for interferometers are the Fabry-Perot Interferometer (FPI), the Exposed-Core microstructured optical fiber (ECF) and Reflectometric Interference Spectroscopy (RIfS).

Different interferometers have been designed for water monitoring. For example, Yaghoubi et al. used an interferometer based on RIfS (Figure 1), whose performance was improved using the Fourier transform (RIFTS). The work describes how they use porous silicon (PSi) substrates functionalized with lectins for the detection of *S. aureus* and *E. coli*, two pathogenic microorganisms commonly found in drinking water [35].

3.2.2. SPR and LSPR

Surface Plasmon Resonance (SPR) is a phenomenon which occurs when the free electrons of a metal are excited by photons, creating an evanescent wave. This is useful for monitoring changes in the refractive index since the evanescent wave is highly sensitive to changes in the vicinity of the surface [61]. SPR occurs only at the nanometer scale in metals (gold and silver are preferred) and are divided into two types: Localized Surface Plasmon Resonance (LSPR) when the phenomenon occurs in metallic nanoparticles and SPR when it occurs in a metallic film [62]. The plasmon generated depends directly on the size of

the nanoparticle or metal film and the material used. As for the material, it is known that from the physical point of view, silver is better since its plasmon is more intense. However, gold is more used because it is chemically inert [63]. One way to take advantage of the characteristics of each material is the use of multilayers or core-shell nanoparticles. It has been shown that metallic multilayer sensors have a wider measuring range and also an improvement in sensitivity compared to single-layer sensors [64]. Examples of the use of more than one metal in SPR substrates are the Ti/Ag/Au combination [64] and the triple layer composed of Au/Ag/Au [65]. In terms of size, the intensity of the plasmon varies according to the thickness of the metal layer or the diameter of the nanoparticles. For SPR propagation, it has been shown that a thickness of 40 nm generates the highest plasmon intensity, while for nanoparticles, the smaller the diameter, the lower the intensity [66].

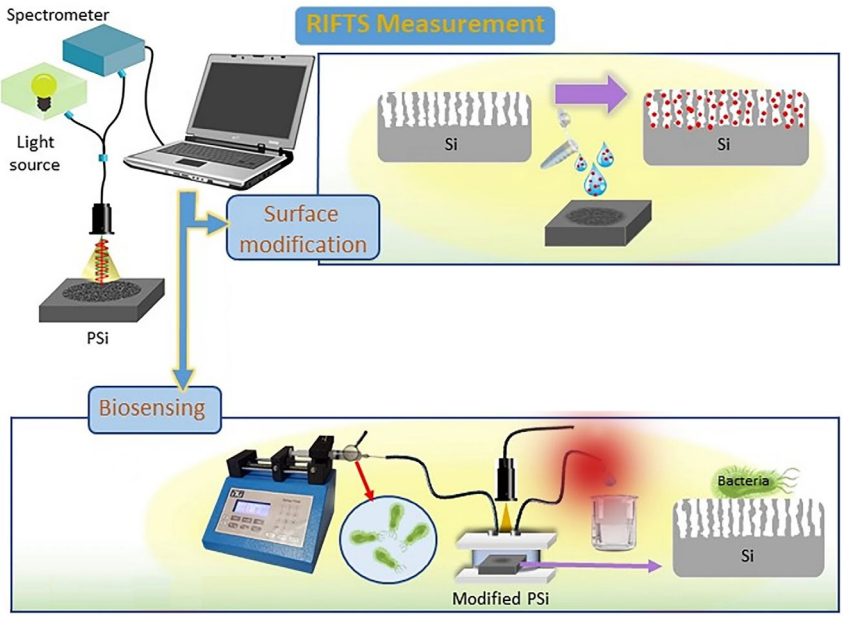

Figure 1. Schematic representation of a reflective interferometric Fourier transform spectroscopy (RIFTS) set up. During surface modification, analyte molecules enter the Si pores. Biosensing monitoring of a bacterial suspension is carried out in a fluidic system. Reproduced from [35].

The simplest SPR/LSPR biosensor includes only a gold layer [67,68]. Nevertheless, recently, the use of multilayers has been implemented, and such is the case of graphene, as this material has gathered interest for the development of SPR biosensors due to its optical and electrical properties. Incorporation of graphene to the SPR biosensors can be achieved via simple methodologies such as the addition of a layer of this material on the gold [69] or more complex arrangements such as the MoS2/Al/MoS2-graphene hybrid structure proposed by L. Wu et al. [70].

One of the benefits of LSPR is the wide variety of nanoparticle geometries available. Optical properties of nanoparticles depend on their size and shape; thus, tailoring these properties can improve the performance of the biosensor. A nanoparticle's SPR can be modified throughout visible and near-infrared (NIR) wavelengths by changing its size, shape, or aspect ratio [71]. For example, spherical and rod nanoparticles have different optical properties and generate varying signal intensities; the surface plasmon shifts from the visible to the NIR region when the shape of nanoparticles is changed from spherical to rod [72]. In addition, nanoparticles with sharp tips such as triangles, stars, or pyramids show higher sensitivity towards refractive index changes and larger near-field enhancements [71]. Gold nanostars with branches and projecting tips have the plasmon in the NIR wavelength. In this case, LSPR signal intensity is proportional to the size of the tips, which improves the local electromagnetic fields significantly and results from the hybridization

of the central core and tips plasmon resonance [73]. The most common nanoparticles are spherical, although there are also triangular, cubes, nanorods and nanostars. For use in SPR sensors, gold is preferred due to its biocompatibility, although silver or copper are also employed.

One of the most recent applications of plasmons is the use of surface plasmon coupled emission (SPCE), which improves the emitted fluorescence signal. Its operation is based on the near-field interaction of the fluorophore and the surface plasmon of the metal. It has remarkable optical qualities, such as high directivity, distinct polarization, wavelength resolution and background suppression. SPCE-based fluorescence is highly sensitive in the context of sensing and imaging [74], and has been successfully employed in optical sensors for detecting tannic acid in water, reaching detection limits at the picomolar scale [75]. Therefore, this is a promising technology that could improve the sensitivity of the environmental biosensors discussed herein.

3.2.3. Optical Resonators

Optical resonators are a type of device in which photons are confined to a certain space. Once confined, the photons accumulate intensity due to interference, which in turn amplifies the signal [76]. When confined, light interacts with itself in a cavity, and only certain optical frequencies can be sustained without incurring significant losses. These are the so-called resonance frequencies. The microcavity functions as a transducer of optical signals and changes in the cavity alter the resonance parameters, which are converted into a change in light intensity [77]. In optical resonators, the sample interacts with light multiple times, which improves detection limits [76]. The Q factor is widely used in the evaluation of a resonator. This parameter describes the behavior of the resonator and is directly related to its geometry and material. The Q-factor has a critical role in determining the magnitude of the resonance shift and the resulting biosensing capacity. A larger cavity has a higher Q-factor. The Q factor of a smaller cavity is lower, but the resonance shift is higher [77].

This type of biosensors is developed in two configurations: Fabry–Perot resonators and ring resonators. The latter are the most common and consist of a circular structure (e.g., a micro-sphere, micro-disk, or micro-toroid), where the light is confined. Resonator biosensors can be found in arrangements such as silicon-on-isolator (SOI) [78], opto-fluidic ring resonator (OFRR) [79], subwavelength grating (SWG) [80] and whispering gallery mode (WGM) [81].

SOI are devices in which the ring is made of silicon. Due to the high refractive index of silicon, the optical modal field is strongly located near the surface of the waveguide, resulting in a high response to surface disturbances [78]. OFRR consists of a microtube that is functionalized on the inside, while a light source is outside. The main advantage of OFRR is that multiple analytes can be detected simultaneously; in addition, the amount of sample to be used is small and the results are very accurate [79]. SWG consists of silicon columns that are in the direction of propagation with a sub wavelength. One of the advantages of SWG is that the effective detection area is increased because in addition to the surface of the waveguide, the space between the silicon columns is also available. SWG offers a higher sensitivity and increased detection surface area and improves the overlap of biomolecules on the surface of the waveguide; that is, the sensitivity on the surface is high despite the accumulation of biomolecules [80]. WGM are found in the cavity as a result of total reflection at the exterior cavity contact. It has a low internal loss and, hence, a weakly constrained near-field, yet a greatly elevated Q factor [81].

Currently, resonators are scarcely used in the detection of water pollutants. Figure 2 illustrates the work by Duan et al., in which liquid crystal microdroplets doped with stearic acid and LC 4-cyano-4′-pentylbiphenyl (5CB) were employed in WGM resonators for the detection of copper in drinking water [36].

high despite the accumulation of biomolecules [80]. WGM are found in the cavity as a result of total reflection at the exterior cavity contact. It has a low internal loss and, hence, a weakly constrained near-field, yet a greatly elevated Q factor [81].

Currently, resonators are scarcely used in the detection of water pollutants. Figure 2 illustrates the work by Duan et al., in which liquid crystal microdroplets doped with stearic acid and LC 4-cyano-4′-pentylbiphenyl (5CB) were employed in WGM resonators for the detection of copper in drinking water [36].

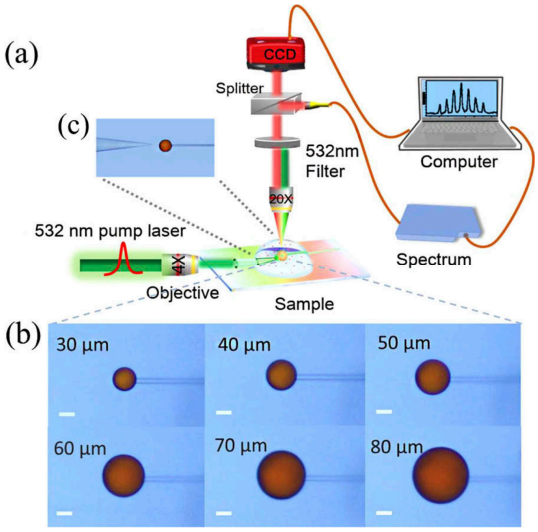

Figure 2. (**a**) Schematic diagram of the whispering gallery mode (WGM) experimental platform. (**b**) Micrographs of the stearic acid-doped 5CB microdroplets with different diameters. (**c**) Micrograph of microdroplet excited by a fiber tip positioned correctly within its vicinity. Reproduced from [36].

3.2.4. Gratings

Gratings are structures that are deposited on a specific surface in varying and periodic patterns. The presence of these structures results in a change in the refractive index [82]. The diffraction effect dominates if the index variation has a period greater than the wavelength of light within the grating. Otherwise, light propagation through the grating will displays characteristics similar to those of the uniform medium, which will become increasingly pronounced as the period of the grating decreases [82]. The grating coupler can be a surface array, in which the light is coupled in the direction of the index variation if the index varies only in one direction. Alternatively, the array can be a subwavelength grating (SWG), which is a grating whose period is small enough to suppress diffraction effects [82]. Gratings are used for biosensing by measuring the attenuation efficiency of the analytes in solution. Detection can also be carried out by measuring the angle of diffraction efficiency. These approaches are used in diffraction grating sensors and in grating waveguide sensors, respectively [83]. If the refractive index varies only in one direction, light is coupled in the direction of the index variation.

Optical gratings are easily coupled to other types of devices to improve their performance. For example, Liu et al. used a grating-coupled SPR to detect environmental estrogen (EE) in tap and bottled water [34]. As shown in Figure 3, SPR was carried out on a tilted fiber Bragg gratings (TFBG), obtaining different additional resonance mechanisms, which were at wavelengths close to the near-IR. Resolution of the refractive index was improved by overlapping with the plasmon. In this biosensor, an estradiol-streptavidin conjugate was used as a recognition element.

3.2.5. Fiber Optic

Among the advantages offered by fiber optics (FO) are immunity to electrostatic and electromagnetic interference, good biological compatibility, corrosion resistance and easy installation and operation [84,85]. Due to these characteristics, it is possible to find resonators, interferometers and SPRs developed with this material. However, by itself, fiber optics are also excellent materials, with optical properties that allow the detection of compounds. The simplest design of a fiber optics biosensor is to immobilize the biological elements in the coating; another option is to add subsequent layers to the coating that improve the performance of the biosensor.

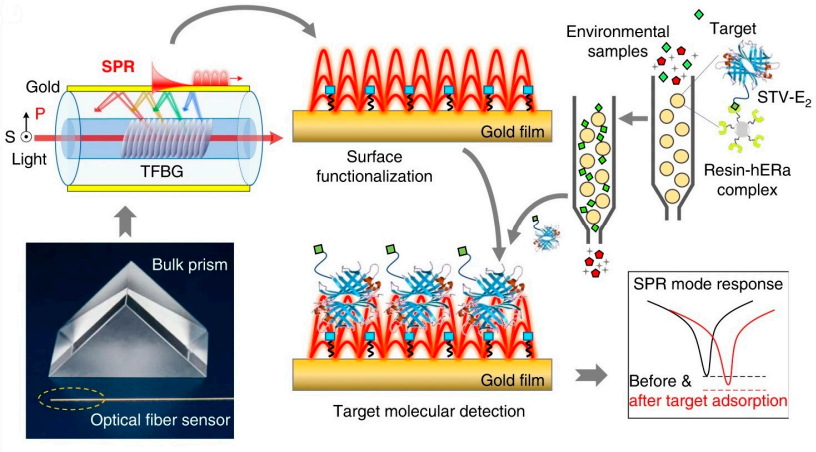

Figure 3. Plasmonic gold film coated TFBG-based SPR biosensor for ultrasensitive estrogen (EE) detection. Reproduced from [34].

3.2.5. Fiber Optics

Among the advantages offered by fiber optics (FO) are immunity to electrostatic and electromagnetic interference, good biological compatibility, corrosion resistance and easy installation and operation [84,85]. Due to these characteristics, it is possible to find resonators, interferometers and SPRs developed with this material. However, by itself, fiber optics are also excellent materials, with optical properties that allow the detection of compounds. The simplest design of a fiber optics biosensor is to immobilize the biological elements in the coating, another option is to add subsequent layers to the coating that improve the performance of the biosensor.

Among the different fluorescence parameters that can be measured for biosensing are the following: (1) Intensity measures the spontaneous emission (fluorescence) after molecular excitation. The intensity of the light emitted at the analytical wavelength is directly related to the concentration of the fluorophore [87]. (2) Luminescence lifetime is the reciprocal of the rate constant of the emission decay that occurs when the luminophore is "instantaneously" excited by a flash of light. Lifetime measurements can be performed using a pulse of radiation with a width that is generally less than the luminophore's decay period [88]. (3) Fluorescence quenching refers to any bi-molecular interaction that decreases the fluorescence intensity of the fluorophore molecule. One of the most problematic aspects of fluorometry is the high level of environment-dependent quenching. Nevertheless, if the fluorophore is the analyte, what was before considered a nuisance has now become a key use of fluorescence-based biosensors [87]. Finally, (4) Förster Resonance Energy Transfer (FRET) is a form of fluorescence quenching that happens when two distinct species—one (a donor) with a fluorescence spectrum that overlaps the excitation spectrum of the other (the acceptor)—are close enough to one other [52]. As a result, the radiation-excited donor can transfer energy non-radiatively to the acceptor, partially quenching the former's fluorescence intensity, regardless of whether the acceptor is fluorescent or not. Thanks to this diversity of quantification methods, it is possible to increase the performance of biosensors in several ways.

3.2.6. Fluorescence

Fluorescence is one of the most utilized transducers in biosensors [31]. Fluorescent materials can be used as sensing probes due to their ability to change their intrinsic fluorescence properties when interacting with other elements. The changes that occur during bio-recognition events are easily transformed into signals that are captured using different transducers [86]. Fluorescent biosensors can be constructed by measuring the intrinsic fluorescence of either the target molecule or the biological recognition element. Materials such as quantum dots (QD) can also be added to improve the fluorescence of the sensor [86].

Among the different fluorescence parameters that can be measured for biosensing are the following: (1) Intensity measures the spontaneous emission (fluorescence) after molecular excitation. The intensity of the light emitted at the analytical wavelength is directly related to the concentration of the fluorophore [87]. (2) Luminescence lifetime is the reciprocal of the rate constant of the emission decay that occurs when the luminophore is "instantaneously" excited by a flash of light. Lifetime measurements can be performed using a pulse of radiation with a width that is generally less than the luminophore's decay period [88]. (3) Fluorescence quenching refers to any bi-molecular interaction that decreases the fluorescence intensity of the fluorophore molecule. One of the most problematic aspects of fluorometry is the high level of environment-dependent quenching. Nevertheless, if the fluorophore is the analyte, what was before considered a nuisance has now become a key use of fluorescence-based biosensors [87]. Finally, (4) Förster Resonance Energy Transfer (FRET) is a form of fluorescence quenching that happens when two distinct species—one (a donor) with a fluorescence spectrum that overlaps the excitation spectrum of the other (the acceptor)—are close enough to one other [52]. As a result, the radiation-excited donor can transfer energy non-radiatively to the acceptor, partially quenching the former's fluorescence intensity, regardless of whether the acceptor is fluorescent or not. Thanks to this diversity of quantification methods, it is possible to increase the performance of biosensors in several ways.

3.2.7. Comparison of Transducers Used in Optical Sensors for Monitoring Water Quality

Among the works for the detection of contaminants in water (analyzed herein, biosensors based on interferometry stand out. These types of biosensors have allowed for the detection of pesticides, pharmaceuticals, and pathogenic microorganisms, where most achieve LOD (below 1 µg/L).

Another advantage of SPR-based biosensors is their relatively simple configuration, i.e., they do not incorporate any other elements besides gold and the biological receptor. However, additional layers can be added to methods, it is possible to increase the performance of biosensors in several ways.

plasmon, allowing considerable signal and sensitivity improvement. One of the benefits of LSPR is that it allows us to experiment with different types, materials, and geometries of nanoparticles. An example of an LSPR biosensor for the detection of contaminants in water is the one developed by Kim and Lee in which gold nanostars are used in conjunction with a combination of aptamers and antibodies for the detection of an antibiotic [53]. In general, SPR and LSPR biosensors have low detection limits below 1 µg/L.

Resonators are not commonly used in the detection of water pollutants, as only two works with these types of biosensors were found, specifically for the detection of pesticides and heavy metals. Both works employed a whispering gallery mode configuration and reached LODs of 0.001 ug/L. In a similar manner, grating couplers are not as common in the development of water quality biosensors. However, there are two examples of their use for the detection of pathogens [50] and pesticides [6], and have also been shown to have low detection limits, being comparable to those mentioned above.

Some examples of fiber optic biosensors used in water quality are the tapered fiber optic designed by Arjmand et al. for pesticide detection [41] and the U-bent developed by Lamarca et al. for antibiotic detection [47]. Both have simple designs, which is an advantage for commercialization, and both have low LODs.

Finally, the use of fluorescence has been extended to all types of analytes, pesticides, pharmaceuticals, microorganisms, heavy metals, and organic compounds. In general, fluorescence biosensors have high LODs, with the lowest being ten to thousands of ug/L. To achieve LODs that compete with other biosensors, it has been necessary to replace traditional fluorometers with more efficient devices. Such is the case of the biosensors designed by Liu et al., in which FO and planar waveguides are used [89]. Another example is the biosensor based on Förster resonance energy transfer, which was also functionalized with graphene [52]. These devices were able to decrease the LOD down to 0.001 ug/L.

4. Detection of Selected Water Pollutants

4.1. Pesticides

Due to their frequent use in cultivation, pesticides reach surface and groundwater bodies during irrigation and precipitation. For example, Atrazine is one of the most ubiquitous pesticides, as its slow degradation makes it persistent, and its presence has been detected in water bodies worldwide [90]. Atrazine is also an endocrine-disrupting compound (EDC) that affects the sexual development of fishes, amphibians, reptiles, and mammals [91]. In addition to atrazine, organophosphate compounds have toxic effects at the neuronal level [92].

Recent research for quantifying pesticides in water via optical biosensors employ different approaches. For example, a fluorescence biosensor with a planar waveguide-based array immunosensor (PWAI) was designed to be able to analyze multiple samples in a single measurement. This biosensor uses a planar waveguide that disperses light into different individual channels (see Figure 4), and detection is performed using fluorophore-labeled antibodies. One of the analytes tested was 2,4-dichlorophenoxyacetic acid (2,4-D), a commonly used herbicide, for which a limit of detection (LOD) of 7.53 µg/L was obtained [89].

Whole cells (i.e., encapsulated algae) have been used to measure chlorophyll fluorescence differences in the cells when exposed to pesticides. Tests were conducted with three different types of algae and three different pesticides, and the best result was a limit of detection of 10 µg/L [55]. Additionally, Scognamiglio et al. [90] presented an alternative whole-cell biosensor, where photosynthetic algae were immobilized on a paper base sensor to measured changes in fluorescence. This biosensor was used for the detection of atrazine, and an LOD of 80 ng/mL was obtained, proving it to be an efficient and sustainable biosensor thanks to the manufacturing materials.

detection of 10 µg/L [55]. Additionally, Scognamiglio et al. [90] presented an alternative whole-cell biosensor, where photosynthetic algae were immobilized on a paper base sensor to measured changes in fluorescence. This biosensor was used for the detection of atrazine, and an LOD of 80 ng/mL was obtained, proving it to be an efficient and sustainable biosensor thanks to the manufacturing materials.

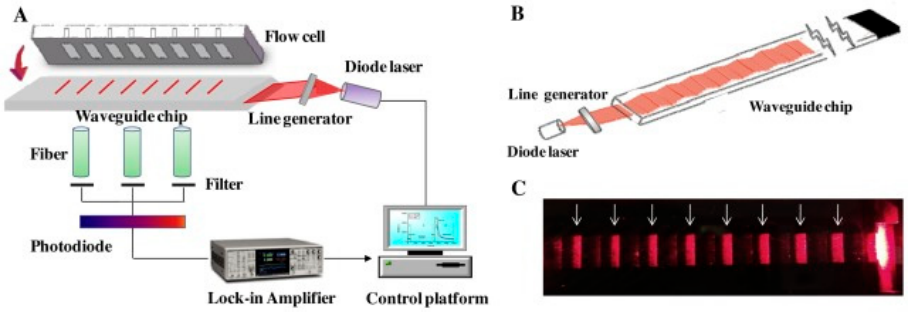

Figure 4. Schematic diagram of (**A**) a prototype array fluorescent biosensor PWAI with a removable multi-channel PDMS flow cell; (**B**) excitation light path inside the planar waveguide transducer; (**C**) photograph of waveguide chip with eight biosensing areas indicated by white arrows. Reproduced from [89].

A different approach is the use of grating couplers complemented by an immunoassay; this study was performed using atrazine as the target molecule resulting in an LOD of 0.05 µg/L [6]. Arimand et al. [41] employed a tapered fiber optic enzyme biosensor for the detection of methyl-parathion, a highly toxic pesticide. With this approach, an LOD of 63.17 ng/L was obtained.

A research group in Greece developed an immunosensor with a simple arrangement to measure interference, and chlorpyrifos, thiabendazole and imazalil were simultaneously detected in water and wine samples. The results obtained were of LODs between 30–40 pg/mL [93]. Subsequently, the same methodology was used to detect atrazine and paraquat, with LODs of 0.04 ng/mL and 0.05 ng/mL, respectively [94].

A liquid crystal resonator has been developed for the detection of pesticides through the presence of enzymes and their inhibitors. This biosensor was tested with two analytes, and the limit of detection reached was 0.1 pg/mL for phenobucarb and 1 pg/mL for dimethoate [42]. More recently, an interferometer was developed for the detection of fenitrothion; this biosensor was based on bimodal waveguides and, using an immunoassay, was able to obtain an LOD of 0.29 ng/mL [46].

As observed in Table 2, most of the recent studies focused on pesticide detection in water. Interferometers achieve high sensitivity and low detection limits, which makes them an ideal technique to detect pesticides in water. On the other hand, in the most recent work, a resonator was developed that was able to detect even lower concentrations. However, the advantage of the interferometer over the resonator is that its configuration is simpler.

Table 2. Published work on detection of pesticides in water.

Target Analyte	Type of Biosensor	Limit of Detection (ppb)	Sample	Bio	Reference
2,4-D	Fluorescence	7.53	Drinking water	Antibody	[89]
2,4-D	Fluorescence	2.17	Deionized water	Antibody	[95]
Diuron	Fluorescence	10	Deionized water	Antibody	[95]
Isoproturon	Fluorescence	10	Deionized water	Cell	[55]
Atrazine	Fluorescence	10	Deionized water	Cell	[55]
Atrazine	Fluorescence	80	Tap water	Cell	[90]
Atrazine	Fluorescence	0.77	Lake water	MIP	[96]

Table 2. *Cont.*

Target Analyte	Type of Biosensor	Limit of Detection (ppb)	Sample	Bio	Reference
Atrazine	Grating couplers	0.05	Tap and river water	Antibody	[6]
Methyl-parathion	Fiber optic	0.063	Deionized water	Enzyme	[41]
Chlorpyrifos Thiabendazole Imazalil	Interferometer	0.03 0.04 0.03	Spiked bottled water	Antibody	[93]
Atrazine Paraquat	Interferometer	0.04 0.05	Deionized water	Antibody	[94]
Fenitrothion	Interferometer	0.29	Tap water	Antibody	[46]
Phenobucarb Dimethoate	Resonator	1×10^{-4} 1×10^{-3}	River water	Enzyme	[42]

4.2. Pharmaceuticals

Pharmaceutical compounds reach the environment through the incorrect disposal of their residues or through excretion. Like pesticides, these compounds are persistent and accumulate in the environment; some also have estrogenic effects in specific organisms and even alter the development of certain species of algae and microalgae [97]. In addition, the presence of antibiotics in water exacerbates the problem of increasing antibiotic-resistant bacteria [98].

SPR and LSPR are commonly employed for the detection of pharmaceuticals in water. For example, Tomasseti et al. [99] developed an immunoassay in a sandwich format for the quantification of ampicillin, obtaining an LOD of 0.3 g/L and showing it to be a biosensor with low sensitivity but good selectivity. One of the innovations in this kind of biosensors is the fabrication of the sensor chip, as was shown in Steinke et al. [100], where glass wafers with imprinted nanopillars were covered with gold and functionalized. This work was carried out for diclofenac detection, and an LOD of 1 µg/L was obtained. SPR can also be used in conjunction with other techniques to improve the sensitivity of the biosensor. An example of this is the biosensor designed by Altintas et al. [101], where molecularly printed polymers were deposited on the surface of the sensor chip. In this work, the detection of metoprolol in drinking water samples was performed, first in a simple way and then by adding gold nanoparticles to the samples so that the LOD improved from 78 µg/mL to 1.9 ng/mL.

Another SPR biosensor with a molecularly printed polymer was developed for the detection of ciprofloxacin, an antibiotic. The detection limit for this biosensor was estimated at 0.08 µg/L [102]. One of the most interesting advances is the biosensor developed by Shrivastav et al. [57], in which SPR and LSPR were combined with fiber optics. In this case, the biosensor was composed of an optical fiber with the core exposed in a section. A layer of silver was deposited onto the core, followed by silver nanoparticles; in this way, the different plasmons were enhanced, resulting in a highly sensitive biosensor. Tetracycline was used as target molecule, obtaining an LOD of 0.97 µg/L.

A similar work published that investigated the detection of tetracycline proposed a SPR/LSPR biosensor with an immunoassay in a sandwich format that integrated gold nanostars and a DNA aptamer. In this work, no limit of detection was established; however, it is reported that the biosensor was able reach attomolar concentrations [53]. A more recent study was conducted to detect the presence of ciprofloxacin in the effluent of water treatment plants. This work was carried out with an optical fiber immunosensor; the result obtained was an LOD of 3.3×10^{-3} ng/L [47].

The latest attempt to detect antibiotics by fluorescence combines a fiber optic sensor with molecularly imprinted composite hydrogel nanoparticle detector. The biosensor was used for the quantification of ciprofloxacin, for which a 6 µM LOD was obtained [58].

Diclofenac is another compound that has been detected using fluorescence; this biosensor was developed with yeast cells that fluoresce in its presence. The detection limit determined was 10 µM [54]. A different approach to the detection of antibiotics was developed by Weber et al. [103] using an interferometer for the quantification of penicillin, with 0.25 µg/mL being the minimum concentration tested.

Detection of estrogens in water has received high interest because of their endocrine-disrupting effect on some marine species [33]. The hormone 17β-estradiol is one of the most widely used hormones for the development of biosensors. One of these studies was conducted by measuring the change in fluorescence intensity in water samples using a fiber optic biosensor that detected fluorescence by evanescent wave. The signal emitted was in response to an estrogen receptor (ER) binding with Cy5.5-labeled streptavadin, as observed in Figure 5. The result was an LOD of 1.5 µg/L, using 17β-estradiol as reference [33].

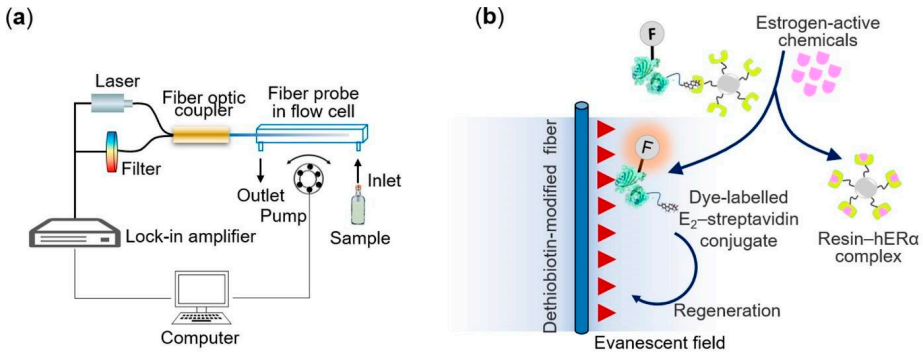

Figure 5. (**a**) Schematic of the optical fiber biosensing platform. (**b**) Sensing scheme of the estrogen receptor-based biosensor using triple-functional fluorescein-labelled E2–STV conjugates for estrogenic activities quantification. Reproduced from [33].

SPR has also been used for this same analyte, both in a classical Kretchmann configuration and in a format combining gratings and SPR mounted on an optical fiber. The latter performed an assay analyzing the interactions between 17β-estradiol and nuclear ER, obtaining an LOD of 0.0015 ng/mL [34], while the classical one used a competitive immunoassay format, achieving 1 pg/mL as the LOD [104].

Overall, SPR biosensors have been the most used technique for pharmaceutical detection (see Table 3, Figure 3). Fiber optic biosensors also stand out, as they offer the lowest LODs using simple configurations, so more research efforts in this area are pertinent.

Table 3. Published work on detection of pharmaceutical compounds in water.

Target Analyte	Type of Biosensor	Limit of Detection (ppb)	Sample	Bio	Reference
Ampicillin	SPR	0.3	Deionized water	Antibody	[99]
Tetracycline	SPR/LSPR	0.97	Deionized water	MIP	[57]
Tetracycline	SPR/LSPR	<ppb	River water	Aptamer and antibody	[53]
Metoprolol	SPR	1.9	Drinking water	MIP	[101]
Ciprofloxacin	SPR	0.08	Deionized water	MIP	[102]
Diclofenac	SPR	1	Deionized water	Antibody	[100]
17β-estradiol	SPR	0.001	Deionized water	Antibody	[104]
17β-estradiol	SPR/Grating	0.0015	Spiked tap and pond water	ER hERα	[34]
17β-estradiol	SPR/Grating	6.8×10^{-5}	Wastewater	MIP	[105]
17β-estradiol	Fluorescence	0.14	Wastewater	DNA	[106]
Sulfadimine	Fluorescence	0.06	Wastewater, lake and bottled water	Antibody	[107]
Diclofenac	Fluorescence	2900	Wastewater	Cell	[54]
Ciprofloxacin	Fluorescence	1900	River water	MIP	[58]

Table 3. *Cont.*

Target Analyte	Type of Biosensor	Limit of Detection (ppb)	Sample	Bio	Reference
Estrogen	Fluorescence	1.05	Wastewater	Estrogen receptors ERα and Erβ	[33]
Ciprofloxacin	Fiber optic	3.3×10^{-6}	Wastewater	Antibody	[47]
Penicillin	Interferometer	250	Deionized water	Antibody	[103]
Amoxicillin	Interferometer	>1	Wastewater, lake and drinking water	Antibody	[108]
Ibuprofen	Interferometer	1000	Deionized water	Chitosan	[109]

4.3. Other Organic Compounds

This classification includes plastic derivatives, industrial supplies, fuels, detergents, or personal care products. Among them are phenolic and halogenated compounds. These attract special attention due to the harmful effects they have on aquatic organisms and even on humans [110].

Shahar et al. [44] proposed a biosensor based on an enzymatic membrane for the detection of organohalide, a halogenated compound, through an optical-fiber reflectometer. Under this scheme, an LOD of 0.908 mg/L was obtained. Furthermore, Cennamon et al. [49] proposed an SPR immunosensor for the detection of naphthalene. This immunosensor was designed using a plastic optical fiber (POF) with an exposed core, where a polymer layer and a gold layer were deposited (Figure 6). The advantages of this type of SPR-POF biosensor are ease of manufacture, installation, and use, as well as a larger fiber diameter. In this work, the presence of naphthalene in seawater was reported, with an LOD of 0.76 ng/mL.

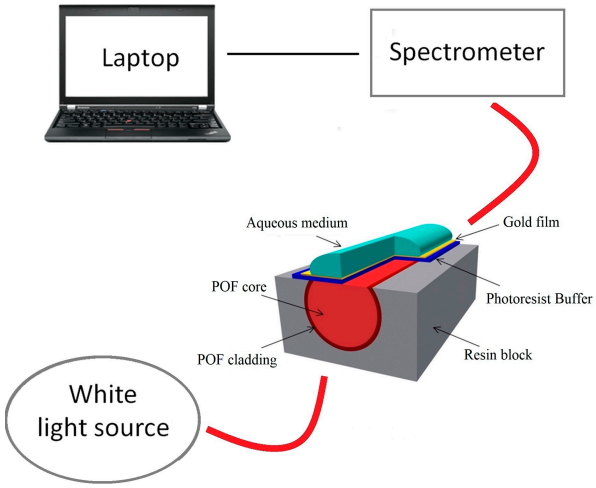

Figure 6. Schematic of the SPR-POF biosensor developed for the detection of naphthalene in water. Reproduced from [49].

Another compound that has been detected via SPR biosensors is bisphenol A (BPA). BPA is used in plastic manufacturing and can act as an endocrine disruptor. In this work, functionalized gold nanoparticles and an inhibition format were used; as a result, a detection limit of 5.2 pg/mL was obtained [48]. The previously mentioned PWAI fluorescent biosensor was also used for the detection of BPA; for this compound, an LOD of 0.038 µg/L was obtained [89]. Another way to use fluorescence as an analytical technique is through Förster Resonance Energy Transfer (FRET). This technique is based on the mechanism of energy transfer in a biological system. FRET was used in conjunction with graphene to develop a biosensor for the detection of BPA; this work resulted in a detection limit of 0.1 ng/mL [52]. Cheng et al. developed a biosensor that uses a smartphone to measure changes in the fluorescence of an immunoassay; the data are processed in an app, where the measurement can be tracked in real time. The immunoassay was performed with

0.1 ng/mL [52]. Cheng et al. developed a biosensor that uses a smartphone to measure changes in the fluorescence of an immunoassay; the data are processed in an app, where the measurement can be tracked in real time. The immunoassay was performed with antibodies labeled with the Cy5.5 dye and was tested on water samples from a lake and tap water for the detection of BPA, achieving an LOD of 0.1 nM in terms of free Cy5.5 [18]. In another work, a simpler fluorescence array was used to test the detection of halogenated compounds. In this study, they tested for five different compounds, for which they obtained LODs in a range between 12.1 and 1.4 mg/L [43].

Table 4 includes the most recent studies published on the detection of organic compounds in water samples. Two works carried out with fluorescence can be seen that have the lowest detection levels. However, the configuration of these biosensors is not simple, and they also require the use of florescent markers. On the other hand, there are the SPR biosensors, which have a good performance, have simpler configurations, do not require markers and their detection limits are competent in relation to chromatography. Finally, there are the fiber-optic biosensors, which have a good detection limit, although they can be improved.

Table 4. Published work on detection of organic compounds in water.

Target Analyte	Type of Biosensor	Limit of Detection (ppb)	Sample	Bio	Reference
Dichloroethane	Fiber optic	1000	River, tap and bottled water	Enzyme	[44]
Naphthalene	SPR	0.76	Sea water	Antibody	[49]
Bisphenol A	SPR	5.2×10^{-3}	Deionized water	Antibody	[48]
Bisphenol A	SPR	0.14	Wastewater	Antibody	[111]
Bisphenol A	SPR	0.04	Drinking water	Antibody	[112]
1,2-dibromoethane	Fluorescence	2400	River water	Enzyme	[43]
1,2,3-trichloropropane		1400			
1,2-di-chloroethane		2700			
3-chloro-2-(chloro-methyl)-1-propene		1400			
γ-hexa-chloro-cyclohexane		12,100			
Bisphenol A	Fluorescence	0.03	Drinking water	Antibody	[89]
Bisphenol A	Fluorescence	0.001	River, tap and bottled water	DNA	[52]
Bisphenol A	Fluorescence	0.076	Lake and tap water	Antibody	[18]
Bisphenol A	Fluorescence	0.025	Deionized water	Antibody	[95]
Bisphenol A	Interferometer	0.5	Treated water	Antibody	[113]

4.4. Microorganisms and Toxins

The presence of microorganisms has special interest in water quality monitoring since these are transmitters of diseases. Likewise, metabolites from some species of fungi contain harmful toxins.

Masdor et al. [114] used a simple SPR system for the detection of *Campylobacter jejuni* via a direct immunoassay, where an LOD of 8×10^6 CFU/mL was obtained. Subsequently, an immunoassay in a sandwich format was performed, which improved the sensitivity of the biosensor, resulting in an LOD of 4×10^4 CFU/mL. An alternative to the traditional SPR is SPR imaging (SPRi). It differs in that the detector is replaced by a CCD camera, which allows us to obtain a complete image of the sensing area. SPRi was employed by Foudeh et al. in the development of a biosensor for the detection of *L. pneumophila*. In this work, genetic material was used in conjunction with quantum dots. The biosensor

A more elaborate set-up was developed for the detection of *E. coli* O157:H7 in water and juice samples, which resulted in an LOD of 5×10^2 CFU/mL [116]. The SPR fi biosensor had an optical fiber to which a mixture of silver nanoparticles with gra added, and then gold nanoparticles and a final gold film on which the biological element was deposited [116]. A different approach for the detection of *E. coli* is the biosen designed by Sanati et al. [117], consisting of two resonator rings of different diam ranged in a vernier structure, which improves the sensitivity of the measurem biosensor was tested with tap water samples by means of an immunoassay, for LOD of 3.33×10^{-5} RIU is reported.

In a different approach for *E. coli* detection, a porous silicon substrate wa conjunction with lectin for the detection of *E. coli* and *Staphylococcus aureus*, obt LOD of 103 cells/mL [15]. Another attempt to detect the presence of *S. aureus* in ronment led to the development of a long-period fiber grating immunosensor. sensor obtained an LOD of 244 CFU/mL [50]. Moreover, in an alternative tech fluorescence, the retroreflector, which reflects light back to the source, has been bacterial detection. With this technique, the presence of *Salmonella typhimurium* w tified using a stem-loop DNA modified with biotin, as shown in Figure 7. The was tested on synthetic samples and reached an LOD of 2.84 pM [118]. More r monolithically integrated silicon interferometer was developed and used in co with an immunoassay for the detection of *E. coli* and *S. typhimurium* in drinki This biosensor achieved an LOD of 40 CFU/mL for *S. typhimurium* and 110 CFU/ *coli* [119].

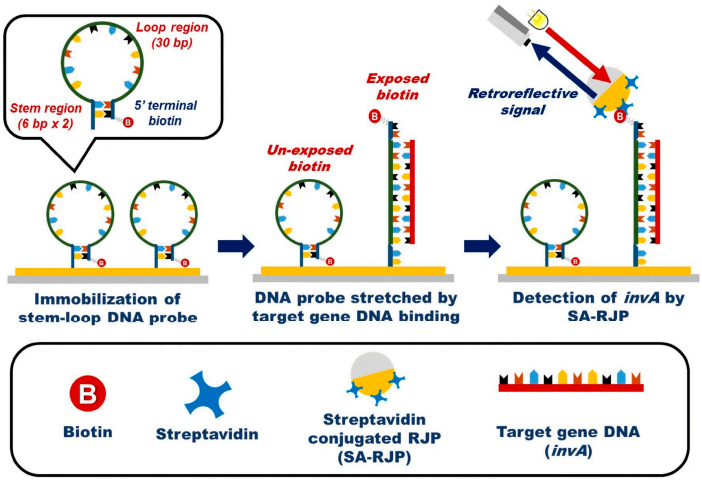

Figure 7. Schematic illustration of the *Salmonella* target gene DNA system detection using retroreflective Janus microparticles. Reproduced from [118].

In the case of toxins, interferometers have been used in conjunction with an noassay for the quantification of ochratoxin A, a mycotoxin produced by more species of fungus. This biosensor reached an LOD of 0.01 ng/L [51]. Another inter for this purpose is the one made by Nabok et al. [120]. The sensor's principal com an optical waveguide made up of a thin silicon nitride layer inserted between tw silicon dioxide layers. The biosensor was tested on synthetic samples for the de zearalenone mycotoxin and reported an LOD of 0.01 ng/L. Microcystin-LR is a t duced by cyanobacteria and is one of the most toxic. Its detection was made in w ples with the TWAI biosensor. In this case, an LOD of 0.67 µg/L was obtained [89].

Table 5 summarizes recent publications on the detection of pathogenic mi isms and toxins in water. Since the units in which the detection limits are rep varied and their homogenization is somewhat complicated, it is difficult to make comparison between them. However, the interferometer and the grating stand ou

between them. However, the interferometer and the grating stand out because they seem to be the most sensitive and have low detection limits; therefore, it would be interesting to carry out more research using these techniques and exploit their potential.

Table 5. Published work on detection of microorganisms and toxins in water.

Target Analyte	Type of Biosensor	Limit of Detection	Sample	Bio	Reference
		Microorganisms			
L. pneumophila	SPRi	3×10^4 CFU/mL	Spiked water from a cooling tower	DNA	[115]
C. jejuni	SPR	4×10^4 CFU/mL	Deionized water	Antibody	[114]
E. coli O157:H7	SPR	5×10^2 CFU/mL	Spiked tap water	Peptide	[116]
E. coli *S. aureus*	Interferometer	10^3 cells/mL 10^3 cells/mL	Deionized water	Lectins of Concanavalin A	[35]
E. coli *S. typhimurium*	Interferometer	110 CFU/mL 40 CFU/mL	Drinking water	Antibody	[119]
E. coli	Resonator	3.33×10^{-5} RIU	Drinking water	Antibody	[117]
E. coli	Fluorescence	10 CFU/mL	Wastewater	DNA	[121]
S. aureus	Grating	244 CFU/mL	Deionized water	Antibody	[50]
S. typhimurium	Retroreflector	2.84 pM	Deionized water	DNA	[118]
		Toxins			
Microcystin-LR	Fluorescence	0.67 ppb	Drinking water	Antibody	[89]
Microcystin-LR	Fluorescence	0.03 ppb	Deionized water	Antibody	[95]
Microcystin-LR	Fluorescence	0.016 ppb	Fresh water	Antibody	[122]
Microcystin-LR	Fluorescence	0.14 ppb	Drinking water	DNA and antibody	[123]
Microcystin-LR	Fluorescence	0.09 ppb	Lake water	Antibody	[124]
Microcystin-LR Microcystin-RR	Fluorescence	0.5 ppb 0.3 ppb	Lake water	DNA	[125]
Ochratoxin A	Interferometer	1×10^{-3} ppb	Deionized water	Antibody	[51]
Zearalenone	Interferometer	0.01 ppb	Deionized water	Antibody	[120]

4.5. Heavy Metals

Heavy metals such as copper, mercury, lead and cadmium are highly dangerous pollutants because they are not chemically or biologically degradable, which causes them to accumulate in soil, water, and air. Human exposure to heavy metals leads to serious diseases, from kidney failure [126] to cancer [36].

In recent years, several types of optical biosensors have been developed for this purpose. An innovative and simple device was proposed by Tagad et al. [45]. In their work they developed an enzymatic biosensor using optical fiber to measure transmittance. This was used for the detection of Hg and resulted in an LOD of 2.5 µM. Years later, Sadani et al. proposed a U-bend fiber optic LSPR biosensor for the detection of Hg, which was functionalized with gold nanoparticles covered with chitosan, as shown in Figure 8a [85]. Meanwhile, Halkare et al. [56] used a similar U-bend fiber optic LSPR biosensor with immobilized *E. coli* cells (Figure 8b), which was able to detect Hg and Cd. Both biosensors were tested with tap water samples, and both achieved detection limits in the ppb range.

A different approach for detecting these compounds is the fluorescence biosensor. The first attempt to use this technique in the detection of heavy metals was by DNA attached to fiber optics. This study was conducted to quantify Hg and Pb, obtaining detection limits of 22 pM and 20 nM, respectively [126]. Several years later, fluorescence was employed to measure Hg via a cell-free expression system. The result was considerably superior, with a LOD of 1 ppb [127]. Similarly, Cu has been analyzed using a resonator, reaching an LOD of 40 pM [36].

Biosensors **2023**, *13*, x FOR PEER REVIEW 18 of 29

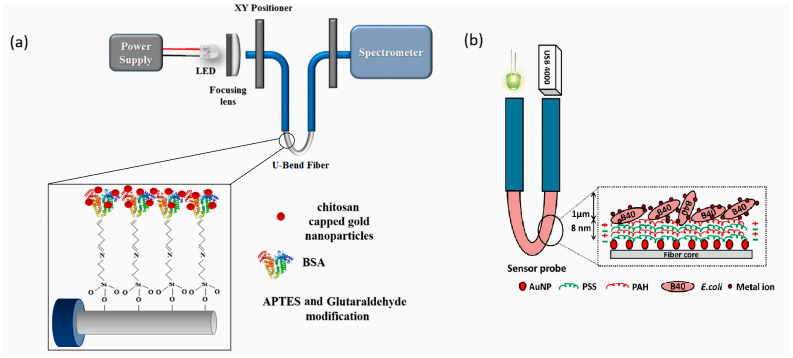

Figure 8. (**a**) Schematic of experimental set up and optical fiber modification with chitosan capped gold nanoparticles. Modified from [85] and (**b**) Schematic of the U-bend optical fiber biosensor for bacteria based heavy metal detection. Modified from [56].

Figure 8. (**a**) Schematic of experimental set up and optical fiber modification with chitosan capped gold nanoparticles. Modified from [85] and (**b**) Schematic of the U-bend optical fiber biosensor for bacteria based heavy metal detection. Modified from [56].

A different approach for detecting these compounds is the fluorescence biosensor. The first attempt to use this technique in the detection of heavy metals was by DNA attached to fiber optics. This study was conducted to quantify Hg and Pb, obtaining detection limits of 22 pM and 20 nM, respectively [126]. Several years later, fluorescence was simply functionalized with multiple layers of polyethylenimine for the detection of Cu. The biosensor was tested with irrigation, ground and tap water samples, showing an LOD of 53 ppb. Moreover, Kumar et al. [129] designed an FPI with DNAzyme, which contained a catalytic region and whose counterpart was coupled to silicon nanoparticles. This was used in ground, irrigation and tap water samples, reporting an LOD of 0.49 ppb.

Recently, the use of FPI for the detection of metals in water was reported. Such is the case of the biosensor developed by Bismuth et al. [128], in which they used porous silica functionalized with multiple layers of polyethylenimine for the detection of Cu. The biosensor was tested with irrigation, ground and tap water samples, showing an LOD of 53 ppb. Moreover, Kumar et al. [129] designed an FPI with DNAzyme, which contained a catalytic region and whose counterpart was coupled to silicon nanoparticles. This was used in ground, irrigation and tap water samples, reporting an LOD of 0.49 ppb.

According to Table 6, the lowest reported LOD corresponds to a WGM-type resonator made with liquid crystals. WGM has a great potential for the detection of compounds at low concentrations; however, few works have been developed in this area. Moreover, the fluorescence biosensors had a good response and low detection limits, so it can be considered as a simpler alternative.

Table 6. Published work on detection of heavy metals in water.

Target Analyte	Type of Biosensor	Limit of Detection (ppb)	Sample	Bio	Reference
Hg	Optical fiber	5001	Deionized water	Enzyme	[45]
Hg	LSPR	0.1	Spiked seawater, wastewater and tap water	BSA and Chitosan	[85]
Hg Cd	LSPR	0.5 0.5	Tap water	Cell	[56]
Hg Cd	SPR	0.01 0.5	Tap water	Cell	[56]
Hg	SPR	0.01	Tap water	DNA	[130]
Hg	SPR	0.2	Tap and pond water	DNA	[131]
Hg Pb	Optical fiber	4.4×10^{-3} 4.14	Drinking water	DNA	[126]
Hg Pb	Optical fiber	4.4×10^{-3} 4.14	Drinking water	DNA	[126]
Pb	Optical fiber	0.21	Wastewater	DNA	[132]
Pb	Optical fiber	0.21	Wastewater	DNA	[132]
Hg	Optical fiber	0.58	Wastewater, tap and bottled water	DNA	[133]
Hg	Optical fiber	0.58	Wastewater, tap and bottled water	DNA	[133]
Hg	Fluorescence	1	Deionized water	DNA	[127]
Hg	Fluorescence	0.24	Surface water	DNA	[134]
Cu	Resonator	2.5×10^{-3}	Drinking water	Stearic acid	[36]
Cu	Interferometer	0.53	Ground water, irrigation water and tap water	Polyethylenimine	[128]
Cu Ag Pb	Interferometer	104 56 125	Tap, irrigation and drain water	Enzyme	[135]
Pb	Interferometer	0.49	Ground water, irrigation water and tap water	DNA	[129]

			and tap water		
Cu Ag Pb	Interferometer	104 56 125	Tap, irrigation and drain water	Enzyme	[135]
Pb	Interferometer	0.49	Ground water, irrigation water and tap water	DNA	[129]

5. Discussion

In this review, 67 papers on optical biosensors applied to the detection of various environmental water pollutants were compiled and considered for analysis. As observed in Figure 9, between the years 2010 and 2014, the number of publications was steady and started to consistently increase between 2015 and 2017. Most of the recent works were published in 2019, and this was followed by a marked decline, suggesting that due to the COVID-19 pandemic, the effort for biosensor development was even more concentrated in healthcare applications.

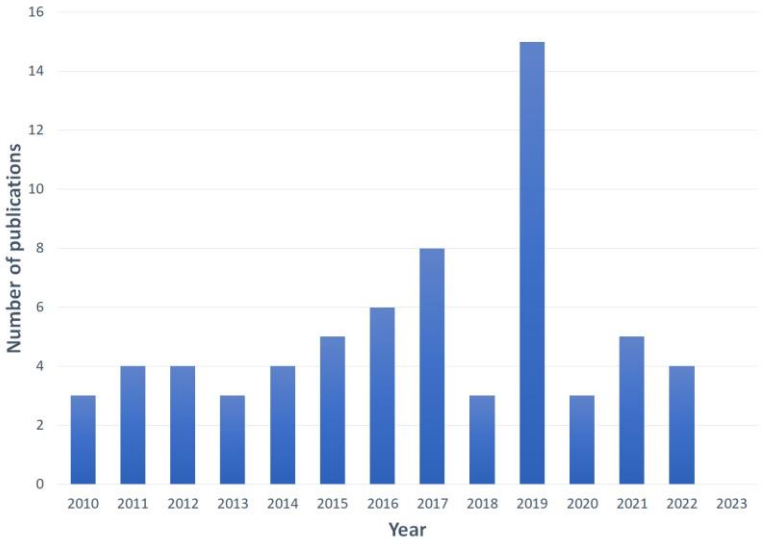

Figure 9. Yearly scientific production regarding biosensors for the detection of pollutants in water.

Figure 10 shows the distribution in terms of (a) the type of biosensor and (b) the biological recognition element. Regarding the type of biosensor, SPR and fluorescence biosensors represent 61% of the literature. As mentioned above, fluorescence is a preferred method because fluorescence transducers allow the measurement of different parameters, and the devices can have a wide variety of configurations. SPR devices can also be developed in various configurations, with the advantage of not using chemical markers (i.e., fluorescent labels). Both transducers can improve their sensitivity with the addition of other elements, e.g., multi-metal or other material layers, nanoparticles, quantum dots, etc. Due to the simplicity of setup and the detection limits they provide, these two transducers have been the most widely used so far.

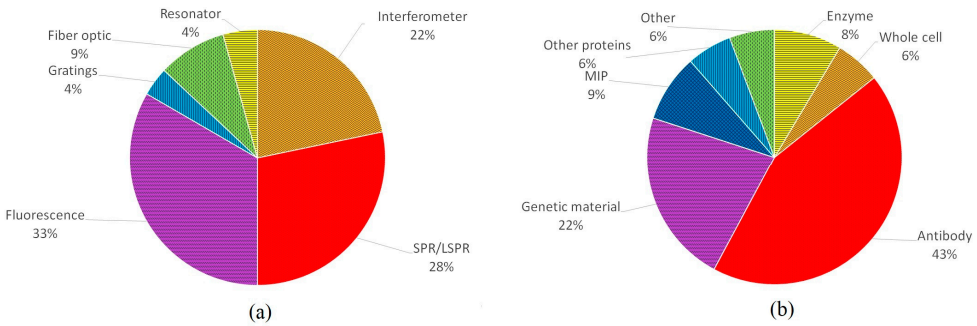

Figure 10. Percentage distribution of the works consulted according to (a) the type of biosensor and (b) the biological recognition element.

Depending on their configuration, fluorescence-based biosensors can detect different analytes, ranging from hundreds of pollutants to the ones that stand out will generally have more complex designs and operating principles. Such is the case for a fluorescence-based biosensor mounted on optical fiber or the use of FRET. However, these biosensors are usually preferred due to their relative simplicity compared to other optical biosensors.

SPR biosensors usually provide low detection limits, although this tends to be limited by the type of immunoassay. Even so, these limits can be further reduced by including

have more complex designs and operating principles. Such is the case for a fluorescence-based biosensor mounted on optical fiber or the use of FRET. However, these biosensors are usually preferred due to their relative simplicity compared to other optical biosensors.

SPR biosensors usually provide low detection limits, although this tends to be limited by the type of immunoassay. Even so, these limits can be further reduced by including other materials (e.g., metal nanoparticles, graphene, optical fiber) to improve device sensitivity. Moreover, SPR has become widespread since the optical arrangement and device has been thoroughly study and is relatively simple. Moreover, an SPR sensor is reusable, so multiple measurements can be performed.

Interferometers have also been shown to achieve low detection limits. Therefore, they account for 27% of the biosensors developed for the detection of contaminants in water. These types of biosensors can also be easily constructed and do not require markers. Meanwhile, fiber optics and grating couplers are often used in biosensor development in combination with other biosensing techniques, such as SPR and fluorescence, which may seem to be of little relevance but are key elements in biosensor design. During the literature search for this review, it was noticed that at the beginning of the decade, resonators were just emerging and being tested, so most of the articles published in those years do not offer a concrete application. However, resonators have been demonstrated to have high sensitivity and achieve low detection limits in the detection of small molecules in water, accounting for 4% of the publications included here. So, it is worthwhile to exploit their potential for environmental applications.

As for biological receptors, antibodies are the most common (43%), followed by genetic material (22%) and MIPs (9%). The use of antibodies is so widespread due to their compatibility with any type of transducer, their high specificity, and their sensitivity. Moreover, they have higher stability than enzymes and can be used for many target analytes, as opposed to DNA. In addition, their affinity for their antigens improves biosensor performance, which—combined with their specificity and the fact that these bonds can be dissociated, allowing the reuse of the sensor—make antibodies the best option in terms of receptors.

So far, the use of whole cells has been limited to fluorescence and SPR. However, with the use of bioreporter cells, their use could be expanded to other transducers [136]; however, these bioreporters have a great performance in fluorescence biosensing [137]. Another receptor that is of great interest at present are MIPs; although their use is relatively recent, it has been shown that these synthetic receptors have the potential to perform as well as natural ones, with the advantages of reducing production costs, being more stable and offering a more homogeneous sensor functionalization [138,139].

In general, sample preparation for biosensors was minimal, consisting of simple filtration if necessary; otherwise, the sample was read directly. This represents a great advantage compared to chromatographic methods, whose sample preparation includes several filtrations, separations, concentration, and in some cases, derivatization, making the pretreatment the most complex part of the analysis. Furthermore, biosensors proved to be competitive with chromatography since their detection limits are similar [56,85,93].

6. Key Trends and Future Perspective

Recent developments in optical sensors have shown considerable improvements in terms of sensitivity, such as SPCE sensors developed for the detection of pollutants such as tannic acid in environmental water samples [75] and perindopril erbumine in water and blood plasma samples [140]. Although these examples did not include a biological recognition element in their sensing platform, SPCE biosensors have been developed for clinical applications [141], proving that this technique could be an excellent alternative for enhancing the sensitivity of environmental biosensors. It is also important to highlight that nanomaterial advances such as soret and cryosoret that promote the generation of hotspots can improve the sensitivity of the biosensors that incorporate nanomaterials [142,143]. With proper biofunctionalization, these types of sensors can offer high-quality platforms for the environmental field. On the other hand, the detection of single molecules is a powerful

technology that avoids bulk averaging and provides direct information on individual molecules [144]. Although single-molecule biosensors do not yet outperform ensemble-averaged approaches in terms of sensitivity, they show considerable improvement in affinity [81]. Single-molecule biosensors have been extensively studied in the healthcare field [145], making them a source of future research if these developments are extrapolated to environmental detection.

An advance in terms of portability and miniaturization is the use of the optical components of smartphones and their implementation in biosensing. Cell phones are one of the technological tools whose progress has been accelerated [146], and one of the features in which more has been invested is the capture of better quality photographs, since it is one of the elements that the user considers when choosing a product. Taking advantage of the high-resolution camera as well as other sensors present in smartphones for photo capture and data acquisition translates into cost reduction in the manufacturing of optical sensing devices [147]. For example, in 2017, McCracken et al. designed a sensor that was able to detect BPA in water samples using fluorescence [148]. This sensor used the camera flash as the excitation source and the camera's complementary metal-oxide-semiconductor (CMOS) sensor as the detector. Once the images were obtained, they were processed in RGB format using ImageJ software. The result was a detection limit of 1004 μg L^{-1}, which is not sufficient to compete with other techniques. However, this sensor represents a first approach to the accessible detection of contaminants in water with cell phones.

Since sensing the data of the aforementioned devices are complex due to variations in light or image aberrations, data processing tools such as machine learning (ML) are useful [149]. ML employs computer systems to replicate human learning and offers an algorithm with the capacity to identify and gain knowledge about the environment. Complicated biological systems are inherently compatible with ML algorithms since they can find hidden patterns [150]. In general, ML can approximate three sorts of problems: classification, regression, and clustering [151]. ML implementation can increase optical biosensor performance by simplifying the examination of raw biosensor output data to approximate a solution to various challenges. For example, (a) classification may be used for detection; (b) regression can be used to forecast and prevent harmful occurrences; and (c) clustering can be used to identify groupings of data that share features [151]; the optical biosensor signals can be analyzed in real time to develop meaningful output pathways in the algorithms, differentiating between good and bad images [14]. Leveraging these tools has facilitated the development of smartphone optical biosensors, which means we are one step closer to the miniaturization of these devices and their use for in situ monitoring. Taking the McCracken sensor as an example [148], it may be inferred that sensor performance could be enhanced by implementing ML for data processing.

Today it is feasible to develop smartphone-based optical biosensors that have low detection limits. An example of this is the biosensor developed by Guo et al. [152], in which they used a strip functionalized with streptavidin-biotinylated DNA probes modified with gold nanoparticles. Once the sample is run, an image is captured by a smartphone and the result is displayed by means of an application. This biosensor achieved an LOD of 0.5 μg L^{-1}, being a remarkable improvement.

Considering all the above, there is still a wide range of research ahead. On the one hand there are the new proven techniques in sensors that can be coupled to biological receptors. Considering the advances in nanomaterials with the promotion of hotspots by means of sorets and cryosorets, this represents an improvement in SPR systems and any other system in which nanomaterials are to be implemented. This also includes the use of SPCE for biosensor fabrication and single-molecule detection. All these methodologies need to be explored in environmental applications.

On the other hand, it is also necessary to continue the research and development of portable, simple, and functional systems. Compared to traditional biosensors, smartphone-based biosensors are straightforward and simple to use. Such evaluations are accomplished at a cheaper cost and may thus be utilized for non-laboratory assessments. For water moni-

toring, this type of biosensor has been developed in two ways: detection through image capture from a chip or sensor cartridge where the measurement to be read is previously carried out, or with a small and portable array, which wirelessly connects to the smartphone and reads the signals. The first one is perhaps the most practical in terms of portability and commercialization. However, the second offers greater versatility in the type of array that can be fabricated, testing different transducers and receivers and with the possibility of integrating nanomaterials and microfluidics.

Although everything up to this point has been projected at the laboratory level, biosensors are a growing market. Previously, there have been biosensors for water quality assessment that have gone on sale, such as Optiqua™ [113], which is an interferometer that uses antibodies to detect contaminants. The use of biological elements is complicated, but technologies such as Optiqua™ are proof that it is possible to overcome this challenge. Additionally, the advancement in the development of MIPs is another possible solution that will improve the development and commercialization of biosensors in the future. With the integration of these new methodologies, the development of portable biosensors capable of detecting low molecular weight compounds at low concentrations is possible.

7. Concluding Remarks

Throughout this review, different types of optical biosensors and their applications in environmental detection have been described. The biosensors are diverse since each one is designed according to the needs and objectives of each application. However, SPR-based biosensors are amongst the most versatile, and their use extends to almost all kinds of pollutants found in water. Similarly, fluorescence is another technique that has been successful in the detection of contaminants in water. Between these two types of biosensors, the SPR-based biosensors have an advantage over fluorescence since, in general, they can reach lower detection limits.

Other types of devices, such as interferometers and resonators, are less commonly used but have been proven to have a high sensitivity and to have low detection limits. The potential shown by these types of biosensors makes it worthwhile to further develop them.

Similarly, each type of biological recognition elements has its advantages and disadvantages. Antibodies are the most versatile and widely used receptors because of their various advantages; however, it is necessary to continue developing research on this subject to make antibodies more affordable. Enzymes are very sensitive to changes in their environment, so this instability limits their potential, while DNA is limited in terms of the variety of analytes it can quantify.

Some of the challenges faced by optical biosensors for their commercialization is the miniaturization of the devices because their optical components are generally delicate and even more expensive than those used in electrochemistry. However, with the increasing development of technology, it is possible to develop biosensors that take advantage of the optical elements of smartphones to develop biosensors. Another challenge is to guarantee the stability of the biological element and to achieve the reusability of the sensors. Continuing to innovate and develop research in biosensors and related areas is of the utmost importance to overcome these barriers and achieve their widespread application for environmental analysis.

Author Contributions: Conceptualization, N.O.-S. and Q.C.; investigation, M.H.-D. and I.A.-H.; writing—original draft preparation, M.H.-D.; writing—review and editing, I.A.-H., M.H.-D., G.M.-L. and N.O.-S.; visualization, G.M.-L. and J.M.; supervision, N.O.-S.; funding acquisition, N.O.-S., Q.C. and J.M. All authors have read and agreed to the published version of the manuscript.

Funding: The authors would like to acknowledge the National Council of Science and Technology of Mexico (CONACyT) for grant # PN2016-4320 and scholarship #855128. Financial support from UC-Mexus CONACyT collaborative grants (grant # CN-20-258) is greatly appreciated.

Institutional Review Board Statement: Not applicable.

Informed Consent Statement: Not applicable.

Data Availability Statement: No new data were created or analyzed in this study. Data sharing is not applicable to this article.

Conflicts of Interest: The authors declare no conflict of interest.

References

1. Richardson, S.D.; Ternes, T.A. Water Analysis: Emerging Contaminants and Current Issues. *Anal. Chem.* **2022**, *94*, 382–416. [CrossRef] [PubMed]
2. Rathi, B.S.; Kumar, P.S.; Vo, D.V.N. Critical Review on Hazardous Pollutants in Water Environment: Occurrence, Monitoring, Fate, Removal Technologies and Risk Assessment. *Sci. Total Environ.* **2021**, *797*, 149134. [CrossRef] [PubMed]
3. Biosensors Market Size, Global Forecast, Growth Drivers, Opportunities 2030. Available online: https://www.marketsandmarkets.com/Market-Reports/biosensors-market-798.html (accessed on 15 October 2022).
4. Monosik, R.; Stredansky, M.; Tkac, J.; Sturdik, E. Application of Enzyme Biosensors in Analysis of Food and Beverages. *Food Anal. Methods* **2012**, *5*, 40–53. [CrossRef]
5. Mohsin, M.; Ahmad, A. Genetically-Encoded Nanosensor for Quantitative Monitoring of Methionine in Bacterial and Yeast Cells. *Biosens. Bioelectron.* **2014**, *59*, 358–364. [CrossRef] [PubMed]
6. Gao, H.; Generelli, S.; Heitger, F. Online Monitoring the Water Contaminations with Optical Biosensor. *Proceedings* **2017**, *1*, 522. [CrossRef]
7. Turner, A.P.F. Biosensors–Sense and Sensitivity. *Science* **2000**, *290*, 1315–1317. [CrossRef]
8. Velasco-Garcia, M.N. Optical Biosensors for Probing at the Cellular Level: A Review of Recent Progress and Future Prospects. *Semin. Cell Dev. Biol.* **2009**, *20*, 27–33. [CrossRef]
9. Xiong, Y.; Huang, Q.; Canady, T.D.; Barya, P.; Liu, S.; Arogundade, O.H.; Race, C.M.; Che, C.; Wang, X.; Zhou, L.; et al. Photonic Crystal Enhanced Fluorescence Emission and Blinking Suppression for Single Quantum Dot Digital Resolution Biosensing. *Nat. Commun.* **2022**, *13*, 4647. [CrossRef]
10. Sansone, L.; Macchia, E.; Taddei, C.; Torsi, L.; Giordano, M. Label-Free Optical Biosensing at Femtomolar Detection Limit. *Sens. Actuators B Chem.* **2018**, *255*, 1097–1104. [CrossRef]
11. Jason-Moller, L.; Murphy, M.; Bruno, J.A. Overview of Biacore Systems and Their Applications. *Curr. Protoc. Protein Sci.* **2006**, *19*, 19.13.1–19.13.14. [CrossRef]
12. Xia, Y.; Hu, J.; Zhao, S.; Tao, L.; Li, Z.; Yue, T.; Kong, J. Build-in Sensors and Analysis Algorithms Aided Smartphone-Based Sensors for Point-of-Care Tests. *Biosens. Bioelectron. X* **2022**, *11*, 100195. [CrossRef]
13. Di Nonno, S.; Ulber, R. Smartphone-Based Optical Analysis Systems. *Analyst* **2021**, *146*, 2749–2768. [CrossRef] [PubMed]
14. Doğan, V.; Isık, T.; Kılıç, V.; Horzum, N. A Field-Deployable Water Quality Monitoring with Machine Learning-Based Smartphone Colorimetry. *Anal. Methods* **2022**, *14*, 3458–3466. [CrossRef] [PubMed]
15. Roda, A.; Zangheri, M.; Calabria, D.; Mirasoli, M.; Caliceti, C.; Quintavalla, A.; Lombardo, M.; Trombini, C.; Simoni, P. A Simple Smartphone-Based Thermochemiluminescent Immunosensor for Valproic Acid Detection Using 1,2-Dioxetane Analogue-Doped Nanoparticles as a Label. *Sens. Actuators B Chem.* **2019**, *279*, 327–333. [CrossRef]
16. Freund, B.; Tatum, W.O. Pitfalls Using Smartphones Videos in Diagnosing Functional Seizures. *Epilepsy Behav. Rep.* **2021**, *16*, 100497. [CrossRef] [PubMed]
17. Yu, Z.; Gong, H.; Li, M.; Tang, D. Hollow Prussian Blue Nanozyme-Richened Liposome for Artificial Neural Network-Assisted Multimodal Colorimetric-Photothermal Immunoassay on Smartphone. *Biosens. Bioelectron.* **2022**, *218*, 114751. [CrossRef] [PubMed]
18. Cheng, Y.; Wang, H.; Zhuo, Y.; Song, D.; Li, C.; Zhu, A.; Long, F. Reusable Smartphone-Facilitated Mobile Fluorescence Biosensor for Rapid and Sensitive on-Site Quantitative Detection of Trace Pollutants. *Biosens. Bioelectron.* **2022**, *199*, 113863. [CrossRef]
19. Ramirez, J.C.; Grajales García, D.; Maldonado, J.; Fernández-Gavela, A. Current Trends in Photonic Biosensors: Advances towards Multiplexed Integration. *Chemosensors* **2022**, *10*, 398. [CrossRef]
20. Sohrabi, H.; Hemmati, A.; Majidi, M.R.; Eyvazi, S.; Jahanban-Esfahlan, A.; Baradaran, B.; Adlpour-Azar, R.; Mokhtarzadeh, A.; de la Guardia, M. Recent Advances on Portable Sensing and Biosensing Assays Applied for Detection of Main Chemical and Biological Pollutant Agents in Water Samples: A Critical Review. *TrAC Trends Anal. Chem.* **2021**, *143*, 116344. [CrossRef]
21. Erdem, A.; Senturk, H.; Yildiz, E. Recent Progress on Biosensors Developed for Detecting Environmental Pollutants. In *Biosensors: Fundamentals, Emerging Technologies, and Application*, 1st ed.; CRC Press: Boca Raton, FL, USA, 2022; pp. 213–231. [CrossRef]
22. Nehra, M.; Dilbaghi, N.; Kumar, R.; Kumar, S. Trends in Point-of-Care Optical Biosensors for Antibiotics Detection in Aqueous Media. *Mater. Lett.* **2022**, *308*, 131235. [CrossRef]
23. Sarkar, A.; Sarkar, K.D.; Amrutha, V.; Dutta, K. An Overview of Enzyme-Based Biosensors for Environmental Monitoring. In *Tools, Techniques and Protocols for Monitoring Environmental Contaminants*, 1st ed.; Elsevier: Amsterdam, The Netherlands, 2019; pp. 307–329. ISBN 9780128146798.
24. Zhu, Y.C.; Mei, L.P.; Ruan, Y.F.; Zhang, N.; Zhao, W.W.; Xu, J.J.; Chen, H.Y. *Enzyme-Based Biosensors and Their Applications*, 1st ed.; Elsevier: Amsterdam, The Netherlands, 2019; ISBN 9780444641144.
25. Zhang, Z.; Zeng, K.; Liu, J. Immunochemical Detection of Emerging Organic Contaminants in Environmental Waters. *TrAC Trends Anal. Chem.* **2017**, *87*, 49–57. [CrossRef]

26. Singh, K.V.; Kaur, J.; Varshney, G.C.; Raje, M.; Suri, C.R. Synthesis and Characterization of Hapten-Protein Conjugates for Antibody Production against Small Molecules. *Bioconjug. Chem.* **2004**, *15*, 168–173. [CrossRef] [PubMed]
27. Wu, J.; Ju, H.X. Clinical Immunoassays and Immunosensing. In *Comprehensive Sampling and Sample Preparation*; Academic Press: Cambridge, MA, USA, 2012; Volume 3, pp. 143–167. [CrossRef]
28. Pohanka, M. Overview of Piezoelectric Biosensors, Immunosensors and DNA Sensors and Their Applications. *Materials* **2018**, *11*, 448. [CrossRef]
29. P Gautam A Review on Recent Advances in Biosensors for Detection of Water. *Int. J. Environ. Sci.* **2012**, *2*, 1565–1574. [CrossRef]
30. Oliveira Brett, A.M. Chapter 4 DNA-Based Biosensors. *Compr. Anal. Chem.* **2005**, *44*, 179–208.
31. Borisov, S.M.; Wolfbeis, O.S. Optical Biosensors. *Chem. Rev.* **2008**, *108*, 423–461. [CrossRef] [PubMed]
32. Sciuto, E.L.; Coniglio, M.A.; Corso, D.; van der Meer, J.R.; Acerbi, F.; Gola, A.; Libertino, S. Biosensors in Monitoring Water Quality and Safety: An Example of a Miniaturizable Whole-Cell Based Sensor for Hg2+ Optical Detection in Water. *Water* **2019**, *11*, 1986. [CrossRef]
33. Liu, L.; Zhou, X.; Lu, Y.; Shi, H.; Ma, M.; Yu, T. Triple Functional Small-Molecule-Protein Conjugate Mediated Optical Biosensor for Quantification of Estrogenic Activities in Water Samples. *Environ. Int.* **2019**, *132*, 105091. [CrossRef]
34. Liu, L.; Zhang, X.; Zhu, Q.; Li, K.; Lu, Y.; Zhou, X.; Guo, T. Ultrasensitive Detection of Endocrine Disruptors via Superfine Plasmonic Spectral Combs. *Light Sci. Appl.* **2021**, *10*, 181. [CrossRef]
35. Yaghoubi, M.; Rahimi, F.; Negahdari, B.; Rezayan, A.H.; Shafiekhani, A. A Lectin-Coupled Porous Silicon-Based Biosensor: Label-Free Optical Detection of Bacteria in a Real-Time Mode. *Sci. Rep.* **2020**, *10*, 16017. [CrossRef]
36. Duan, R.; Li, Y.; Li, H.; Yang, J. Detection of Heavy Metal Ions Using Whispering Gallery Mode Lasing in Functionalized Liquid Crystal Microdroplets. *Biomed. Opt. Express* **2019**, *10*, 6073. [CrossRef] [PubMed]
37. Jiang, B.; Song, Y.; Liu, Z.; Huang, W.E.; Li, G.; Deng, S.; Xing, Y.; Zhang, D. Whole-Cell Bioreporters for Evaluating Petroleum Hydrocarbon Contamination. *Crit. Rev. Environ. Sci. Technol.* **2021**, *51*, 272–322. [CrossRef]
38. Van Der Meer, J.R.; Tropel, D.; Jaspers, M. Illuminating the Detection Chain of Bacterial Bioreporters. *Environ. Microbiol.* **2004**, *6*, 1005–1020. [CrossRef] [PubMed]
39. Zhu, Y.; Elcin, E.; Jiang, M.; Li, B.; Wang, H.; Zhang, X.; Wang, Z. Use of Whole-Cell Bioreporters to Assess Bioavailability of Contaminants in Aquatic Systems. *Front. Chem.* **2022**, *10*, 1018124. [CrossRef] [PubMed]
40. Haupt, K.; Mosbach, K. Molecularly Imprinted Polymers and Their Use in Biomimetic Sensors. *Chem. Rev.* **2000**, *100*, 2495–2504. [CrossRef]
41. Arjmand, M.; Saghafifar, H.; Alijanianzadeh, M.; Soltanolkotabi, M. A Sensitive Tapered-Fiber Optic Biosensor for the Label-Free Detection of Organophosphate Pesticides. *Sens. Actuators B Chem.* **2017**, *249*, 523–532. [CrossRef]
42. Duan, R.; Hao, X.; Li, Y.; Li, H. Detection of Acetylcholinesterase and Its Inhibitors by Liquid Crystal Biosensor Based on Whispering Gallery Mode. *Sens. Actuators B Chem.* **2020**, *308*, 127672. [CrossRef]
43. Bidmanova, S.; Kotlanova, M.; Rataj, T.; Damborsky, J.; Trtilek, M.; Prokop, Z. Fluorescence-Based Biosensor for Monitoring of Environmental Pollutants: From Concept to Field Application. *Biosens. Bioelectron.* **2016**, *84*, 97–105. [CrossRef]
44. Shahar, H.; Tan, L.L.; Ta, G.C.; Heng, L.Y. Optical Enzymatic Biosensor Membrane for Rapid in Situ Detection of Organohalide in Water Samples. *Microchem. J.* **2019**, *146*, 41–48. [CrossRef]
45. Tagad, C.K.; Kulkarni, A.; Aiyer, R.C.; Patil, D.; Sabharwal, S.G. A Miniaturized Optical Biosensor for the Detection of Hg2+ Based on Acid Phosphatase Inhibition. *Optik* **2016**, *127*, 8807–8811. [CrossRef]
46. Ramirez-Priego, P.; Estévez, M.C.; Díaz-Luisravelo, H.J.; Manclús, J.J.; Montoya, Á.; Lechuga, L.M. Real-Time Monitoring of Fenitrothion in Water Samples Using a Silicon Nanophotonic Biosensor. *Anal. Chim. Acta* **2021**, *1152*, 338276. [CrossRef] [PubMed]
47. Lamarca, R.S.; Franco, D.F.; Nalin, M.; de Lima Gomes, P.C.F.; Messaddeq, Y. Label-Free Ultrasensitive and Environment-Friendly Immunosensor Based on a Silica Optical Fiber for the Determination of Ciprofloxacin in Wastewater Samples. *Anal. Chem.* **2020**, *92*, 14415–14422. [CrossRef] [PubMed]
48. Xue, C.S.; Erika, G.; Jiří, H. Surface Plasmon Resonance Biosensor for the Ultrasensitive Detection of Bisphenol A. *Anal. Bioanal. Chem.* **2019**, *411*, 5655–5658. [CrossRef] [PubMed]
49. Cennamo, N.; Zeni, L.; Ricca, E.; Isticato, R.; Marzullo, V.M.; Capo, A.; Staiano, M.; D'Auria, S.; Varriale, A. Detection of Naphthalene in Sea-Water by a Label-Free Plasmonic Optical Fiber Biosensor. *Talanta* **2019**, *194*, 289–297. [CrossRef]
50. Yang, F.; Chang, T.L.; Liu, T.; Wu, D.; Du, H.; Liang, J.; Tian, F. Label-Free Detection of Staphylococcus Aureus Bacteria Using Long-Period Fiber Gratings with Functional Polyelectrolyte Coatings. *Biosens. Bioelectron.* **2019**, *133*, 147–153. [CrossRef]
51. Al-Jawdah, A.; Nabok, A.; Jarrah, R.; Holloway, A.; Tsargorodska, A.; Takacs, E.; Szekacs, A. Mycotoxin Biosensor Based on Optical Planar Waveguide. *Toxins* **2018**, *10*, 272. [CrossRef]
52. Gupta, S.; Wood, R. Development of FRET Biosensor Based on Aptamer/Functionalized Graphene for Ultrasensitive Detection of Bisphenol A and Discrimination from Analogs. *Nano-Struct. Nano-Objects* **2017**, *10*, 131–140. [CrossRef]
53. Kim, S.; Lee, H.J. Gold Nanostar Enhanced Surface Plasmon Resonance Detection of an Antibiotic at Attomolar Concentrations via an Aptamer-Antibody Sandwich Assay. *Anal. Chem.* **2017**, *89*, 6624–6630. [CrossRef]
54. Schirmer, C.; Posseckardt, J.; Schröder, M.; Gläser, M.; Howitz, S.; Scharff, W.; Mertig, M. Portable and Low-Cost Biosensor towards on-Site Detection of Diclofenac in Wastewater. *Talanta* **2019**, *203*, 242–247. [CrossRef]
55. Gosset, A.; Oestreicher, V.; Perullini, M.; Bilmes, S.A.; Jobbágy, M.; Dulhoste, S.; Bayard, R.; Durrieu, C. Optimization of Sensors Based on Encapsulated Algae for Pesticide Detection in Water. *Anal. Methods* **2019**, *11*, 6193–6203. [CrossRef]

56. Halkare, P.; Punjabi, N.; Wangchuk, J.; Nair, A.; Kondabagil, K.; Mukherji, S. Bacteria Functionalized Gold Nanoparticle Matrix Based Fiber-Optic Sensor for Monitoring Heavy Metal Pollution in Water. *Sens. Actuators B Chem.* **2019**, *281*, 643–651. [CrossRef]
57. Shrivastav, A.M.; Mishra, S.K.; Gupta, B.D. Localized and Propagating Surface Plasmon Resonance Based Fiber Optic Sensor for the Detection of Tetracycline Using Molecular Imprinting. *Mater. Res. Express* **2015**, *2*, 35007. [CrossRef]
58. Huang, Q.D.; Lv, C.H.; Yuan, X.L.; He, M.; Lai, J.P.; Sun, H. A Novel Fluorescent Optical Fiber Sensor for Highly Selective Detection of Antibiotic Ciprofloxacin Based on Replaceable Molecularly Imprinted Nanoparticles Composite Hydrogel Detector. *Sens. Actuators B Chem.* **2021**, *328*, 129000. [CrossRef]
59. Malacara, D. *Óptica Básica*, 3rd ed.; FCE—Fondo de Cultura Económica: Mexico City, Mexico, 2015; ISBN 9786071634139.
60. Hariharan, P. *Optical Interferometry*, 2nd ed.; Elsevier: Amsterdam, The Netherlands, 2003; ISBN 9780123116307.
61. Islam, M.S.; Kouzani, A.Z.; Dai, X.J.; Michalski, W.P.; Gholamhosseini, H. Comparison of Performance Parameters for Conventional and Localized Surface Plasmon Resonance Graphene Biosensors. In Proceedings of the 2011 Annual International Conference of the IEEE Engineering in Medicine and Biology Society, Boston, MA, USA; 2011; pp. 1851–1854. [CrossRef]
62. Estevez, M.C.; Otte, M.A.; Sepulveda, B.; Lechuga, L.M. Trends and Challenges of Refractometric Nanoplasmonic Biosensors: A Review. *Anal. Chim. Acta* **2014**, *806*, 55–73. [CrossRef]
63. Schasfoort, R.B.M.; McWhirter, A. Chapter 3: SPR Instrumentation. In *Handbook of Surface Plasmon Resonance*, 1st ed; Royal Society of Chemistry: Cambridge, UK, 2010; pp. 35–80.
64. Chen, Y.; Yu, Y.; Li, X.; Tan, Z.; Geng, Y. Experimental Comparison of Fiber-Optic Surface Plasmon Resonance Sensors with Multi Metal Layers and Single Silver or Gold Layer. *Plasmonics* **2015**, *10*, 1801–1808. [CrossRef]
65. Kamaruddin, N.H.; Bakar, A.A.A.; Yaacob, M.H.; Mahdi, M.A.; Zan, M.S.D.; Shaari, S. Enhancement of Chitosan-Graphene Oxide SPR Sensor with a Multi-Metallic Layers of Au–Ag–Au Nanostructure for Lead(II) Ion Detection. *Appl. Surf. Sci.* **2016**, *361*, 177–184. [CrossRef]
66. Schasfoort, R.B.M. History and Physics of Surface Plasmon Resonance. In *Handbook of Surface Plasmon Resonance*, 2nd ed; Royal Society of Chemistry: Cambridge, UK, 2017; pp. 27–59.
67. Thakur, A.; Qiu, G.; NG, S.P.; Guan, J.; Yue, J.; Lee, Y.; Wu, C.M.L. Direct Detection of Two Different Tumor-Derived Extracellular Vesicles by SAM-AuNIs LSPR Biosensor. *Biosens. Bioelectron.* **2017**, *94*, 400–407. [CrossRef]
68. Morales-Luna, G.; Herrera-Domínguez, M.; Pisano, E.; Balderas-Elizalde, A.; Hernandez-Aranda, R.I.; Ornelas-Soto, N. Plasmonic Biosensor Based on an Effective Medium Theory as a Simple Tool to Predict and Analyze Refractive Index Changes. *Opt. Laser Technol.* **2020**, *131*, 106332. [CrossRef]
69. Hossain, M.B.; Rana, M.M. DNA Hybridization Detection Based on Resonance Frequency Readout in Graphene on Au SPR Biosensor. *J. Sens.* **2016**, *2016*, 6070742. [CrossRef]
70. Wu, L.; Jia, Y.; Jiang, L.; Guo, J.; Dai, X.; Xiang, Y.; Fan, D. Sensitivity Improved SPR Biosensor Based on the MoS2/Graphene-Aluminum Hybrid Structure. *J. Light. Technol.* **2017**, *35*, 82–87. [CrossRef]
71. Kelly, K.L.; Coronado, E.; Zhao, L.L.; Schatz, G.C. The Optical Properties of Metal Nanoparticles: The Influence of Size, Shape, and Dielectric Environment. *J. Phys. Chem. B* **2003**, *107*, 668–677. [CrossRef]
72. Fathi, F.; Rashidi, M.R.; Omidi, Y. Ultra-Sensitive Detection by Metal Nanoparticles-Mediated Enhanced SPR Biosensors. *Talanta* **2019**, *192*, 118–127. [CrossRef] [PubMed]
73. Hao, F.; Nehl, C.L.; Hafner, J.H.; Nordlander, P. Plasmon Resonances of a Gold Nanostar. *Nano Lett.* **2007**, *7*, 729–732. [CrossRef] [PubMed]
74. Xu, L.T.; Chen, M.; Weng, Y.H.; Xie, K.X.; Wang, J.; Cao, S.H.; Li, Y.Q. Label-Free Fluorescent Nanofilm Sensor Based on Surface Plasmon Coupled Emission: In Situ Monitoring the Growth of Metal-Organic Frameworks. *Anal. Chem.* **2022**, *94*, 6430–6435. [CrossRef]
75. Bhaskar, S.; Ramamurthy, S.S. Mobile Phone-Based Picomolar Detection of Tannic Acid on Nd2O3 Nanorod-Metal Thin-Film Interfaces. *ACS Appl. Nano Mater.* **2019**, *2*, 4613–4625. [CrossRef]
76. Vollmer, F.; Arnold, S.; Braun, D.; Teraoka, I.; Libchaber, A. Multiplexed DNA Quantification by Spectroscopic Shift of Two Microsphere Cavities. *Biophys. J.* **2003**, *85*, 1974–1979. [CrossRef]
77. Chen, C.; Wang, J. Optical Biosensors: An Exhaustive and Comprehensive Review. *Analyst* **2020**, *145*, 1605–1628. [CrossRef] [PubMed]
78. Talebi Fard, S.; Grist, S.M.; Donzella, V.; Schmidt, S.A.; Flueckiger, J.; Wang, X.; Shi, W.; Millspaugh, A.; Webb, M.; Ratner, D.M.; et al. Label-Free Silicon Photonic Biosensors for Use in Clinical Diagnostics. *Silicon Photonics VIII* **2013**, *8629*, 862909. [CrossRef]
79. Li, H.; Fan, X. Characterization of Sensing Capability of Optofluidic Ring Resonator Biosensors. *Appl. Phys. Lett.* **2010**, *97*, 11105. [CrossRef]
80. Yan, H.; Huang, L.; Xu, X.; Tang, N.; Chakravarty, S.; Chen, R.T. Enhanced Surface Sensitivity in Microring Resonator Biosensor Based on Subwavelength Grating Waveguides. *Front. Biol. Detect. Nanosensors Syst. IX* **2017**, *10081*, 100810G. [CrossRef]
81. Dey, S.; Dolci, M.; Zijlstra, P. Single-Molecule Optical Biosensing: Recent Advances and Future Challenges. *ACS Phys. Chem. Au* **2023**. [CrossRef]
82. Cheng, L.; Mao, S.; Li, Z.; Han, Y.; Fu, H.Y. Grating Couplers on Silicon Photonics: Design Principles, Emerging Trends and Practical Issues. *Micromachines* **2020**, *11*, 666. [CrossRef]

83. Wei, X.; Weiss, S.M. Guided Mode Biosensor Based on Grating Coupled Porous Silicon Waveguide. *Opt. Express* **2011**, *19*, 11330. [CrossRef] [PubMed]
84. Jiao, L.; Zhong, N.; Zhao, X.; Ma, S.; Fu, X.; Dong, D. Recent Advances in Fiber-Optic Evanescent Wave Sensors for Monitoring Organic and Inorganic Pollutants in Water. *TrAC Trends Anal. Chem.* **2020**, *127*, 115892. [CrossRef]
85. Sadani, K.; Nag, P.; Mukherji, S. LSPR Based Optical Fiber Sensor with Chitosan Capped Gold Nanoparticles on BSA for Trace Detection of Hg (II) in Water, Soil and Food Samples. *Biosens. Bioelectron.* **2019**, *134*, 90–96. [CrossRef]
86. Jeong, Y.; Kook, Y.M.; Lee, K.; Koh, W.G. Metal Enhanced Fluorescence (MEF) for Biosensors: General Approaches and a Review of Recent Developments. *Biosens. Bioelectron.* **2018**, *111*, 102–116. [CrossRef] [PubMed]
87. Benito-Peña, E.; Valdés, M.G.; Glahn-Martínez, B.; Moreno-Bondi, M.C. Fluorescence Based Fiber Optic and Planar Waveguide Biosensors. A Review. *Anal. Chim. Acta* **2016**, *943*, 17–40. [CrossRef] [PubMed]
88. Orellana, G. Fluorescence-Based Sensors. In *Optical Chemical Sensors*, 1st ed.; Springer: Dordrecht, The Netherlands, 2006; pp. 99–116. ISBN 978-1-4020-4611-7.
89. Liu, L.; Zhou, X.; Lu, M.; Zhang, M.; Yang, C.; Ma, R.; Memon, A.G.; Shi, H.; Qian, Y. An Array Fluorescent Biosensor Based on Planar Waveguide for Multi-Analyte Determination in Water Samples. *Sens. Actuators B Chem.* **2017**, *240*, 107–113. [CrossRef]
90. Scognamiglio, V.; Antonacci, A.; Arduini, F.; Moscone, D.; Campos, E.V.R.; Fraceto, L.F.; Palleschi, G. An Eco-Designed Paper-Based Algal Biosensor for Nanoformulated Herbicide Optical Detection. *J. Hazard. Mater.* **2019**, *373*, 483–492. [CrossRef]
91. Hayes, T.B.; Anderson, L.L.; Beasley, V.R.; De Solla, S.R.; Iguchi, T.; Ingraham, H.; Kestemont, P.; Kniewald, J.; Kniewald, Z.; Langlois, V.S.; et al. Demasculinization and Feminization of Male Gonads by Atrazine: Consistent Effects across Vertebrate Classes. *J. Steroid Biochem. Mol. Biol.* **2011**, *127*, 64–73. [CrossRef]
92. Smulders, C.J.G.M.; Bueters, T.J.H.; Vailati, S.; van Kleef, R.G.D.M.; Vijvergberg, H.P.M. Block of Neuronal Nicotinic Acetylcholine Receptors by Organophosphate Insecticides. *Toxicol. Sci.* **2004**, *82*, 545–554. [CrossRef] [PubMed]
93. Koukouvinos, G.; Tsialla, Z.; Petrou, P.S.; Misiakos, K.; Goustouridis, D.; Ucles Moreno, A.; Fernandez-Alba, A.R.; Raptis, I.; Kakabakos, S.E. Fast Simultaneous Detection of Three Pesticides by a White Light Reflectance Spectroscopy Sensing Platform. *Sens. Actuators B Chem.* **2017**, *238*, 1214–1223. [CrossRef]
94. Stavra, E.; Petrou, P.S.; Koukouvinos, G.; Kiritsis, C.; Pirmettis, I.; Papadopoulos, M.; Goustouridis, D.; Economou, A.; Misiakos, K.; Raptis, I.; et al. Simultaneous Determination of Paraquat and Atrazine in Water Samples with a White Light Reflectance Spectroscopy Biosensor. *J. Hazard. Mater.* **2018**, *359*, 67–75. [CrossRef]
95. Xiao-Hong, Z.; Bao-Dong, S.; Han-Chang, S.; Lan-Hua, L.; Hong-Li, G.; Miao, H. An Evanescent Wave Multi-Channel Immunosensor System for the Highly Sensitive Detection of Small Analytes in Water Samples. *Sens. Actuators B Chem.* **2014**, *198*, 150–156. [CrossRef]
96. Liu, R.; Guan, G.; Wang, S.; Zhang, Z. Core-Shell Nanostructured Molecular Imprinting Fluorescent Chemosensor for Selective Detection of Atrazine Herbicide. *Analyst* **2011**, *136*, 184–190. [CrossRef]
97. Kümmerer, K. Pharmaceuticals in the Environment. *Annu. Rev. Environ. Resour.* **2010**, *35*, 57–75. [CrossRef]
98. Sharma, V.K.; Johnson, N.; Cizmas, L.; McDonald, T.J.; Kim, H. A Review of the Influence of Treatment Strategies on Antibiotic Resistant Bacteria and Antibiotic Resistance Genes. *Chemosphere* **2016**, *150*, 702–714. [CrossRef]
99. Tomassetti, M.; Conta, G.; Campanella, L.; Favero, G.; Sanzò, G.; Mazzei, F.; Antiochia, R. A Flow SPR Immunosensor Based on a Sandwich Direct Method. *Biosensors* **2016**, *6*, 22. [CrossRef]
100. Steinke, N.; Döring, S.; Wuchrer, R.; Kroh, C.; Gerlach, G.; Härtling, T. Plasmonic Sensor for On-Site Detection of Diclofenac Molecules. *Sens. Actuators B Chem.* **2019**, *288*, 594–600. [CrossRef]
101. Altintas, Z.; France, B.; Ortiz, J.O.; Tothill, I.E. Computationally Modelled Receptors for Drug Monitoring Using an Optical Based Biomimetic SPR Sensor. *Sens. Actuators B Chem.* **2016**, *224*, 726–737. [CrossRef]
102. Luo, Q.; Yu, N.; Shi, C.; Wang, X.; Wu, J. Surface Plasmon Resonance Sensor for Antibiotics Detection Based on Photo-Initiated Polymerization Molecularly Imprinted Array. *Talanta* **2016**, *161*, 797–803. [CrossRef] [PubMed]
103. Weber, P.; Vogler, J.; Gauglitz, G. Development of an Optical Biosensor for the Detection of Antibiotics in the Environment. *Opt. Sensors* **2017**, *10231*, 102312L. [CrossRef]
104. Kumbhat, S.; Gehlot, R.; Sharma, K.; Singh, U.; Joshi, V. Surface Plasmon Resonance Based Indirect Immunoassay for Detection of 17β-Estradiol. *J. Pharm. Biomed. Anal.* **2019**, *163*, 211–216. [CrossRef] [PubMed]
105. Tan, Y.; Wei, T. Detection of 17β-Estradiol in Water Samples by a Novel Double-Layer Molecularly Imprinted Film-Based Biosensor. *Talanta* **2015**, *141*, 279–287. [CrossRef] [PubMed]
106. Yildirim, N.; Long, F.; Gao, C.; He, M.; Shi, H.-C.; Gu, A.Z. Aptamer-Based Optical Biosensor For Rapid and Sensitive Detection of 17β-Estradiol In Water Samples. *Environ. Sci. Technol.* **2012**, *46*, 3288–3294. [CrossRef] [PubMed]
107. Liu, L.H.; Zhou, X.H.; Xu, W.Q.; Song, B.D.; Shi, H.C. Highly Sensitive Detection of Sulfadimidine in Water and Dairy Products by Means of an Evanescent Wave Optical Biosensor. *RSC Adv.* **2014**, *4*, 60227–60233. [CrossRef]
108. Scott, I.M.; Kraft, L.J.; Parker, J.D.; Daniel, K.; Kustick, S.; Kennen, D.; McMurry, J.L. A Real Time Optical Biosensor Assay for Amoxicillin and Other β-Lactams in Water Samples. *Georg. J. Sci.* **2010**, *68*, 2010.
109. Sciacca, B.; Secret, E.; Pace, S.; Gonzalez, P.; Geobaldo, F.; Quignard, F.; Cunin, F. Chitosan-Functionalized Porous Silicon Optical Transducer for the Detection of Carboxylic Acid-Containing Drugs in Water. *J. Mater. Chem.* **2011**, *21*, 2294–2302. [CrossRef]

110. Stackelberg, P.E.; Furlong, E.T.; Meyer, M.T.; Zaugg, S.D.; Henderson, A.K.; Reissman, D.B. Persistence of Pharmaceutical Compounds and Other Organic Wastewater Contaminants in a Conventional Drinking-Water-Treatment Plant. *Sci. Total Environ.* **2004**, *329*, 99–113. [CrossRef]
111. Hegnerová, K.; Piliarik, M.; Šteinbachová, M.; Flegelová, Z.; Černohorská, H.; Homola, J. Detection of Bisphenol A Using a Novel Surface Plasmon Resonance Biosensor. *Anal. Bioanal. Chem.* **2010**, *398*, 1963–1966. [CrossRef]
112. Hegnerová, K.; Homola, J. Surface Plasmon Resonance Sensor for Detection of Bisphenol A in Drinking Water. *Sens. Actuators B Chem.* **2010**, *151*, 177–179. [CrossRef]
113. Ma, K.; Ekblad, T.; Koerkamp, M.K.; Kelderman, H.; van Wijlen, M.; Duarah, A.; Yue, J.; Zhang, L.; Wong, M.V.M.; Lim, M.H. Contaminant Detection in Treated Water Using Optiqua's MiniLab^{TM} Biosensing System: A Case Study for Bisphenol A. *Int. J. Environ. Anal. Chem.* **2015**, *95*, 366–378. [CrossRef]
114. Masdor, N.A.; Altintas, Z.; Tothill, I.E. Surface Plasmon Resonance Immunosensor for the Detection of Campylobacter Jejuni. *Chemosensors* **2017**, *5*, 16. [CrossRef]
115. Foudeh, A.M.; Trigui, H.; Mendis, N.; Faucher, S.P.; Veres, T.; Tabrizian, M. Rapid and Specific SPRi Detection of L. Pneumophila in Complex Environmental Water Samples. *Anal. Bioanal. Chem.* **2015**, *407*, 5541–5545. [CrossRef] [PubMed]
116. Zhou, C.; Zou, H.; Li, M.; Sun, C.; Ren, D.; Li, Y. Fiber Optic Surface Plasmon Resonance Sensor for Detection of E. Coli O157:H7 Based on Antimicrobial Peptides and AgNPs-RGO. *Biosens. Bioelectron.* **2018**, *117*, 347–353. [CrossRef]
117. Sanati, P.; Hashemi, S.S.; Bahadoran, M.; Babadi, A.A.; Akbari, E. Detection of Escherichia Coli K12 in Water Using Slot Waveguide in Cascaded Ring Resonator. *Silicon* **2022**, *14*, 851–857. [CrossRef]
118. Kim, D.W.; Chun, H.J.; Kim, J.H.; Yoon, H.; Yoon, H.C. A Non-Spectroscopic Optical Biosensor for the Detection of Pathogenic Salmonella Typhimurium Based on a Stem-Loop DNA Probe and Retro-Reflective Signaling. *Nano Converg.* **2019**, *6*, 16. [CrossRef]
119. Angelopoulou, M.; Petrou, P.; Misiakos, K.; Raptis, I.; Kakabakos, S. Simultaneous Detection of Salmonella Typhimurium and Escherichia Coli O157:H7 in Drinking Water with Mach–Zehnder Interferometers Monolithically Integrated on Silicon Chips †. *Eng. Proc.* **2022**, *16*, 12269. [CrossRef]
120. Nabok, A.; Al-Jawdah, A.M.; Gémes, B.; Takács, E.; Székács, A. An Optical Planar Waveguide-Based Immunosensors for Determination of Fusarium Mycotoxin Zearalenone. *Toxins* **2021**, *13*, 89. [CrossRef]
121. Yildirim, N.; Long, F.; Gu, A.Z. Aptamer Based E-Coli Detection in Waste Waters by Portable Optical Biosensor System. In Proceedings of the 2014 40th Annual Northeast Bioengineering Conference (NEBEC), Boston, MA, USA, 25–27 April 2014; pp. 1–3. [CrossRef]
122. Herranz, S.; Marazuela, M.D.; Moreno-Bondi, M.C. Automated Portable Array Biosensor for Multisample Microcystin Analysis in Freshwater Samples. *Biosens. Bioelectron.* **2012**, *33*, 50–55. [CrossRef]
123. Liu, M.; Zhao, H.; Chen, S.; Yu, H.; Quan, X. Colloidal Graphene as a Transducer in Homogeneous Fluorescence-Based Immunosensor for Rapid and Sensitive Analysis of Microcystin-LR. *Environ. Sci. Technol.* **2012**, *46*, 12567–12574. [CrossRef]
124. Shi, H.C.; Song, B.D.; Long, F.; Zhou, X.H.; He, M.; Lv, Q.; Yang, H.Y. Automated Online Optical Biosensing System for Continuous Real-Time Determination of Microcystin-LR with High Sensitivity and Specificity: Early Warning for Cyanotoxin Risk in Drinking Water Sources. *Environ. Sci. Technol.* **2013**, *47*, 4434–4441. [CrossRef] [PubMed]
125. Shi, Y.; Wu, J.; Sun, Y.; Zhang, Y.; Wen, Z.; Dai, H.; Wang, H.; Li, Z. A Graphene Oxide Based Biosensor for Microcystins Detection by Fluorescence Resonance Energy Transfer. *Biosens. Bioelectron.* **2012**, *38*, 31–36. [CrossRef] [PubMed]
126. Han, S.; Zhou, X.; Tang, Y.; He, M.; Zhang, X.; Shi, H.; Xiang, Y. Practical, Highly Sensitive, and Regenerable Evanescent-Wave Biosensor for Detection of Hg2+ and Pb2+ in Water. *Biosens. Bioelectron.* **2016**, *80*, 265–272. [CrossRef]
127. Gupta, S.; Sarkar, S.; Katranidis, A.; Bhattacharya, J. Development of a Cell-Free Optical Biosensor for Detection of a Broad Range of Mercury Contaminants in Water: A Plasmid DNA-Based Approach. *ACS Omega* **2019**, *4*, 9480–9487. [CrossRef] [PubMed]
128. Bismuth, M.; Zaltzer, E.; Muthukumar, D.; Suckeveriene, R.; Shtenberg, G. Real-Time Detection of Copper Contaminants in Environmental Water Using Porous Silicon Fabry-Pérot Interferometers. *Analyst* **2021**, *146*, 5160–5168. [CrossRef]
129. Kumar, D.N.; Reingewirtz, S.; Shemesh, M.; Suckeveriene, R.; Shtenberg, G. DNAzyme-Based Biosensor for Sub Ppb Lead Ions Detection Using Porous Silicon Fabry-Pérot Interferometer. *Sens. Actuators B Chem.* **2022**, *362*, 131761. [CrossRef]
130. Zhang, H.; Yang, L.; Zhou, B.; Liu, W.; Ge, J.; Wu, J.; Wang, Y.; Wang, P. Ultrasensitive and Selective Gold Film-Based Detection of Mercury (II) in Tap Water Using a Laser Scanning Confocal Imaging-Surface Plasmon Resonance System in Real Time. *Biosens. Bioelectron.* **2013**, *47*, 391–395. [CrossRef]
131. Chang, C.C.; Lin, S.; Wei, S.C.; Chen, C.Y.; Lin, C.W. An Amplified Surface Plasmon Resonance "Turn-on" Sensor for Mercury Ion Using Gold Nanoparticles. *Biosens. Bioelectron.* **2011**, *30*, 235–240. [CrossRef]
132. Yildirim, N.; Long, F.; He, M.; Gao, C.; Shi, H.C.; Gu, A.Z. A Portable DNAzyme-Based Optical Biosensor for Highly Sensitive and Selective Detection of Lead (II) in Water Sample. *Talanta* **2014**, *129*, 617–622. [CrossRef]
133. Long, F.; Gao, C.; Shi, H.C.; He, M.; Zhu, A.N.; Klibanov, A.M.; Gu, A.Z. Reusable Evanescent Wave DNA Biosensor for Rapid, Highly Sensitive, and Selective Detection of Mercury Ions. *Biosens. Bioelectron.* **2011**, *26*, 4018–4023. [CrossRef] [PubMed]
134. Long, F.; Zhu, A.; Shi, H.; Wang, H.; Liu, J. Rapid On-Site/in-Situ Detection of Heavy Metal Ions in Environmental Water Using a Structure-Switching DNA Optical Biosensor. *Sci. Rep.* **2013**, *3*, 1175. [CrossRef] [PubMed]
135. Shtenberg, G.; Massad-Ivanir, N.; Segal, E. Detection of Trace Heavy Metal Ions in Water by Nanostructured Porous Si Biosensors. *Analyst* **2015**, *140*, 4507–4514. [CrossRef] [PubMed]

136. Eltzov, E.; Yehuda, A.; Marks, R.S. Creation of a New Portable Biosensor for Water Toxicity Determination. *Sens. Actuators B Chem.* **2015**, *221*, 1044–1054. [CrossRef]
137. Xu, T.; Close, D.M.; Sayler, G.S.; Ripp, S. Genetically Modified Whole-Cell Bioreporters for Environmental Assessment. *Ecol. Indic.* **2013**, *28*, 125–141. [CrossRef]
138. Refaat, D.; Aggour, M.G.; Farghali, A.A.; Mahajan, R.; Wiklander, J.G.; Nicholls, I.A.; Piletsky, S.A. Strategies for Molecular Imprinting and the Evolution of MIP Nanoparticles as Plastic Antibodies—Synthesis and Applications. *Int. J. Mol. Sci.* **2019**, *20*, 6304. [CrossRef]
139. Parisi, O.I.; Francomano, F.; Dattilo, M.; Patitucci, F.; Prete, S.; Amone, F.; Puoci, F. The Evolution of Molecular Recognition: From Antibodies to Molecularly Imprinted Polymers (MIPs) as Artificial Counterpart. *J. Funct. Biomater.* **2022**, *13*, 12. [CrossRef]
140. Bhaskar, S.; Thacharakkal, D.; Ramamurthy, S.S.; Subramaniam, C. Metal-Dielectric Interfacial Engineering with Mesoporous Nano-Carbon Florets for 1000-Fold Fluorescence Enhancements: Smartphone-Enabled Visual Detection of Perindopril Erbumine at a Single-Molecular Level. *ACS Sustain. Chem. Eng.* **2023**, *11*, 78–91. [CrossRef]
141. Yuk, J.S.; Guignon, E.F.; Lynes, M.A. Highly Sensitive Grating Coupler-Based Surface Plasmon-Coupled Emission (SPCE) Biosensor for Immunoassay. *Analyst* **2013**, *138*, 2576–2582. [CrossRef]
142. Rai, A.; Bhaskar, S.; Ganesh, K.M.; Ramamurthy, S.S. Hottest Hotspots from the Coldest Cold: Welcome to Nano 4.0. *ACS Appl. Nano Mater.* **2022**, *5*, 12245–12264. [CrossRef]
143. Bhaskar, S.; Srinivasan, V.; Ramamurthy, S.S. Nd2O3-Ag Nanostructures for Plasmonic Biosensing, Antimicrobial, and Anticancer Applications. *ACS Appl. Nano Mater.* **2022**, *6*, 1129–1145. [CrossRef]
144. Gaddam, R.R.; Narayan, R.; Raju, K.V.S.N. Fluorescence Spectroscopy of Nanofillers and Their Polymer Nanocomposites. In *Spectroscopy of Polymer Nanocomposites*, 1st ed.; William Andrew Publishing: Norwich, NY, USA, 2016; pp. 158–180. ISBN 9780323401838.
145. Akkilic, N.; Geschwindner, S.; Höök, F. Single-Molecule Biosensors: Recent Advances and Applications. *Biosens. Bioelectron.* **2020**, *151*, 111944. [CrossRef]
146. Ruby, R. A Snapshot in Time: The Future in Filters for Cell Phones. *IEEE Microw. Mag.* **2015**, *16*, 46–59. [CrossRef]
147. Wang, H.; Heintzmann, R.; Diederich, B. The Power in Your Pocket—Uncover Smartphones for Use as Cutting-Edge Microscopic Instruments in Science and Research. *Adv. Opt. Technol.* **2021**, *10*, 89–108. [CrossRef]
148. McCracken, K.E.; Tat, T.; Paz, V.; Yoon, J.Y. Smartphone-Based Fluorescence Detection of Bisphenol A from Water Samples. *RSC Adv.* **2017**, *7*, 9237–9243. [CrossRef]
149. Zhang, Z.Y.; Liu, X.; Shen, L.; Chen, L.; Fang, W.H. Machine Learning with Multilevel Descriptors for Screening of Inorganic Nonlinear Optical Crystals. *J. Phys. Chem. C* **2021**, *125*, 25175–25188. [CrossRef]
150. Fairbairn, C.E.; Kang, D.; Bosch, N. Using Machine Learning for Real-Time BAC Estimation from a New-Generation Transdermal Biosensor in the Laboratory. *Drug Alcohol Depend.* **2020**, *216*, 108205. [CrossRef]
151. Arano-Martinez, J.A.; Martínez-González, C.L.; Salazar, M.I.; Torres-Torres, C. A Framework for Biosensors Assisted by Multiphoton Effects and Machine Learning. *Biosensors* **2022**, *12*, 710. [CrossRef]
152. Guo, Z.; Kang, Y.; Liang, S.; Zhang, J. Detection of Hg(II) in Adsorption Experiment by a Lateral Flow Biosensor Based on Streptavidin-Biotinylated DNA Probes Modified Gold Nanoparticles and Smartphone Reader. *Environ. Pollut.* **2020**, *266*, 115389. [CrossRef]

Chemosphere xxx (xxxx) 139156

Contents lists available at ScienceDirect

Chemosphere

journal homepage: www.elsevier.com/locate/chemosphere

Development of a surface plasmon resonance based immunosensor for diclofenac quantification in water

Marcela Herrera-Domínguez [a], Alexander S. Lambert [b], Gesuri Morales-Luna [c], Eduardo Pisano [d], Iris Aguilar-Hernandez [a], Jürgen Mahlknecht [a], Quan Cheng [b, **], Nancy Ornelas-Soto [a, *]

[a] Tecnologico de Monterrey, Escuela de Ingeniería y Ciencias, Ave. Eugenio Garza Sada 2501, Monterrey, NL, 64849, Mexico
[b] Department of Chemistry, University of California, Riverside, CA, 92521, USA
[c] Departamento de Física y Matemáticas, Universidad Iberoamericana, Ciudad de Mexico, Prolongación Paseo de La Reforma 880, Ciudad de Mexico, 01219, Mexico
[d] CONACYT – Centro de Investigación en Materiales Avanzados, S.C., Monterrey, Parque PIIT, 66628, Apodaca, Nuevo León, Mexico

ARTICLE INFO

Handling editor: Carlos Alberto Martínez-Huitle

Keywords:
Surface plasmon resonance
Optical biosensor
Diclofenac
Immunosensor
Emerging pollutants
Pharmaceuticals

ABSTRACT

A Surface Plasmon Resonance (SPR) biosensor based on an inhibition immunoassay was developed for the detection of diclofenac (DCF) in aqueous solution. Due to the small size of DCF, an hapten-protein conjugate was produced by coupling DCF to bovine serum albumin (BSA). DCF-BSA conjugate formation was confirmed via MALDI-TOF mass spectrometry. The resulting conjugate was immobilized onto the surface of a sensor fabricated via e-beam deposition of a 2 nm chromium adhesion layer followed by a 50 nm gold layer onto precleaned BK7 glass slides. Immobilization onto the nano thin gold surface was accomplished by covalent amide linkage through a self-assembled monolayer. Samples were composed of a mixture of antibody at a fixed concentration and DCF at different known concentrations in deionized water, causing the inhibition of *anti*-DCF on the sensor. The DCF-BSA was obtained with a ratio of 3 DCF molecules per BSA. A calibration curve was performed using concentrations between 2 and 32 μg L^{-1}. The curve was fitted using the Boltzmann equation, reaching a limit of detection (LOD) of 3.15 μg L^{-1} and limit of quantification (LOQ) of 10.52 μg L^{-1}, the inter-day precision was calculated and an RSD value of 1.96% was obtained; and analysis time of 10 min. The developed biosensor is a preliminary approach to the detection of DCF in environmental water samples, and the first SPR biosensor developed for DCF detection using a hapten-protein conjugate.

1. Introduction

Emerging contaminants (ECs) are compounds of diverse origins and chemical nature, for which no environmental or public health risks have been established. These contaminants include personal hygiene and household products, as well as pharmaceutical and industrial chemical compounds (Sauvé and Desrosiers, 2014). Diclofenac (DCF) is one of the most widely prescribed anti-inflammatory drugs worldwide and is also sold over the counter in several countries. Studies have revealed that the chronic exposure of marine species to the presence of DCF in their habitat causes alterations in tissues in vertebrates, changes in gill physiology that leads to affect the oxygen supply in fishes and generate oxidative stress in mollusks (Hoeger et al., 2005; Quinn et al., 2011; Sathishkumar et al., 2020). DCF has been found globally in surface water, groundwater, drinking water and wastewater, at concentrations ranging from less than 1 ng L^{-1} to 57 μg L^{-1} (Sathishkumar et al., 2020).

Detection and quantification of ECs typically imply the use of labor-intensive analytical methods such as gas chromatography (GC) or liquid chromatography (LC) complemented using specific detectors such as mass spectrometry (MS) (Comtois-Marotte et al., 2017; Richardson and Ternes, 2018). Chromatographic techniques, although accurate and reliable, can have some drawbacks. They require specialized equipment, highly skilled operators, and the use of high purity reagents and standards. In addition, extensive pretreatment or sample preparation steps may be required for the analysis of ECs at low concentrations, including sequential filtration, solid phase extraction, derivatization, among others. For example, in a comprehensive study by Kostich, Batt and Lazorchak analyzing the occurrence of ECs in samples from different wastewater treatment plants, it was emphasized that "because of the large number of sampling sites and chemical analytes, it was logistically too

* Corresponding author.
** Corresponding author.
E-mail addresses: quan.cheng@ucr.edu (Q. Cheng), ornel@tec.mx (N. Ornelas-Soto).

https://doi.org/10.1016/j.chemosphere.2023.139156
Received 6 December 2022; Received in revised form 26 May 2023; Accepted 5 June 2023
0045-6535/© 20XX

difficult and expensive to collect and analyze field blanks as well as duplicates from each location" (Kostich et al., 2014). This is especially relevant in Latin America (LA), due to the lack of information in this region about this type of pollutants.

So far, the presence of ECs has been studied in only a few countries, primarily Argentina, Brazil, Mexico, and Colombia, where ECs have been detected not only in wastewater, but also in surface, ground and drinking water (Peña-Guzmán et al., 2019). So far, in studies carried out in Latin America, DCF has been found in concentrations between at concentrations of 95–6360 ng L^{-1} in wastewater, 0.04–500 ng L^{-1} in surface water and an average concentration of 44275 ng L^{-1} in drinking water (Peña-Guzmán et al., 2019). Specifically in Mexico, DCF has been detected in groundwater at concentrations ranging from 1 to 130 ng L^{-1} (Peña-Guzmán et al., 2019), in hospital wastewater at 1.79 μg L^{-1} and in the influent of a wastewater treatment plant at 0.85 μg L^{-1} (Calderón et al., 2019). While in Brazil, two points of a river were sampled for six months and the concentrations of DCF varied between 0.01 and 0.19 mg L^{-1}, the latter being the highest concentrations (Veras et al., 2019). Among the emerging contaminants that have been analyzed in the region, DCF has some of the lowest reported concentrations in samples like surface waters. However, its constant presence in surface, ground and drinking water is a cause for concern, as this compound has a detection frequency between 70 and 100% (Calderón et al., 2019; Peña-Guzmán et al., 2019; Veras et al., 2019). Highly selective and simple analytical methods would not only help to facilitate the detection of target ECs, but it would promote access to information, which could in turn contribute to the regulation of ECs into water bodies. Presently, Brazil, Mexico and Argentina have published most of the literature on the presence of ECs in the environment, however, this research has not been used to develop regulatory measures (Souza et al., 2022).

Methodologies based on immunological reactions such as ELISA and its variants are high-throughput alternatives that have proven to be viable analytical tools for the quantification of analytes in different matrices (Zhang et al., 2017). Residues of the pesticide carbofuran have been detected in water, soil and food samples (Yang et al., 2008); the psychiatric drug carbamazepine has been found in water (Calisto et al., 2011) and the antimicrobial triclocarban was revealed in human blood, serum and urine (Ahn et al., 2012). Although ELISA is reliable, sensitive, and specific compared to other immunoassays, it also has certain drawbacks. Laboratory procedures are also laborious which leads to errors in the assay, multiplexing options are limited, centralized laboratory equipment is needed and markers are often required (Hosseini et al., 2018); for this reason, new methodologies are required that are simple to carry out and at the same time are sensitive, accurate and reliable.

Typically, an immunosensor comprises the attachment one of the immunological binding pairs to the sensor surface to monitor its reaction with the antigen or complementary antibody (Flanagan and Pantell, 2007). Currently, the use of immunosensors based on the surface plasmon resonance (SPR) phenomenon has extended its use to the development of biosensors in the medical, food and environmental fields (Lu et al., 2020; Souto et al., 2019; Zhou et al., 2019). In this context, the key feature of the immunoassay is the high affinity and specificity of the antibodies towards their counterpart, while SPR brings the ability to monitor surface reactions without relevant interference from the bulk of the solution, without the need to use labels, and allowing real-time monitoring.

In this work, we propose the development of an SPR immunosensor for the detection of DCF in aqueous samples. DCF is a small molecule (considering small molecules as those with a molecular weight ≤1000 Da) and molecules of this size, called haptens, have low to no antigenic response, so coupling to carrier macromolecules is required to promote the antibody response (Singh et al., 2004). The biosensor was designed as an inhibition immunoassay where DCF was first bound to BSA as a carrier protein. The DCF-BSA conjugate was made using the anhydride mixing method, which has been previously reported for other applications, for example, in the development of an immunochromatographic lateral flow strip test for the detection of DCF in medicinal wine samples (Yang et al., 2020). In this study, the DCF-BSA conjugate approach is used for the first time in an SPR sensor configuration. So far only one other work has been published for the detection of DCF in aqueous samples using an SPR immunosensor (Steinke et al., 2019). In said work, the SPR sensor was based on gold nanopillars fabricated in-house, and no modifications were made to the DCF molecule prior to the inhibition immunoassay. Therefore, the enhanced sensitivity of the sensor was solely provided by the nanofabricated tailored gold structures. In contrast, in the present work a chemical approach was used as follows: DCF was conjugated to a carrier protein (BSA) via the anhydride mixture method to ensure its immunodetection, and the gold SPR sensor was fabricated by depositing a simple 50 nm gold layer on a glass substrate. In this case, signal detection was defined by the correct conjugation between BSA and DCF, and the LOD (3.29 μg L^{-1}) was comparable with the only other studied published so far (1 μg L^{-1}). Therefore, we consider this work provides a valuable contribution, since levels of quantification comparable to the concentrations of DCF found in some environmental water samples were achieved with an accessible and straightforward method.

2. Materials and methods

2.1. Reagents

1,4-dioxane, tributylamine, isobutyl chloroformate, bovine serum albumin (BSA), diclofenac sodium salt, ethanol, 16-mercaptohexadecanoic (MHDA), 11- mercaptoundecanoic acid (MUD), ethanolamine, trifluoroacetic acid (TFA), acetonitrile and α-cyano-3,4-hydroxycinnamic acid (CHCA) were purchased from Sigma-Aldrich. *N*-(3-Dimethylaminopropyl)-*N*′-ethylcarbodiimide hydrochloride (EDC) and *N*-hydroxysulfosuccinimide (NHS) are from CHEM-IMPEX Int'l Inc, the antibody used was *Anti*-Diclofenac antibody rabbit polyclonal LS-C185241 purchased from LSBio.

2.2. DCF-BSA conjugate

The mixed anhydride method was used to couple DCF to BSA as a carrier protein (Gendloff et al., 1986). Briefly, 0.08 mmol of DFC in its acid form were dissolved in 5 mL of 1,4-dioxane, and tributylamine and isobutyl chloroformate were added in equimolar amounts. The mixture was allowed to react for 2 h at 4 °C. Then, 5 mL of BSA aqueous solution (pH 8.5) were dripped and stirred for 4 h at room temperature to allow the DCF to react with the free amine groups and bind via an amide bond. Finally, the resulting mixture was purified by dialysis for three days using a 12–14 kDa membrane, lyophilized and stored at −20 °C.

2.3. DCF-BSA conjugate characterization

An AB Sciex 5800 MALDI-TOF mass spectrometer was used to characterize the DCF-BSA conjugate. To carry out the analysis, a 1:1 mixture of 5% trifluoroacetic acid (TFA) aqueous solution and acetonitrile (ACN) was prepared, and 10 mg mL^{-1} of α-cyano-3,4-hydroxycinnamic acid (CHCA) were added to the mixture to obtain the ionization matrix. Then, 2 μL of the respective conjugate and unmodified protein (200 μg mL^{-1} both) were deposited on the MALDI-TOF plate; once the samples were dry, 2 μL of the matrix were added over. Spectra were acquired in the positive reflector mode with a laser intensity between 4700 and 5400. Four replicates per sample were placed in the dish, and at least five shots were taken per sample.

2.4. Diclofenac quantification by SPR

2.4.1. SPR setup

The dual-channel NanoSPR 6–321 spectrometer was used for all conventional SPR measurements. The device used a GaAs semiconductor laser light source (λ = 670 nm), a manufacturer-supplied prism of high refractive index (n = 1.61 and a 30 μL flow cell. 50 nm gold layer SPR substrates previously modified with a self-assembled monolayer (SAM) of alkanethiols were inserted, and online analysis was conducted in an angular scanning mode with a 17-degree angular window that tracked the resonance angle every 5 s while simultaneously collecting the angular spectrum.

2.4.2. Sensor functionalization

SPR substrates were fabricated by e-beam deposition of a 2 nm chromium adhesion layer followed by a 50 nm gold layer onto precleaned BK7 glass slides. Before functionalization, the sensors were rinsed with ethanol and dried under compressed air. The clean gold substrates were incubated overnight in a mixture of alkanethiols, 16-mercaptohexadecanoic acid and 11-mercaptoundecanol acid (1:10 M ratio), to form a SAM on the surface. Then, one chemically modified sensor was placed in the SPR device and 0.01 M PBS buffer was injected at a rate of 5 μL s^{-1} until the signal was stabilized. Subsequently, 80 μL of an EDC/NHS mixture were injected at a ratio of 0.3:0.1 M, and the mixture was incubated for 30 min. Next, 150 μL of the DCF-BSA conjugate at a concentration of 50 μg mL^{-1} were injected and incubated for 1.5 h until the signal stabilized. Finally, 80 μL of a 1 M aqueous ethanolamine solution were injected for 20 min; Fig. 1 shows a schematic of the functionalized sensor.

2.4.3. Antibody affinity test

Prior to analyte quantification, a test was performed to verify the affinity of the *anti*-DCF for the conjugate. *Anti*-DCF was injected into a functionalized sensor at concentrations of 10, 20, 40, 60, 80 and 100 μg mL^{-1}. The injections were performed consecutively with PBS buffer re-equilibration steps between each measurement. These tests were performed in triplicate.

2.4.4. Specificity test

An interference test was performed to determine the specificity of the biosensor and to rule out its interaction with naproxen, ibuprofen, and ketorolac, three common anti-inflammatory drugs. The analytes were injected on the functionalized surface of the biosensor. The injections were consecutive, with a concentration of 15 μg L^{-1} in ultrapure water and an incubation time of 10 min per injection.

2.4.5. Inhibition assay for DCF detection

For this assay, 2, 7, 12, 17, 22, 27 and 32 μg L^{-1} of DCF in PBS were preincubated with 40 μg mL^{-1} of *anti*-DCF in a total volume of 100 μL for 30 min. During preincubation, the antibody is bound to the analyte until equilibrium of the reaction is reached. After preincubation, 80 μL were injected and allowed to flow continuously over the sensor surface at a flow rate of 5 μL s^{-1} for 10 min and re-equilibrated with PBS buffer. Only antibodies with antigen-binding sites not occupied by analyte molecules are able to react with the functionalized sensor surface, as shown in Fig. 1, resulting in a signal inversely related to the analyte concentration in the sample. Experiments were performed in triplicate. For data analysis, results were normalized in terms of the mean and standard deviation.

3. Results and discussion

3.1. MALDI-TOF characterization

In the MALDI-TOF mass/charge spectra (found in supplementary information S1) the mass difference between the pure BSA and the conjugate is clearly observed, demonstrating that the conjugate was successfully formed, and according to our calculations, there were 3 DCF molecules per molecule of BSA. The same batch of DCF-BSA conjugate was used for all experiments, and no changes suggesting loss of stability were observed when carrying out the experiments.

3.2. Sensor functionalization

It is well known that the quality of the recognition element and the way it is immobilized onto the surface greatly impact the performance of an SPR biosensor. For the inhibition assay, the DCF-BSA conjugate was immobilized on the sensor surface, and to obtain a sufficiently high response, functionalization was carried out by activating the carboxyl groups. Initially, a half hour contact time between the DCF-BSA conjugate and the sensor was established. However, it was necessary to extend this step to reach saturation and stability. The ideal incubation time was determined as 1.5 h; additional information regarding the conditions established for the immobilization of the DCf-BSA can be found in the supplementary information. Fig. 2 (a) shows the sensogram in which a drop in the angle caused by the washing step, used to remove the molecules that were not covalently bound, is observed after

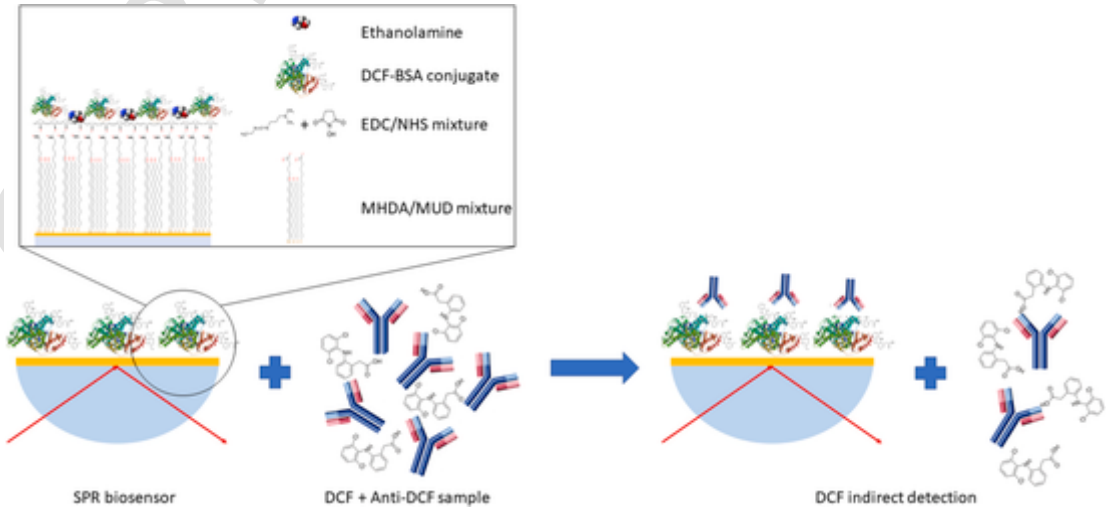

Fig. 1. Schematic of the functionalized surface of the biosensor and the inhibition immunoassay for DCF detection.

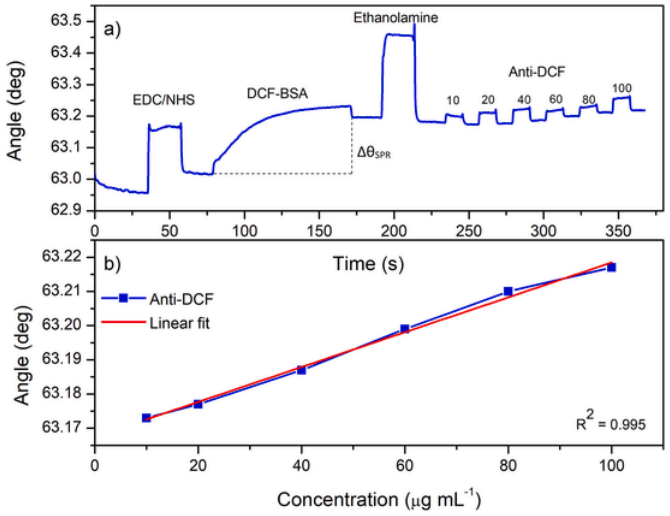

Fig. 2. A) Sensogram of the functionalization steps and the subsequent calibration curve performed with *anti*-DCF and b) linear fit from the *Anti*-DCF affinity test.

each functionalization stage. The change in the SPR angle before and after DCF-BSA conjugate injection ($\Delta\theta_{SPR}$) indicates an excellent immobilization due to the large increase in the angle. Finally, blocking with ethanolamine reduces non-specific binding of the analyte to the surface.

The % coverage can be estimated in terms of saturation; the change in angle after the total functionalization process (including hapten immobilization and ethanolamine blocking) is 0.194°, where the change in angle corresponding to the deposition of conjugate is 0.18° and the change by ethanolamine is 0.014°. Considering that ethanolamine has the function of occupying any place where the conjugate has not adhered, it can be inferred that the conjugate occupies 92.7% of the surface.

In a similar published work in which a hapten-protein conjugate was used for the detection of 17-β estradiol, several injections of the conjugate were carried out for its immobilization (four injections of 10, 50, 100 and 150 μg mL^{-1}), taking a total of 1 h to reach saturation (Kumbhat et al., 2019). The authors concluded that the same result could obtained in a single step by injecting the conjugate at 200 μg mL^{-1}. Hence, for future work it is proposed to increase the concentration of the conjugate and thus reduce the incubation time.

3.3. Antibody affinity test

To determine the affinity of the antibody towards the functionalized sensor, consecutive injections of *Anti*-DCF at different concentrations were performed. The objective of this test was to observe the behavior of the sensor with different concentrations of the antibody, as well as to assess possible sensor saturation after consecutive sample injections. A slight negative difference between the baseline before and after the first sample injection is observed in Fig. 2 (a), which may be due to the removal of molecules that were unable to covalently bind to the sensor surface. Subsequent injections confirmed that the antibody was indeed interacting and binding to the sensor.

As can be seen in the trend line, Fig. 2 (b), the change in SPR angle increases on average from the 40 μg mL^{-1} injection onwards and then remains almost constant. Therefore, to visualize a positive difference in the SPR angle after each injection, a higher concentration of antibody (40 μg mL^{-1}) was employed to perform the competitive assay. Antibody response had a linear behavior, indicating a direct relationship between antibody concentration and changes in the SPR angle. Furthermore, despite the increased concentrations, the sensor does not seem to reach a point of total saturation up to this point. This indicates that the sensor can be used to read several consecutive samples. Measurements were performed in triplicate and results were consistent for every replicate, thus demonstrating reproducibility.

3.4. Biosensor specificity

Fig. 3 shows the results from the interference test, where the response to naproxen, ibuprofen and ketorolac is observed as a drop in the angle. This drop is attributed to a change of medium (from buffer to ultrapure water), and after the incubation and washing steps, the baseline returns to its original value for naproxen and ibuprofen, indicating there is no interaction with BSA. Only ketorolac produced a change in the SPR angle, with a shift of 0.0032°, marked by the red line, this is because at the conditions at which the interferents were tested, the carboxyl group of ketorolac is more reactive towards BSA. An insert was added in Fig. 3 showing a fragment of the diclofenac detection curve; the angle shift for the lowest diclofenac concentration (2 μg L^{-1}) was 0.061°, showing that the interference of ketorolac (15 μg L^{-1}) is about 5%. However, it should be noted that after reviewing the limited available literature where the occurrence of ketorolac is analyzed in real samples, for example the case of hospital wastewater, the concentration of ketorolac was 0.47 μg L^{-1}, whereas a diclofenac concentration of 6.17 μg L^{-1} has been reported (Calderón et al., 2019; Oliveira et al., 2015). In general, regardless of the type of real environmental sample analyzed, a lower incidence of ketorolac is reported. Hence, interference by this pharmaceutical in real samples is expected to be insignificant.

3.5. Inhibition immunoassay

Due to the small size of DCF molecules, an indirect competitive (inhibition) assay was performed. Four repetitions of the assay were carried out, and results were normalized prior to data analysis. Fig. 4 shows the obtained calibration curve after a fit using the sigmoidal Boltzmann function (Xue et al., 2019) according to Equation (1). Consequential to the fit used, an R2-value of 0.99 was obtained. For the calculation of LOD and LOQ, the 3SD and 10SD criteria were used, resulting in 3.15 μg L^{-1} and 10.52 μg L^{-1} respectively. The detection range is 2–32 μg L^{-1}, corresponding to the concentrations tested during the assay. The precision of the method was evaluated in terms of repeatability (inter-day) and was expressed as the percentage of the Relative Standard Deviation (RSD%), for which a value of 1.96% was obtained, as

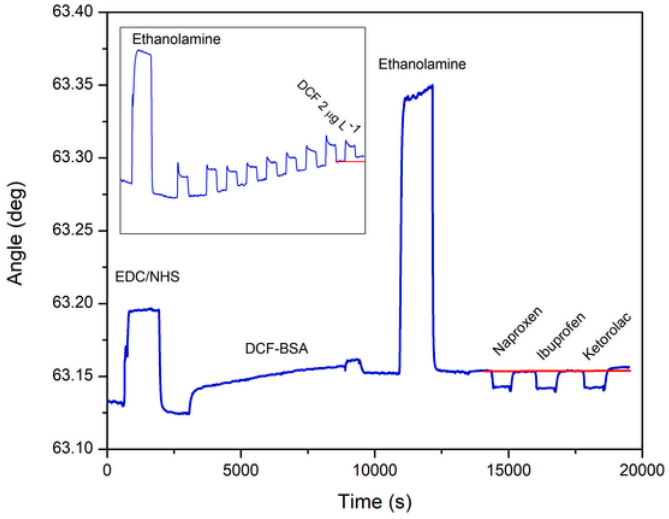

Fig. 3. Interference test sensogram. Naproxen, ibuprofen, and ketorolac in ultrapure water were tested. Inset shows a section of the DCF detection curve.

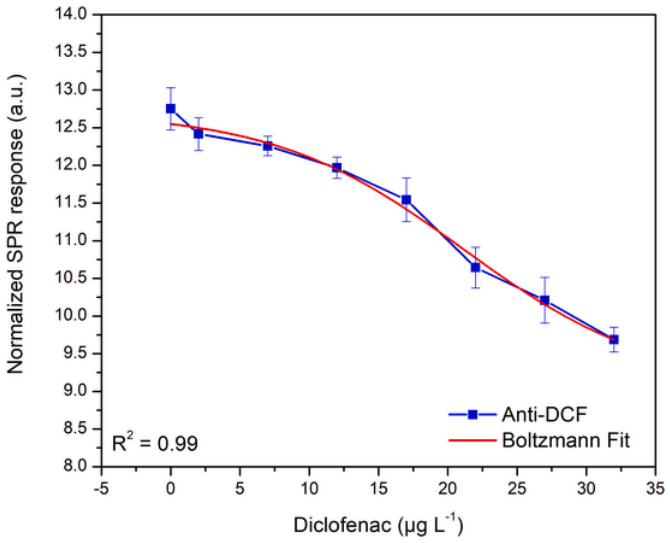

Fig. 4. Calibration curve from the competitive assay for the detection of DCF.

can be seen in the error bars in Fig. 4. Finally, the analysis time per sample is 10 min.

$$y = 9.06 + \frac{12.71 - 9.06}{1 + e^{\frac{x-21.12}{6.88}}} \quad (1)$$

Equation (1). Boltzmann function used for fitting.

A search of previously published papers for the detection of DCF by SPR was performed and only one article was found. Hence, the search was extended to other techniques involving other types of biosensors, the information from these papers is given in Table 1. Most of these works do not report all the analytical data, being the QCM based biosensor the only one that is comparable in terms of LOD with the biosensor developed here (2.8 and 3.15 μg L-1 respectively). The SPR biosensor shows an advantage in measurement time, achieving detection in only 10 min compared to 60 min for QCM. In addition, we found studies that have lower LOD like the work reported by Okoth et al. (2018) and others with higher LOD like the work performed by Guenther et al. (2019). The lowest LOD corresponds to a photoelectrochemical biosensor, which in addition to the biological element, is functionalized with CdS-doped graphene and gold nanoparticles, making it a complex system, which instead of the typical electrochemical station requires an external lamp to induce the photocurrent. On the other hand, the measurement time is much longer (90 min) than that required for this SPR biosensor (10 min).

To the best of our knowledge, only one work has addressed the use of an SPR immunosensor for DCF, in which a sensor with imprinted nanopillars was used (Steinke et al., 2019). In that work, DCF molecules were directly deposited on the sensor and an inhibition immunoassay was performed. The authors reported a detection range of 1 μg L^{-1} and 10 μg L^{-1}, and the LOD obtained herein (3.29 μg L^{-1}) is comparable to their results. The main differences between both works are (a) the immobilization strategy, i.e., pure DCF instead of a DCF hapten-protein conjugate, and (b) the use of nanostructured sensors based on nanopillars by Steinke et al. instead of a gold coated glass slide. The nanopillars intensify the SPR signal therefore eliminating the need for conjugating DCF to a bigger molecule, while in contrast in this work similar detection limits were reached without having to design complex nanostructures since the conjugate improves sensitivity. Having a biosensor whose configuration is simpler is highly advantageous in terms of accessibility, as it can reduce production time and costs and infrastructure requirements.

The DCF concentrations used during the study are close to the values reported previously in some works, especially those that sampled wastewater and for the Latin American region. Table 2 summarizes the DCF values reported in other works, indicating the country of origin and the type of water sampled. Therefore, it can be inferred that these results are a good first approximation to the detection of DCF in environmental aqueous samples using a rapid and simple analytical method.

The disparity in DCF concentrations between these two regions could be attributed to poor waste management and lack of regulation for emerging pollutants. Moreover, diclofenac prescription has undergone regulatory label changes in some European countries (Morales et al., 2021), while it's still an over-the-counter medication in LA, suggesting a higher overall consumption. In the case of Mexico for example, after an exhaustive review, only six works were found where diclofenac was quantified in environmental water samples. Three of these studies worked with fortified samples (Calderón et al., 2019; Félix-Cañedo et al., 2013; Rivera-Jaimes et al., 2018). The three works where real samples were analyzed are from 2011 to 2019, and focused on highly localized sampling points (i.e., the sampling campaigns were limited and might not represent the overall concentration in the country) (Arguello-Pérez et al., 2019; Chávez et al., 2011; Isaac-Olivé and Navarro-Frómeta, 2019). This indicates that the values in Table 2 should not be used yet as a definitive reference framework, as more studies are needed to generate significant information on real environmental concentrations in México. In Latin American countries where more research regarding emerging pollutants has been carried out, such as Brazil, environmental concentration ranges from 19 to 193 μg/L can be found. Given the high concentrations of ECs, biosensors could be a viable alternative in LA countries for fast quantification of this pollutant.

4. Conclusions

A DCF-BSA conjugate was developed for the detection of DCF. The conjugate was successfully synthesized, achieving binding of approximately 3 DCF molecules to each BSA molecule. The biosensor showed specificity towards DCF since other anti-inflammatory drugs such as ibuprofen and naproxen could not bind to the surface, only ketorolac showed affinity for the biosensor. However, interference by ketorolac is not significant since its concentrations in ambient water are minimal. The SPR biosensor fabricated using the DCF-BSA conjugate was able to detect DCF in concentrations of parts per billion, which are in the same order of magnitude than those quantified in wastewater, with a LOD of 3.15 μg L^{-1} and LOQ of 10.52 μg L^{-1}, the measurements were performed in a time of 10 min and with a RSD of 1.96%, which improves

Table 1
Comparison between biosensors developed for DCF detection.

Biosensor type	LOD μg L^{-1}	LOQ μg L^{-1}	Range μg L^{-1}	SD (%)	Analysis time	Sample tested	Reference
SPR	**3.15**	**10.52**	**2–32**	**1.96**	**10 min**	**Deionized water**	**This work**
Photoelectrochemical	0.23	–	0.29–44.4	2.92	90 min	Lake water	Okoth et al. (2018)
Optical/impedimetric	180	–	1970–21700	–	0.5 min	Deionized water	Guenther et al. (2019)
Fluorescence	–	–	2961.4–14807.4	–	12 h	Wastewater	Schirmer et al. (2019)
SPR (with nanostructures)	–	–	1–10	–	–	Deionized water	Steinke et al. (2019)
QCM	2.8	4.5	4.4–13.6	–	60 min	River water	Mazouzi et al. (2021)

Table 2
Reported DCF concentrations in water samples in Latin America and Europe.

Country	Sample	Concentration μg L^{-1}	Reference
Mexico	Hospital wastewater	6.17	Calderón et al. (2019)
	Urban wastewater	5.47	
	Tap water	4.51	
Brazil	River	19 to 193	Veras et al. (2019)
Colombia	River 1	12.20–67.54	Gallego-Ríos and Peñuela (2021)
	River 2	0.68–7.29	
Colombia	Hospital wastewater	1.72	Botero-Coy et al. (2018)
	Wastewater influent	0.40	
Antarctic Peninsula	Stream	0.077–7.76	González-Alonso et al. (2017)
	Wastewater	15.08	
Germany	Wastewater	0.14–2.4	Deng et al. (2003)
Portugal	Seawater	0.002–0.004	Paíga et al. (2017)
France	Groundwater	0.005	Vulliet and Cren-Olivé (2011)
	Surface water	0.01	
Italy	River water	0.1	Patrolecco et al. (2013)
	Wastewater influent	0.21	
	Wastewater effluent	0.11	
Switzerland	Wastewater effluent	0.99	Tixier et al. (2003)

the results of previous published works. Moreover, compared to the only other SPR biosensor built for the quantification of this molecule, detection limits and ranges were analogous considering the different approach used in each case (i.e., nanofabricated structures vs. a chemical-based method). An advantage of a chemical-based method is that there is little to no requirement for specialized infrastructure (e.g., clean rooms) or expensive top-down nanofabrication equipment, which can translate into higher accessibility, especially for Latin America (Kumar et al., 2018). The developed biosensor should be able to easily DCF present in water samples, although research will continue to improve the biosensor. Moreover, we believe the results from this work are highly valuable as they could be combined with the metal-nanostructures approach to obtain superior detection limits.

Credit authorship contribution statement

Marcela Herrera Domínguez: Formal analysis, Investigation, Writing – original draft. Alexander S. Lambert: Validation, Methodology, Supervision., Gesuri Morales-Luna: Formal analysis, Validation, Writing – review & editing, Eduardo Pisano: Formal analysis, Validation, Iris Aguilar Hernández: Writing – review & editing, Visualization, Jürgen Mahlknecht: Resources, Funding acquisition, Quan Cheng: Methodology, Validation, Resources, Supervision, Nancy Ornelas-Soto: Conceptualization, Methodology, Resources, Supervision, Project administration.

Declaration of competing interest

The authors declare that they have no known competing financial interests or personal relationships that could have appeared to influence the work reported in this paper.

Data availability

Data will be made available on request.

Acknowledgments

The authors would like to acknowledge the National Council of Science and Technology of Mexico (CONACyT) for grant # PN 2016-4320 and scholarship #855128. Financial support from UC-Mexus CONACyT collaborative grants (grant # CN-20-258) is greatly appreciated. The Chair of Circular Economy of Water FEMSA at Tecnologico de Monterrey is thanked for providing complementary funds; FEMSA had no role in the study design, data collection and analysis, decision to publish, or preparation of the manuscript.

References

Ahn, K.C., Kasagami, T., Tsai, H.J., Schebb, N.H., Ogunyoku, T., Gee, S.J., Young, T.M., Hammock, B.D., 2012. An immunoassay to evaluate human/environmental exposure to the antimicrobial triclocarban. Environ. Sci. Technol. 46, 374–381. https://doi.org/10.1021/es202494d.

Arguello-Pérez, M. ángel, Mendoza-Pérez, J.A., Tintos-Gómez, A., Ramírez-Ayala, E., Godínez-Domínguez, E., Silva-Bátiz, F. de A., 2019. Ecotoxicological analysis of emerging contaminants from wastewater discharges in the Coastal Zone of Cihuatlán (Jalisco, Mexico). Water (Switzerland) 11, 1386. https://doi.org/10.3390/w11071386.

Botero-Coy, A.M., Martínez-Pachón, D., Boix, C., Rincón, R.J., Castillo, N., Arias-Marín, L.P., Manrique-Losada, L., Torres-Palma, R., Moncayo-Lasso, A., Hernández, F., 2018. 'An investigation into the occurrence and removal of pharmaceuticals in Colombian wastewater. Sci. Total Environ. 642, 842–853. https://doi.org/10.1016/j.scitotenv.2018.06.088.

Calderón, A., Meraz, M., Tomasini, A., 2019. Pharmaceuticals present in urban and hospital wastewaters in Mexico city. J. Water Chem. Technol. 41, 105–112. https://doi.org/10.3103/s1063455x19020073.

Calisto, V., Bahlmann, A., Schneider, R.J., Esteves, V.I., 2011. Application of an ELISA to the quantification of carbamazepine in ground, surface and wastewaters and validation with LC-MS/MS. Chemosphere 84, 1708–1715. https://doi.org/10.1016/j.chemosphere.2011.04.072.

Chávez, A., Maya, C., Gibson, R., Jiménez, B., 2011. The removal of microorganisms and organic micropollutants from wastewater during infiltration to aquifers after irrigation of farmland in the Tula Valley, Mexico. Environ. Pollut. 159, 1354–1362. https://doi.org/10.1016/j.envpol.2011.01.008.

Comtois-Marotte, S., Chappuis, T., Vo Duy, S., Gilbert, N., Lajeunesse, A., Taktek, S., Desrosiers, M., Veilleux, É., Sauvé, S., 2017. Analysis of emerging contaminants in water and solid samples using high resolution mass spectrometry with a Q Exactive orbital ion trap and estrogenic activity with YES-assay. Chemosphere 166, 400–411. https://doi.org/10.1016/j.chemosphere.2016.09.077.

Deng, A., Himmelsbach, M., Zhu, Q.Z., Frey, S., Sengl, M., Buchberger, W., Niessner, R., Knopp, D., 2003. Residue analysis of the pharmaceutical diclofenac in different water types using ELISA and GC-MS. Environ. Sci. Technol. 37, 3422–3429. https://doi.org/10.1021/es0341945.

Félix-Cañedo, T.E., Durán-Álvarez, J.C., Jiménez-Cisneros, B., 2013. The occurrence and distribution of a group of organic micropollutants in Mexico City's water sources. Sci. Total Environ. 454, 109–118. https://doi.org/10.1016/j.scitotenv.2013.02.088. . –455. .

Flanagan, M.T., Pantell, R.H., 2007. Surface plasmon resonance and immunosensors. Electron. Lett. 20, 968. https://doi.org/10.1049/el:19840660.

Gallego-Ríos, S.E., Peñuela, G.A., 2021. Evaluation of ibuprofen and diclofenac in the main rivers of Colombia and striped catfish Pseudoplatystoma magdaleniatum. Environ. Monit. Assess. 193, 1–17. https://doi.org/10.1007/s10661-021-08922-5.

Gendloff, E.H., Casale, W.L., Ram, B.P., Tai, J.H., Pestka, J.J., Hart, L.P., 1986. Hapten-protein conjugates prepared by the mixed anhydride method. Cross-reactive antibodies in heterologous antisera. J. Immunol. Methods 92, 15–20. https://doi.org/10.1016/0022-1759(86)90497-7.

González-Alonso, S., Merino, L.M., Esteban, S., López de Alda, M., Barceló, D., Durán, J.J., López-Martínez, J., Aceña, J., Pérez, S., Mastroianni, N., Silva, A., Catalá, M., Valcárcel, Y., 2017. Occurrence of pharmaceutical, recreational and psychotropic drug residues in surface water on the northern Antarctic Peninsula region. Environ. Pollut. 229, 241–254. https://doi.org/10.1016/j.envpol.2017.05.060.

Guenther, M., Altenkirch, F., Ostermann, K., Rödel, G., Tobehn-Steinhäuser, I., Herbst, S., Görlandt, S., Gerlach, G., 2019. Optical and impedimetric study of genetically modified cells for diclofenac sensing. J. Sensors Sens. Syst. 8, 215–222. https://doi.org/10.5194/jsss-8-215-2019.

Hoeger, B., Köllner, B., Dietrich, D.R., Hitzfeld, B., 2005. Water-borne diclofenac affects kidney and gill integrity and selected immune parameters in brown trout (Salmo trutta f. fario). Aquat. Toxicol. 75, 53–64. https://doi.org/10.1016/j.aquatox.2005.07.006.

Hosseini, S., Vázquez-Villegas, P., Rito-Palomares, M., Martinez-Chapa, S.O., 2018. Advantages, Disadvantages and modifications of conventional ELISA. SpringerBriefs Appl. Sci. Technol. 67–115. https://doi.org/10.1007/978-981-10-6766-2_5/COVER.

Isaac-Olivé, K., Navarro-Frómeta, A.E., 2019. Detection of pharmaceuticals in the environment. In: Handbook of Environmental Chemistry. Springer Verlag, pp. 57–74. https://doi.org/10.1007/698_2017_165.

Kostich, M.S., Batt, A.L., Lazorchak, J.M., 2014. Concentrations of prioritized pharmaceuticals in effluents from 50 large wastewater treatment plants in the US and implications for risk estimation. Environ. Pollut. 184, 354–359. https://doi.org/

10.1016/j.envpol.2013.09.013.
Kumar, S., Bhushan, P., Bhattacharya, S., 2018. Fabrication of nanostructures with bottom-up approach and their utility in diagnostics, therapeutics, and others. In: Energy, Environment, and Sustainability. Springer Nature, pp. 167–198. https://doi.org/10.1007/978-981-10-7751-7_8.
Kumbhat, S., Gehlot, R., Sharma, K., Singh, U., Joshi, V., 2019. Surface plasmon resonance based indirect immunoassay for detection of 17β-estradiol. J. Pharm. Biomed. Anal. 163, 211–216. https://doi.org/10.1016/j.jpba.2018.10.015.
Lu, X., Sun, J., Sun, X., 2020. Recent advances in biosensors for the detection of estrogens in the environment and food. TrAC, Trends Anal. Chem. 127, 115882. https://doi.org/10.1016/J.TRAC.2020.115882.
Mazouzi, Y., Miche, A., Loiseau, A., Beito, B., Méthivier, C., Knopp, D., Salmain, M., Boujday, S., 2021. Design and analytical performances of a diclofenac biosensor for water Resources monitoring. ACS Sens. 6, 3485–3493. https://doi.org/10.1021/acssensors.1c01607.
Morales, D.R., Morant, S.V., MacDonald, T.M., Hallas, J., Ernst, M.T., Pottegard, A., Herings, R.M.C., Smits, E., Overbeek, J.A., Mackenzie, I.S., Doney, A.S.F., Mitchell, L., Bennie, M., Robertson, C., Wei, L., Nicholson, L., Morris, C., Flynn, R.W.V., 2021. Impact of EU regulatory label changes for diclofenac in people with cardiovascular disease in four countries: interrupted time series regression analysis. Br. J. Clin. Pharmacol. 87, 1129–1140. https://doi.org/10.1111/bcp.14478.
Okoth, O.K., Yan, K., Feng, J., Zhang, J., 2018. Label-free photoelectrochemical aptasensing of diclofenac based on gold nanoparticles and graphene-doped CdS. Sensor. Actuator. B Chem. 256, 334–341. https://doi.org/10.1016/j.snb.2017.10.089.
Oliveira, T.S., Murphy, M., Mendola, N., Wong, V., Carlson, D., Waring, L., 2015. Characterization of Pharmaceuticals and Personal Care products in hospital effluent and waste water influent/effluent by direct-injection LC-MS-MS. Sci. Total Environ. 518–519, 459–478. https://doi.org/10.1016/j.scitotenv.2015.02.104.
Paíga, P., Santos, L.H.M.L.M., Delerue-Matos, C., 2017. Development of a multi-residue method for the determination of human and veterinary pharmaceuticals and some of their metabolites in aqueous environmental matrices by SPE-UHPLC–MS/MS. J. Pharm. Biomed. Anal. 135, 75–86. https://doi.org/10.1016/j.jpba.2016.12.013.
Patrolecco, L., Ademollo, N., Grenni, P., Tolomei, A., Barra Caracciolo, A., Capri, S., 2013. Simultaneous determination of human pharmaceuticals in water samples by solid phase extraction and HPLC with UV-fluorescence detection. Microchem. J. 107, 165–171. https://doi.org/10.1016/j.microc.2012.05.035.
Peña-Guzmán, C., Ulloa-Sánchez, S., Mora, K., Helena-Bustos, R., Lopez-Barrera, E., Alvarez, J., Rodriguez-Pinzón, M., 2019. Emerging pollutants in the urban water cycle in Latin America: a review of the current literature. J. Environ. Manag. 237, 408–423. https://doi.org/10.1016/j.jenvman.2019.02.100.
Quinn, B., Schmidt, W., O'Rourke, K., Hernan, R., 2011. Effects of the pharmaceuticals gemfibrozil and diclofenac on biomarker expression in the zebra mussel (Dreissena polymorpha) and their comparison with standardised toxicity tests. Chemosphere 84, 657–663. https://doi.org/10.1016/j.chemosphere.2011.03.033.
Richardson, S.D., Ternes, T.A., 2018. Water analysis: emerging contaminants and current issues. Anal. Chem. 90, 398–428. https://doi.org/10.1021/acs.analchem.7b04577.
Rivera-Jaimes, J.A., Postigo, C., Melgoza-Alemán, R.M., Aceña, J., Barceló, D., López de Alda, M., 2018. Study of pharmaceuticals in surface and wastewater from Cuernavaca, Morelos, Mexico: occurrence and environmental risk assessment. Sci. Total Environ. 613–614, 1263–1274. https://doi.org/10.1016/j.scitotenv.2017.09.134.
Sathishkumar, P., Meena, R.A.A., Palanisami, T., Ashokkumar, V., Palvannan, T., Gu, F.L., 2020. Occurrence, interactive effects and ecological risk of diclofenac in environmental compartments and biota - a review. Sci. Total Environ. https://doi.org/10.1016/j.scitotenv.2019.134057.
Sauvé, S., Desrosiers, M., 2014. A review of what is an emerging contaminant. Chem. Cent. J. 8, 15. https://doi.org/10.1186/1752-153X-8-15.
Schirmer, C., Posseckardt, J., Schröder, M., Gläser, M., Howitz, S., Scharff, W., Mertig, M., 2019. Portable and low-cost biosensor towards on-site detection of diclofenac in wastewater. Talanta 203, 242–247. https://doi.org/10.1016/j.talanta.2019.05.058.
Singh, K.V., Kaur, J., Varshney, G.C., Raje, M., Suri, C.R., 2004. Synthesis and characterization of hapten-protein conjugates for antibody production against small molecules. Bioconjugate Chem. 15, 168–173. https://doi.org/10.1021/bc034158v.
Souto, D.E.P., Volpe, J., Gonçalves, C. de C., Ramos, C.H.I., Kubota, L.T., 2019. A brief review on the strategy of developing SPR-based biosensors for application to the diagnosis of neglected tropical diseases. Talanta 205, 120122. https://doi.org/10.1016/J.TALANTA.2019.120122.
Souza, M.C.O., Rocha, B.A., Adeyemi, J.A., Nadal, M., Domingo, J.L., Barbosa, F., 2022. Legacy and emerging pollutants in Latin America: a critical review of occurrence and levels in environmental and food samples. Sci. Total Environ. 848. https://doi.org/10.1016/j.scitotenv.2022.157774.
Steinke, N., Döring, S., Wuchrer, R., Kroh, C., Gerlach, G., Härtling, T., 2019. Plasmonic sensor for on-site detection of diclofenac molecules. Sensor. Actuator. B Chem. 288, 594–600. https://doi.org/10.1016/j.snb.2019.02.069.
Tixier, C., Singer, H.P., Oellers, S., Müller, S.R., 2003. Occurrence and fate of carbamazepine, clofibric acid, diclofenac, ibuprofen, ketoprofen, and naproxen in surface waters. Environ. Sci. Technol. 37, 1061–1068. https://doi.org/10.1021/es025834r.
Veras, T.B., Luiz Ribeiro de Paiva, A., Duarte, M.M.M.B., Napoleão, D.C., da Silva Pereira Cabral, J.J., 2019. Analysis of the presence of anti-inflammatories drugs in surface water: a case study in Beberibe river - PE, Brazil. Chemosphere 222, 961–969. https://doi.org/10.1016/j.chemosphere.2019.01.167.
Vulliet, E., Cren-Olivé, C., 2011. Screening of pharmaceuticals and hormones at the regional scale, in surface and groundwaters intended to human consumption. Environ. Pollut. 159, 2929–2934. https://doi.org/10.1016/J.ENVPOL.2011.04.033.
Xue, C.S., Erika, G., Jiří, H., 2019. Surface plasmon resonance biosensor for the ultrasensitive detection of bisphenol A. Anal. Bioanal. Chem. 411, 5655–5658. https://doi.org/10.1007/s00216-019-01996-8.
Yang, J., Wang, H., Jiang, Y., Sun, Y., Pan, K., Lei, H., Wu, Q., Shen, Y., Xiao, Z., Xu, Z., 2008. Development of an enzyme-linked immuno-sorbent assay (ELISA) method for carbofuran residues. Molecules 13, 871–881. https://doi.org/10.3390/molecules13040871.
Yang, X., Wang, Y., Yang, J., Sun, Z., Chu, C., Yue, Z., Li, L., Hu, X., 2020. Development of an immunochromatographic lateral flow strip test for the rapid detection of diclofenac in medicinal wine. Food Agric. Immunol. 31, 205–216. https://doi.org/10.1080/09540105.2020.1712331.
Zhang, Z., Zeng, K., Liu, J., 2017. Immunochemical detection of emerging organic contaminants in environmental waters. TrAC, Trends Anal. Chem. 87, 49–57. https://doi.org/10.1016/j.trac.2016.12.002.
Zhou, J., Qi, Q., Wang, C., Qian, Y., Liu, G., Wang, Y., Fu, L., 2019. Surface plasmon resonance (SPR) biosensors for food allergen detection in food matrices. Biosens. Bioelectron. 142, 111449. https://doi.org/10.1016/J.BIOS.2019.111449.

sensors

MDPI

Article

Detection of Acetaminophen in Groundwater by Laccase-Based Amperometric Biosensors Using MoS_2 Modified Carbon Paper Electrodes

Marcela Herrera-Domínguez [1], Koun Lim [2], Iris Aguilar-Hernández [1], Alejandra García-García [3], Shelley D. Minteer [2], Nancy Ornelas-Soto [1,*] and Raúl Garcia-Morales [4,*]

[1] Laboratorio de Nanotecnología Ambiental, Escuela de Ingeniería y Ciencias, Tecnológico de Monterrey, Ave. Eugenio Garza Sada 2501, Monterrey 64849, NL, Mexico
[2] Department of Chemistry and Materials Science & Engineering, University of Utah, Salt Lake City, UT 84112, USA
[3] Laboratorio de Síntesis y Modificación de Nanoestructuras y Materiales Bidimensionales, Centro de Investigación en Materiales Avanzados S.C., Unidad Monterrey, Parque PIIT, Apodaca 66628, NL, Mexico
[4] Centro de Nanociencias y Nanotecnología, Universidad Nacional Autónoma de México, Carretera Tijuana-Ensenada Km. 107, Ensenada 22860, BC, Mexico
* Correspondence: ornel@tec.mx (N.O.-S.); raul.garmo@ens.cnyn.unam.mx (R.G.-M.)

Abstract: The use of enzyme-based biosensors for the detection and quantification of analytes of interest such as contaminants of emerging concern, including over-the-counter medication, provides an attractive alternative compared to more established techniques. However, their direct application to real environmental matrices is still under investigation due to the various drawbacks in their implementation. Here, we report the development of bioelectrodes using laccase enzymes immobilized onto carbon paper electrodes modified with nanostructured molybdenum disulfide (MoS_2). The laccase enzymes were two isoforms (LacI and LacII) produced and purified from the fungus *Pycnoporus sanguineus* CS43 that is native to Mexico. A commercial purified enzyme from the fungus *Trametes versicolor* (TvL) was also evaluated to compare their performance. The developed bioelectrodes were used in the biosensing of acetaminophen, a drug widely used to relieve fever and pain, and of which there is recent concern about its effect on the environment after its final disposal. The use of MoS_2 as a transducer modifier was evaluated, and it was found that the best detection was achieved using a concentration of 1 mg/mL. Moreover, it was found that the laccase with the best biosensing efficiency was LacII, which achieved an LOD of 0.2 µM and a sensitivity of 0.108 µA/µM cm^2 in the buffer matrix. Moreover, the performance of the bioelectrodes in a composite groundwater sample from Northeast Mexico was analyzed, achieving an LOD of 0.5 µM and a sensitivity of 0.015 µA/µM cm^2. The LOD values found are among the lowest reported for biosensors based on the use of oxidoreductase enzymes, while the sensitivity is the highest currently reported.

Keywords: electrochemical biosensor; acetaminophen; laccases; MoS_2; emerging pollutants

Citation: Herrera-Domínguez, M.; Lim, K.; Aguilar-Hernández, I.; García-García, A.; Minteer, S.D.; Ornelas-Soto, N.; Garcia-Morales, R. Detection of Acetaminophen in Groundwater by Laccase-Based Amperometric Biosensors Using MoS_2 Modified Carbon Paper Electrodes. *Sensors* **2023**, *23*, 4633. https://doi.org/10.3390/s23104633

Academic Editor: Shimshon Belkin

Received: 6 April 2023
Revised: 27 April 2023
Accepted: 5 May 2023
Published: 10 May 2023

1. Introduction

Water pollution is a global environmental concern, and recently particular attention has been paid to a group of organic pollutants found in low concentrations (ng/L to mg/L) [1], as they may represent a real hazard to aquatic ecosystems due to their bioaccumulation and long-term effects. These pollutants are known as contaminants of emerging concern (CEC), and in many cases they are not regulated by environmental laws. Therefore, it is of vital importance to investigate the possible effects of these pollutants at the concentrations found in the environment [2].

The term CEC includes pharmaceutical active compounds (PhACs). Among these compounds, pharmaceuticals sold without a medical prescription are especially concerning since they are more frequently discharged into water bodies either directly or indirectly [3].

Acetaminophen (ACE), also known as paracetamol, is a widely used analgesic whose presence has been detected in aquatic ecosystems [4]. ACE is the first step in pain management according to the World Health Organization (WHO) ladder [5] and has been commonly recommended for many clinical practice guidelines since its inception in the 1950s [6]. It has been estimated that the annual production of ACE is as high as 145,000 t [7], and indicators have ranked its usage in countries such as the United States (5790 t in 2002) and France (3303 t in 2005) in the top 10 [8].

Several studies have demonstrated that ACE may interfere with the endocrine system of fish, causing abnormal embryonic development, growth, and have negative effects in reproduction; furthermore, possible deleterious effects in kidney and liver have been found [9,10]. ACE has been found worldwide in the environment in concentrations up to 230 μg/L [8,11]. Due to these reasons, some organizations, such as the Minnesota Department of Health (MDH) in the US, have determined a guidance value for acetaminophen in drinking water of 200 μg/L, since the liver is the most sensitive organ to ACE exposure [12].

ACE has been quantified in environmental samples using well-established techniques such as chromatography, spectroscopy, and capillary electrophoresis. Nevertheless, these present some drawbacks, such as high costs, long analysis times, and exhaustive sample preparation steps [13–15]. Therefore, the development of environmental electrochemical biosensors has been increasing recently due to their advantages, such as short response times, minimal sample preparation, and relatively easy construction and operation coupled with high sensitivity and selectivity [16]. Among electrochemical biosensors, enzymatic-based biosensors have shown advantages in the detection of a wide variety of chemical compounds. These devices consist of a transducer and a biological component. In enzyme-based biosensors, the enzyme chemically interacts with the target compound, and this interaction is then transduced into a measurable signal [17–19]. Moreover, it is important to note that the determination of ACE by electrochemical sensors has been mostly studied in pharmaceuticals and human body fluids, and few studies have been conducted on environmental samples [9].

In fact, since these types of electrochemical sensors still have some limitations when being used in real environments, it has become necessary to use other technologies and approaches, such as the development of conductive polymers, the use of nanomaterials, and the obtaining of new biological components, to improve their electrochemical response. Among the biological elements being developed, laccase enzymes are multicopper oxidoreductases that catalyze the oxidation of phenolic and amino aromatic-like compounds into their oxidized form, accompanied by the reduction of molecular oxygen [20–22]. Furthermore, the use of laccases provides other advantages compared to other oxidoreductases, such as biocatalysis without additional cofactors, good thermostability, stability to pH, and denaturing substances [23]. Specifically, two laccase isoforms from the native strain *Pycnoporus sanguineus CS43*, LacI and LacII, have been demonstrated to possess high resistance to inhibitors and thermal stability up to 60 °C [24]. According to previous studies, both isoforms are promising recognition elements for electrochemical biosensors, since they have exhibited an onset potential of over +650 mV vs. Ag/AgCl at pH 4 [25].

On the other hand, nanostructured electrochemical transducers can be used to improve a biosensor [18,26], as these materials can exhibit enhanced conductivity and catalytic activity [27–29]. Molybdenum sulfide (MoS_2) presents interesting structural, physicochemical, thermal, mechanical, and electrocatalytic properties (10–15 mA/cm^2) [30,31], and has been employed in the development of a series of sensors for the detection of analytes such as NO in as gas sensor, glucose, DNA, dopamine, and bisphenol A in biological and pharmaceutical samples [27,32–36].

In this work, a laccase-based biosensor for the environmental determination of acetaminophen in water was developed. The biosensor comprises carbon paper functionalized with MoS_2, a two-dimensional nanomaterial, and laccase enzyme. The performance of purified laccase isoforms from the native *Pycnoporus sanguineus* CS43 fungus was compared to a commercially available laccase from *Trametes versicolor* (TvL). This is the only work

in which a laccase-based biosensor has been specifically developed for the environmental determination of ACE in water. ACE quantification was evaluated in real samples (i.e., a pool of 31 groundwater samples from northern Mexico), and the pharmaceutical was successfully detected at environmentally relevant concentrations. Moreover, high sensitivity was achieved due to the presence of MoS_2.

2. Materials and Methods

2.1. Reagents

Acetaminophen (ACE), potassium hydroxide, dibasic sodium phosphate, ammonium heptamolybdate tetrahydrate (AHMo), thiourea (TU), molybdenum (VI) oxide (MoO_3) and sulfur powder, bicinchoninic acid (BCA), tetra-n-butylammonium bromide (TBAB), Nafion solution, and ABTS (2,2′-azino-bis(3-ethylbenzthiazoline-6-sulphonic acid)) reagents were purchased from Sigma-Aldrich. (Sigma Aldrich, Saint Louis, MO, USA) Citric acid monohydrate was purchased from Fisher Scientific (Thermo Fischer Scientific, Waltham, MA, USA). Toray Paper (TGP-H-060) was purchased from Fuel Cell Earth (Fuel Cell Earth, Woburn, MA, USA). All reagents were of analytical grade and were used without further purification, and all solutions were prepared using deionized water (18 mΩ·cm).

2.2. Laccase Enzymes

A Laccase isoform (EC 1.10.3.2) from *P. sanguineus* CS43 (LacI and LacII) was obtained as described in our previous work [24]. Briefly, mycelia were recovered from a tomato medium supernatant after 10 days of culture by filtration (0.2 µm pore size). Then, the sample was concentrated by ultrafiltration with a tangential-flow filter (Membrane cut-off of 10 kDa, Sartorius Sartojet). The ultra-filtered sample was purified with a DEAE-cellulose ion exchange column eluted with a 20 to 300 mM phosphate buffer of pH 6.0 at a flow rate of 2 mL/min. Finally, laccase fractions were collected and concentrated. Commercially purified laccase from *Trametes versicolor* (EC 1.10.3.2) was kindly provided by Amano Enzyme Inc. (TvL). Laccase activity was determined as in a previous work [37], where the oxidation of 0.54 mM ABTS 50 mM citric/phosphate buffer of pH 4 was monitored by the increase in the absorbance at 420 nm. Total protein content was determined with the BCA reagents using bovine serum albumin (BSA) as standard and measured at 562 nm. Absorbance was measured using a Thermo 50 Scientific© Evolution 260 Bio UV-Visible Spectrophotometer (Thermo Fischer Scientific, Waltham, MA, USA). Measurements were triplicated. All solutions were prepared in MQ water. *P. sanguineus* CS43 fungal laccases were used as obtained from a freshly purified culture, and TvL was prepared according to previous work [37], where it was demonstrated to have an efficient electrochemical signal. Concentrations and/or enzymatic activities were not modified for the following experiments. Characterization of laccase enzymes is shown in Table 1.

Table 1. Enzymatic characterization of laccases from *P. sanguineus* CS43 and *Trametes versicolor*.

Sample	Conc. (mg/mL)	Activity (U/mL)	Specific Activity (U/mg)
TvL	1.32 ± 0.64	81.00 ± 30	61.50 ± 3.29
LacI	0.31 ± 0.48	33.87 ± 1.38	108.17 ± 7.35
LacII	0.48 ± 0.17	74.49 ± 0.97	155.11 ± 1.50

2.3. Synthesis of MoS_2 Nanostructured Material

The hydrothermal synthesis of MoS_2 was performed following the procedure reported by Najmaei et al. [38] with modifications. The modified synthesis is registered under patent MX-a-2017-016742 [39]. The first step consisted of the obtention of MoO_3 nanoribbons through the hydrothermal method: a dispersion of 2 mL of a saturated ammonium molybdate in HCl mixed by magnetic stirring for 30 min was then transferred to a Teflon-lined autoclave and left at 185 °C for 12 h. MoO_3 and sulfur powder were put into a tube furnace at 600 °C under nitrogen flow; afterward, the temperature was increased to 800 °C and

was heated for 1 h. After the heating process, the furnace was left to cool down to room temperature under nitrogen flow. Then powder was stored for further use.

2.4. Immobilization of Laccase onto MoS_2 Modified Electrodes

Different solutions containing 0.5, 1, 2, and 5 mg/mL of MoS_2 were prepared and sonicated for 15 min. After a homogeneous solution was obtained, 10 µL of each solution was drop-casted onto the carbon paper (CP) electrode surface (0.25 cm^2) and left to dry at room temperature (CP-MoS_2). TBAB-Nafion polymer was used for enzyme immobilization according to the procedure previously reported [40,41]. Briefly, a solution of each purified enzyme (LacI, LacII, and TvL) was mixed with a solution of TBAB-Nafion to obtain a ratio of 3:1 (enzyme: TBAB-Nafion). Then, the solution was vortexed at 2000 rpm for 30 s. After a homogeneous solution was obtained, 10 µL was taken and drop-casted onto (a) pristine electrodes and (b) electrodes modified with MoS_2 to obtain the CP-Lac and CP-MoS_2-Lac working electrodes, respectively.

2.5. Electrochemical Measurements in the Optimization of Acetaminophen Detection

Voltametric and amperometric measurements were carried out on a CHI 611E Electrochemical Workstation (CH Instruments, Shanghai, China) with a conventional three-electrode system. Either carbon paper (CP) electrode or CP modified electrode was used as the working electrode, saturated calomel as the reference electrode (SCE), and a platinum mesh as the auxiliary electrode. All experiments were conducted at room temperature (~20 °C) in a beaker containing 5 mL of a 0.1 M citric acid/2 M KOH buffer (pH 4). The steady state amperometric response of working electrodes at different ACE concentrations was determined by successive additions of a 66.15 mM of ACE solution in MQ water. First, the working electrodes were equilibrated in 0.1 M citrate buffer at a constant potential of −0.1 V until a constant current was obtained, known as background current (I1). Then, aliquots of the ACE solution were added to the electrochemical cell and the obtained steady-state current response was recorded (I2). The obtained current difference ($\Delta I = I2 - I1$) was used to plot a calibration curve of ΔI vs. concentration of dopamine ([ACE]). All measurements were taken by triplicate.

2.6. Characterization Techniques

Raman spectra of modified electrodes were acquired using a Renishaw InVia spectrometer under ambient conditions with a 50× objective lens. Laser excitation was 633 nm using an Argon ion laser in the range of 100–1900 cm^{-1}. Laser power on the sample was set around 1.0 mW to avoid laser-induced heating. The modification of carbon paper electrodes with MoS_2 was verified with SEM micrographs. A Nova NanoSEM 200 (FEI Company, Hillsboro, OR, USA) Scanning Electron Microscope with an acceleration voltage of 15 kV in high vacuum conditions with a BSE detector with the capacity to acquire high magnification images (>5000×) was used. Electrochemical impedance spectroscopic (EIS) measurements were carried out on a BioLogic SP-150 potentiostat with a conventional three-electrode system; the frequency range was between 100 kHz and 10 MHz, with the single sine amplitudes of 100 µA.

2.7. Application of Optimized Electrodes for the Detection of Acetaminophen in Groundwater Samples

To evaluate the practical effectiveness of the modified electrodes in a real environment, optimal working electrodes were used for the determination of ACE in groundwater. Groundwater samples were obtained from several aquifers located in the state of Nuevo Leon in northeastern Mexico. Sample pH varied between 6.77 and 7.88, indicating neutral to slightly alkaline water conditions within the studied area. Their concentration of major ions, Na^+, K^+, Ca^{2+}, Mg^{2+}, Cl^-, $SO_4{}^{2-}$, $NO_3{}^-$, and $HCO_3{}^-$, is related to water–rock interaction (lutites and limestones) [42]. The groundwater samples were pooled, and the pooled sample was preconditioned by adding 50mM citric acid and adjusting pH to 4 with KOH (2M).

Electrochemical measurements were performed by successive injections of ACE into a 5 mL preconditioned groundwater sample.

3. Results and Discussion

3.1. Immobilization of Laccases onto MoS_2 Modified Electrodes

Michaelis–Menten kinetic parameters of the free and immobilized laccase enzymes on carbon paper electrodes modified with MoS_2 (CP-MoS_2-Lac) were determined using ABTS as a substrate. The values of the kinetic parameters shown in Table 2 were obtained by non-linear curve fitting of the reaction rate versus substrate concentration from the Michaelis–Menten equation. As observed, when laccases were subjected to the immobilization process, an increase in K_{Mapp} of 1.93 and 2.41 was obtained for TvL and LacI. Conversely, this effect was not observed when LacII (35.57 ± 4.79 µM) was immobilized, as no significant changes in its K_{Mapp} value were observed. The rise in K_{Mapp} is in general complemented by a decrease in affinity and may be a result of the enzyme's substrate diffusional restriction or the conformational changes caused by its entrapment in polymer micelles, which prevent substrate and laccase from interacting properly [43–45]. These findings indicate the existence and functioning of laccase enzymes after they were immobilized.

Table 2. Michaelis-Menten kinetic constants for both free and immobilized laccase enzymes on the carbon paper electrode surface.

Laccase	K_{Mapp}	
	Free	Immobilized
TvL	42.07 ± 3.136	123 ± 26.96
LacI	16.64 ± 2.548	58.68 ± 10.12
LacII	34.51 ± 5.857	35.57 ± 4.79

Bioelectrocatalytic activity was studied by cyclic voltammetry to corroborate the presence of immobilized laccase enzymes on the electrodes. Figure 1 shows the CVs taken at every film used in the construction of modified electrodes for ACE detection based on the immobilization of laccases onto CP-MoS_2 electrodes. CVs showed a quasi-reversible system with cathodic and anodic peaks at around 0.45 V and 0.55 V, respectively. Pristine CP presented a reduction peak of 0.45 V and a maximum current of 20 µA; when CP was modified with MoS_2 (1 mg/mL), current decrease and shift in the reduction peak

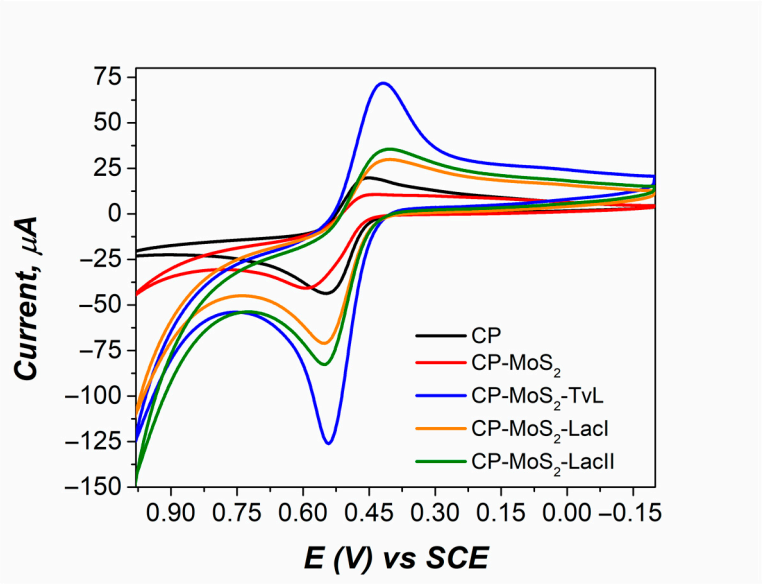

Figure 1. Cyclic voltammograms of electrodes in each immobilization step in a 0.5 mM ACE solution in 0.1 M citrate buffer (pH 4) at a scan rate of 50 mV/s.

Laccase immobilization was also studied with Raman spectroscopy; this technique takes advantage of the fingerprint of specific molecules in a sample. Commonly, the analysis of enzymes (proteins) by Raman is based on bands associated with their peptide chains [46]. Figure 2 shows the Raman spectra of laccase-MoS_2 modified carbon paper electrodes in the range 500–1450 cm^{-1}; it was possible to observe characteristic peaks for

Nonetheless, after adding laccase enzymes to CP-MoS_2 modified electrodes, it was possible to observe an increase in the current of the cathodic peak for three enzymes of around 30, 36, and 72 μA for LacI, LacII, and TvL respectively. Peak shifting and current increase in peak reduction for all bioelectrodes proved that laccases had been adsorbed on the surface of modified electrode, thus decreasing laccase biocatalytic activity while also causing a slower electron transfer due to the diffusion restriction attained by these layers. All bioelectrodes failed to exhibit a redox reaction in the absence of ACE at potentials between 1.0 and −0.2 V (Supplementary Materials Figure S1).

Laccase immobilization was also studied with Raman spectroscopy; this technique takes advantage of the fingerprint of specific molecules in a sample. Commonly, the analysis of enzymes (proteins) by Raman is based on bands associated with their peptide chains [46]. Figure 2 shows the Raman spectra of laccase-MoS_2 modified carbon paper electrodes in the range 500–1450 cm^{-1}; it was possible to observe characteristic peaks for CP, MoS_2, TBAB-Nafion, and laccases. Peaks at 1333 cm^{-1} correspond to disorder and defects in the carbon lattice (D-line) from the carbon paper [47]. For MoS_2, the signal at 645 cm^{-1} corresponds to a combination of the LA(M) frequency and the A1g mode, and the peak at around 820 cm^{-1} is due to the presence of a small amount of MoO_3 [48,49]. TBAB-Nafion (TB-Naf) presented several peaks in this region. The most prominent peaks at 732 and 1048 cm^{-1} correspond to CF_2 stretching and sulfonate (SO_3) symmetric stretch, respectively [50]. Most of the signals for laccase enzymes were overlapped by TBAB-Nafion polymer signals; this condition was expected since it is known that this polymer entraps enzymes through the formation of a semi-permeable membrane that allows the diffusion of substrates and products [51,52]. Nonetheless, LacI and LacII presented a small peak at around 930 cm^{-1} probably for stretching of the γOH in the carboxylic groups in amino acids (glutamic acid and aspartic acid) [53]. TvL showed a more prominent peak at around 995 cm^{-1} probably due to the glycoproteic portion of laccase (C-O ribose); this higher signal may be associated with the fact that TvL was more concentrated than LacI and LacII [54,55].

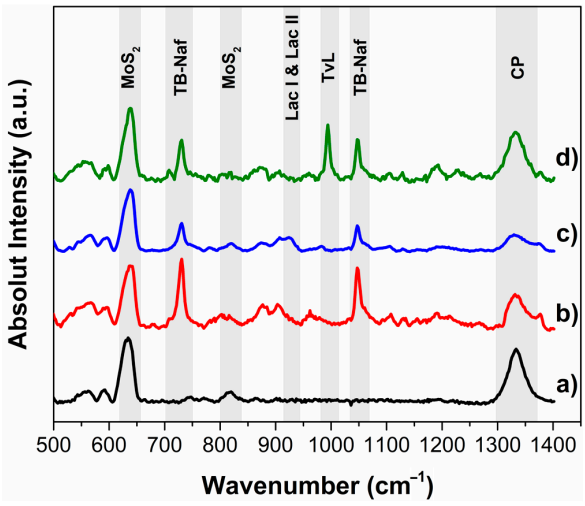

Figure 2. Raman spectra of (a) CP−MoS_2, (b) CP−MoS_2-LacI, (c) CP-MoS_2-LacII, and (d) CP−MoS_2−TvL.

The ACE molecule has a hydroxyl and amino derivative functional group; therefore, based on laccase reactivity, the presence of functional groups acting as electron-donating groups (EDG) such as hydroxyl (-OH) and amines (-NH_2) makes ACE susceptible to laccase attack [56]. The role of MoS_2 in this mechanism is the modification of the working electrode (carbon paper) to improve its conductive properties (transducer modifier), due to its features as a bandgap ranging from 1.2 to 1.8 eV, as well as higher adsorption capacity of ACEox [57–59]. Hence, according to this and CVs results, the proposed electron transfer mechanism for the developed CP-MoS_2-Lac biosensor is defined as follows: first, acetaminophen (ACEred) is oxidized enzymatically by laccase in the presence of oxygen to its respective N-acetyl-p-benzoquinoneimine form (ACEox), and then ACEox is electrochemically reduced back at the electrode surface to its ACEred form, which is reflected as an electrical current (Figure 3). For amperometric experiments, measurements were made at a potential of −0.1 V to ensure the electrochemical reduction of ACEox. Moreover, this potential avoids possible interference from MoS_2 precursors, specifically the remaining MoO_3 (See Figure S3 in Supplementary Materials). This low potential that was used

groups (EDG) such as hydroxyl (-OH) and amines (-NH_2) makes ACE susceptible to laccase attack [56]. The role of MoS_2 in this mechanism is the modification of the working electrode (carbon paper) to improve its conductive properties (transducer modifier), due to its features as a bandgap ranging from 1.2 to 1.8 eV, as well as higher adsorption capacity of ACEox [57–59]. Hence, according to this and CVs results, the proposed electron transfer mechanism for the developed CP-MoS_2-Lac biosensor is defined as follows: first, acetaminophen (ACEred) is oxidized enzymatically by laccases in the presence of oxygen to its respective N-acetyl-p-benzoquinoneimine form (ACEox), and then ACEox is electrochemically reduced back at the electrode surface to its ACEred form, which is reflected as an electrical current (Figure 3). For amperometric experiments, measurements were made at a potential of −0.1 V to ensure the electrochemical reduction of ACEox. Moreover, this potential avoids possible interference from MoS_2 precursors, specifically the remaining $MoCl_5$ (see Figure S3 in Supplementary Materials). This potential was used in accordance with previously reported studies [13,60].

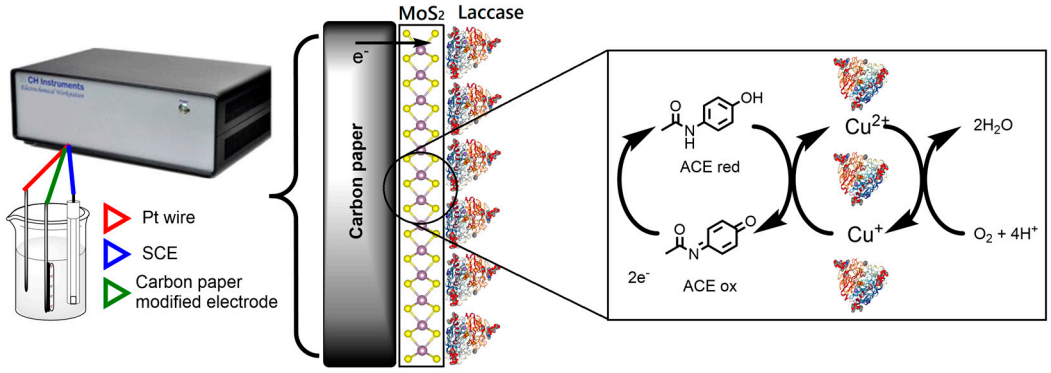

Figure 3. Electron transfer mechanism for our developed CP−MoS_2 Lac bioelectrodes in the detection of acetaminophen.

3.2. Optimum MoS_2 Concentration for Laccase Bioelectrode Modification

All nonlinear regression of the Michaelis–Menten model was used to evaluate the apparent electrochemical enzymatic kinetics of the bioelectrodes toward the substrate. This model can be used to study the influence of factors such as temperature, pH, immobilization technique, and diffusion-limiting membranes on an enzymatic system [61,62]. In this sense, the following modified equation was used:

$$J = \frac{J_{max}[S]}{KM_{app} + [S]}$$

where J is the current density, K_{Mapp} is the apparent Michaelis constant which quantifies the enzymatic affinity for the substrate, and J_{max} is the maximum current density [63,64]. Since the recognition system of the proposed enzymatic bioelectrode depends on the enzymatic kinetics, ACE detection was evaluated under steady-state conditions to compare the apparent affinity of K_{Mapp} and J_{max} of ACE at the bioelectrodes. Consecutive injections of ACE into a stirred buffer solution measured at a potential of −0.1V were made. Representative amperometric curves for 1 mg/mL of MoS_2 modified electrodes (Figure 4) showed an evident electrocatalytic effect obtained after adding ACE into the system.

Sensors 2023, 23, x FOR PEER REVIEW 7 of 16

groups (EDG) such as hydroxyl (-OH) and amines (-NH_2) makes ACE susceptible to laccase attack [56]. The role of MoS_2 in this mechanism is the modification of the working electrode (carbon paper) to improve its conductive properties (transducer modifier), due to its features as a bandgap ranging from 1.2 to 1.8 eV, as well as higher adsorption capacity of ACEox [57–59]. Hence, according to this and CVs results, the proposed electron transfer mechanism for the developed CP-MoS_2-Lac biosensor is defined as follows: first, acetaminophen (ACEred) is oxidized enzymatically by laccases in the presence of oxygen to its respective N-acetyl-p-benzoquinoneimine form (ACEox), and then ACEox is electrochemically reduced back at the electrode surface to its ACEred form, which is reflected as an electrical current (Figure 3). For amperometric experiments, measurements were made at a potential of −0.1 V to ensure the electrochemical reduction of ACEox. Moreover, this potential avoids possible interference from MoS_2 precursors, specifically the remaining $MoCl_5$ (see Figure S3 in Supplementary Materials). This potential was used in accordance with previously reported studies [13,60].

All nonlinear regression of the Michaelis–Menten model was used to evaluate the apparent electrochemical enzymatic kinetics of the bioelectrodes toward the substrate. This model can be used to study the influence of factors such as temperature, pH, immobilization technique, and diffusion-limiting membranes on an enzymatic system [61,62]. In this sense, the following modified equation was used:

$$J = \frac{J_{max}[S]}{KM_{app} + [S]}$$

where J is the current density, K_{Mapp} is the apparent Michaelis constant which quantifies the enzymatic affinity for the substrate, and J_{max} is the maximum current density [63,64]. Since the recognition system of the proposed enzymatic bioelectrode depends on the enzymatic kinetics, ACE detection was evaluated under steady-state conditions to compare the apparent affinity of K_{Mapp} and J_{max} of ACE at the bioelectrodes. Consecutive injections of ACE into a stirred buffer solution measured at a potential of −0.1V were made. Representative amperometric curves for 1 mg/mL of MoS_2 modified electrodes (Figure 4) showed an evident electrocatalytic effect obtained after adding ACE into the system.

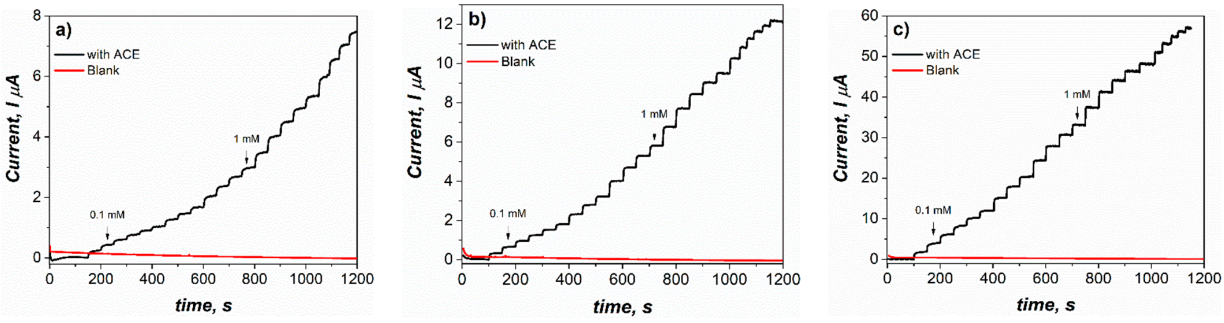

Figure 4. Amperometric i–t curves for the CP-MoS_2-Lac modified electrodes with successive addition of ACE into 0.1 M citric acid/2M KOH pH 4 recorded at −0.1 V. For (**a**) CP-MoS_2-TvL, (**b**) CP-MoS_2-LacI, and (**c**) CP-MoS_2-LacII.

All the bioelectrodes demonstrated a Michaelis–Menten kinetic behavior, as can be seen in Figure 5. It is also possible to observe that modification of MoS_2 in a concentration of 0.5–5 mg/mL did not cause a noteworthy increase in the electrochemical detection of ACE when using LacI and TvL, where maximum current densities were around 45 μA/cm². On the other hand, for LacII, a significant increase in current density was ob-

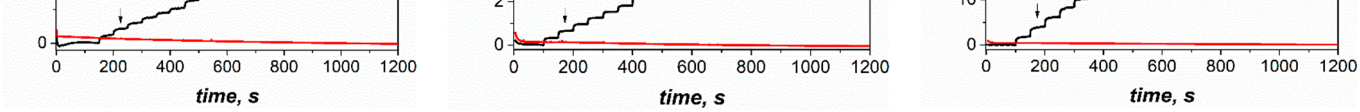

Figure 4. Amperometric i–t curves for the CP-MoS_2-Lac modified electrodes with successive addition of ACE into 0.1 M citric acid/2M KOH pH 4 recorded at −0.1 V. For (**a**) CP-MoS_2-TvL, (**b**) CP-MoS_2-LacI, and (**c**) CP-MoS_2-LacII.

All the bioelectrodes demonstrated a Michaelis–Menten kinetic behavior, as can be seen in Figure 5. It is also possible to observe that modification of MoS_2 in a concentration of 0.5–5 mg/mL did not cause a noteworthy increase in the electrochemical detection of ACE when using LacI and TvL, where maximum current densities were around 45 µA/cm^2. On the other hand, for LacII, a significant increase in current density was observed using 1 and 2 mg/mL of MoS_2. The maximum current density for LacII was around 210 µA/cm^2 when using 1 mg/mL of MoS_2.

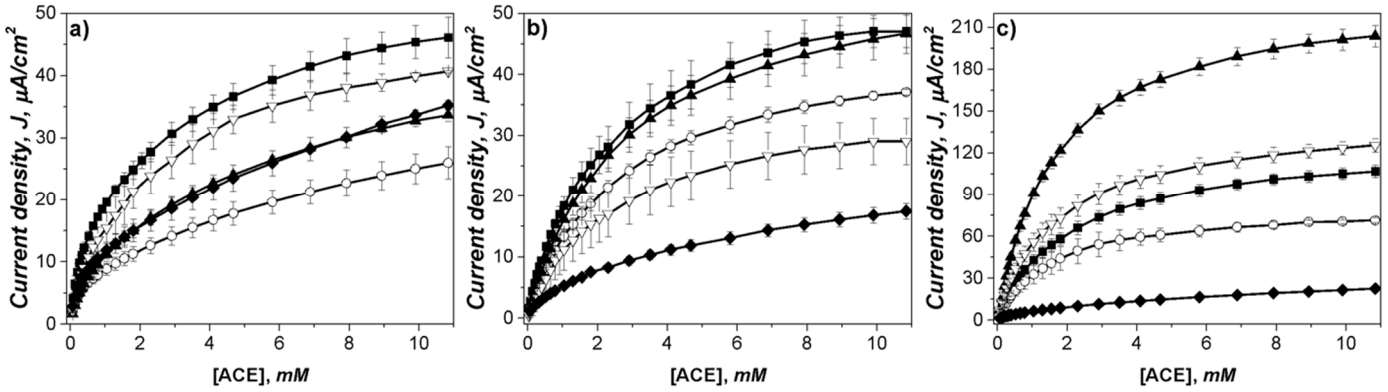

Figure 5. Apparent steady-state Michaelis–Menten kinetics of ACE for (**a**) CP-MoS_2-TvL, (**b**) CP-MoS_2-LacI, and (**c**) CP-MoS_2-LacII, determined in stirred citric acid/KOH (pH 4, 500 rpm) at an applied potential of −0.1 V vs. SCE. MoS_2 concentrations were: 0 mg/mL (■), 0.5 mg/mL (○), 1 mg/mL (▲), 2 mg/mL (▽), and 5 mg/mL (♦). Error bars represent standard deviation (n = 3).

Values for K_{Mapp} and J_{max} from nonlinear regression of the Michaelis–Menten model are reported in Table 3. Usually, low KM values are associated with high affinity [65]; taking this into account, the results for LacI and TvL modified bioelectrodes confirm that MoS_2 did not have a significant effect on the concentrations that were studied. Contrarily, for LacII, lower K_{Mapp} and higher J_{max} were achieved when 1 and 2 mg/mL of MoS_2 were used. From these results, the MoS_2 concentration considered to be optimum for further uses was 1 mg/mL since low K_{Mapp} and the highest J_{max} were obtained.

Table 3. Apparent steady-state Michaelis–Menten kinetic values of LacI, LacII, and TvL MoS_2 modified bioelectrodes for ACE, determined in stirred citric acid/KOH (pH 4, 50 mM, 500 rpm) at an applied potential of −0.1 V vs. SCE.

MoS_2 Concentration	TvL		LacI		LacII	
	K_{Mapp} (µM)	J_{max} (µA/cm^2)	K_{Mapp} (µM)	J_{max} (µA/cm^2)	K_{Mapp} (µM)	J_{max} (µA/cm^2)
Unmodified						
-	1659 ± 250	51.11 ± 2.59	2164 ± 151	53.68 ± 1.43	1908 ± 77	129.3 ± 1.76
Modified with MoS_2						
0.5mg/mL	2613 ± 254	29.80 ± 1.09	2474 ± 65	45.39 ± 0.44	1501 ± 99	81.05 ± 1.68
1 mg/mL	2952 ± 155	41.03 ± 0.85	2702 ± 143	58.01 ± 1.17	1656 ± 37	234.7± 1.65
2 mg/mL	1791 ± 99	49.84 ± 0.91	2429 ± 232	34.34 ± 1.30	1604 ± 66	142.2± 1.81
5 mg/mL	2733 ± 253	40.33 ± 1.43	3535 ± 250	22.07 ± 0.65	4176 ± 331	29.54 ± 1.04

3.3. Characterization of Optimum MoS_2 Modified Electrodes

According to the above results, the electrode with the best efficiency in ACE determination was the one modified with MoS_2 at 1 mg/mL. SEM and electrochemical impedance spectroscopy (EIS) were carried out to study the electrode properties. SEM micrographs of CP and CP-MoS_2 modified with 1 mg/mL are shown in Figure 6. From Figure 6a, it is possible to observe that CP is composed of carbon fibers with an average diameter

of 6.72 ± 0.65 µm, and that no impurities were observed. When CP was modified with 1 mg/mL of MoS_2 (Figure 6b), it was well distributed throughout the CP surface; uniform distribution was confirmed by EDS mapping (Figure 6e,f). At high magnification (Figure 6c), it is possible to observe that MoS_2 morphology resembles ribbons with an average length of 5 µm and an average width of 0.4 µm. Moreover, some nano-platelets grown over the surface (indicated with arrows in Figure 6d) were observed, which can serve as electroactive sites that are more accessible for the substrate to experience reduction reactions. No visible gaps between the stacked MoS_2 ribbons were visible, suggesting that, as the concentration of ribbon increases, they tend to stack in an ordered manner, ensuring a good contact between adjacent ribbons and the surface of the electrode, which suggests that the electron transfer process is favored. EDS analysis (Figure 6g) was performed to characterize the chemical composition of CP-MoS_2, confirming the existence of the element C, and Mo and S in a 1:2 ratio.

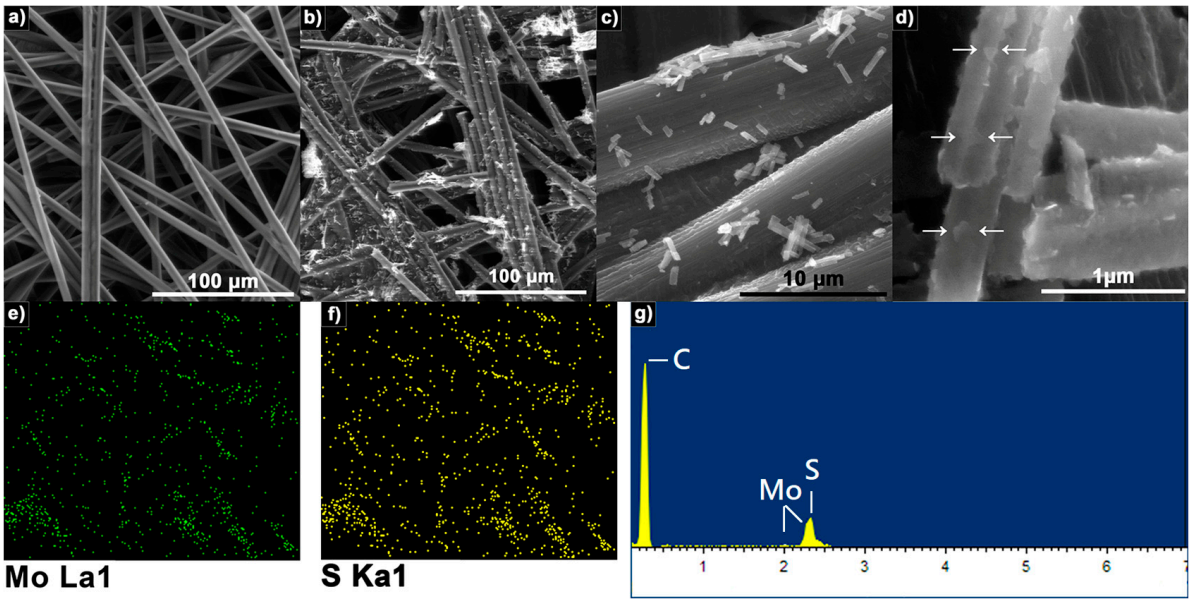

Figure 6. Representative SEM micrographs of electrodes. (**a**) bare CP; (**b**–**d**) CP modified with 1 mg/mL of MoS_2; (**e**,**f**) EDS mapping of Mo and S elements distribution within CP; (**g**) EDS spectrum of MoS_2 onto CP.

The Nyquist plot (Figure 7) shows the electrochemical impedance spectra (EIS) of CP, CP-MoS_2, CP-MoS_2-TvL, and CP-MoS_2-LacII. TvL was taken for comparison. All plots show the typical semicircle portion at high frequencies that correspond to an electron-transfer limited process with the transfer of electrons between the electrolyte and the electrode surface. Symbols represent the experimental data, and solid lines represent the fitted data to an equivalent circuit (inset Figure 7) to determine the charge transfer resistance (Rct) and double-layer capacitance (Cdl) at the interface of the developed electrodes. The basic Randles circuit was modified by an additional parallel RC circuit for a better fit. This additional circuit was required possibly due to the higher roughness of CP [66]. It was possible to observe that CP unmodified by MoS_2 or laccase had an Rct of 61.21 ± 0.21 Ω. After that, when MoS_2 was added to the electrode, a slight decrease in Rct to 59.73 ± 0.73 was obtained, this result may be associated with the electrical conductivity given by MoS_2, promoting direct electron transfer reactions. When TvL was added, an Rct of 63.84 ± 0.62 was obtained, while, for LacII, an Rct to 61.34 ± 0.27 was observed. The hindered electron transfer shown for CP-MoS_2-TvL and CP-MoS_2-LacII may be due to the addition of laccase enzymes to the electrode [67]. Despite this increase in transfer-resistant charge compared to CP-MoS_2, LacII had a lower Rct compared to TvL.

The characterization of electrodes in optimal conditions showed that the use of MoS_2 as a CP modifier agent in the manufacture of bioelectrodes produces a positive effect, facilitating the transfer of electrons in the system.

Sensors **2023**, *23*, x FOR PEER REVIEW 11 of 18

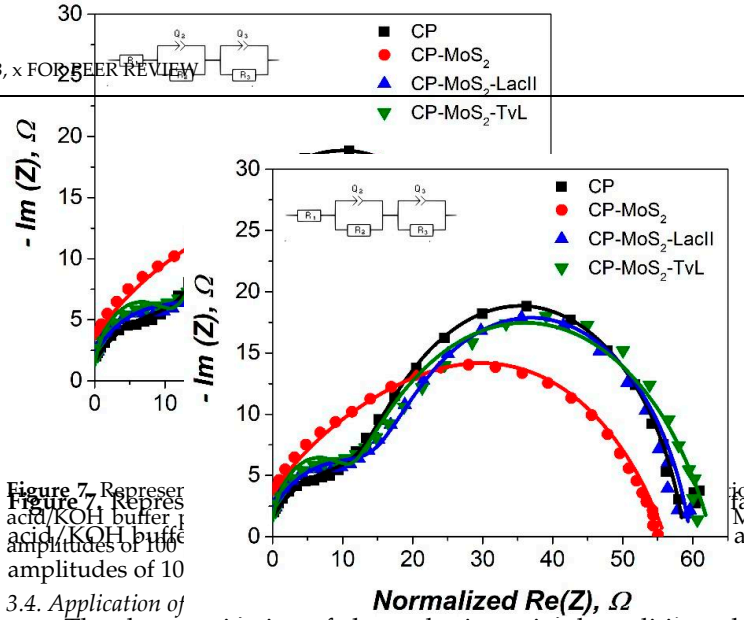

Figure 7. Represen ion. Measured in citric acid/KOH buffer MHz, with single sine amplitudes of 10

Figure 7. Represen ion. Measured in citric acid/KOH buffe and 10 MHz, with single sine amplitudes of 100 amplitudes of 10

3.4. Application of

The characterization of electrodes in optimal conditions showed that the use of MoS_2 as a CP modifier agent in the manufacture of bioelectrodes produces a positive effect facilitating the transfer of electrons in the system.

Based on enzymatic electrodes by using the lowest and highest values, the optimal combination of enzyme/MoS_2 concentration for electrode modification was the one fabricated with LacII and a concentration of 1 mg/mL. Thus, further analyses were performed to determine the linear ranges and limits of detection for ACE. As stated before, commercially available TvL was used for comparison against native LacII. Figure 8 and Table 4 show the results for electrodes unmodified and modified with 1 mg/mL of MoS_2 and with LacII and TvL.

3.4. Application of Modified Electrodes in the Detection of Acetaminophen

Based on enzymatic electrodes by using the lowest and highest values, the optimal combination of enzyme/MoS_2 concentration for electrode modification was the one fabricated with LacII and a concentration of 1 mg/mL. Thus, further analyses were performed to determine the linear ranges and limits of detection for ACE. As stated before, commercially available TvL was used for comparison against native LacII. Figure 8 and Table 4 show the results for electrodes unmodified and modified with 1 mg/mL of MoS_2 and with LacII and TvL.

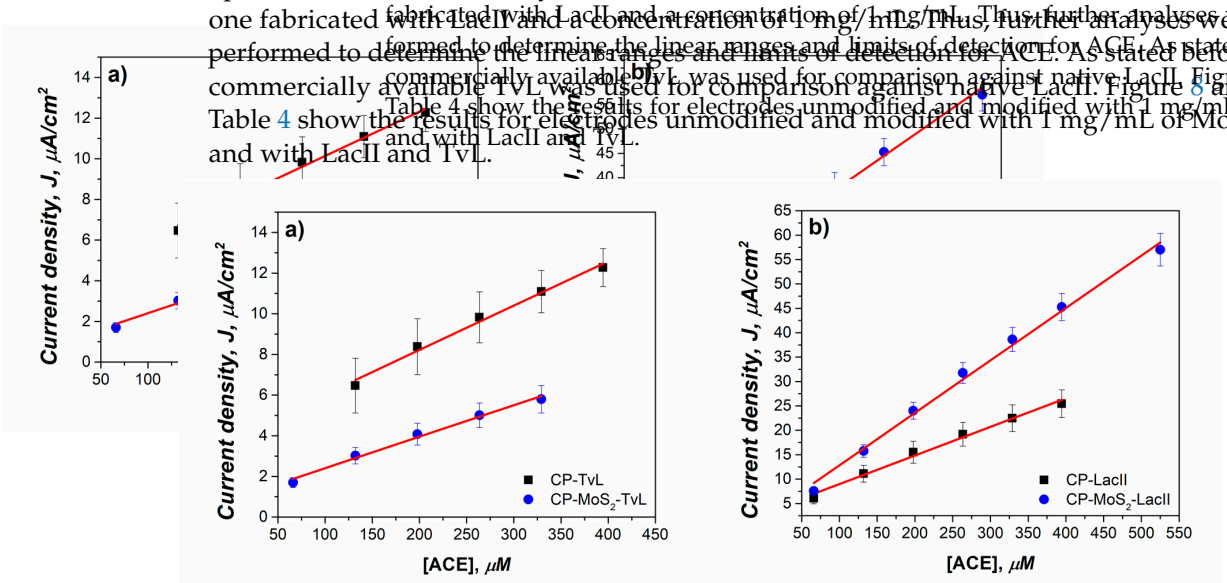

Figure 8. Calibration curves using the electrodes unmodified and modified with 1 mg/mL of MoS_2 in citric acid/KOH buffer pH 4 for (**a**) LacII, and (**b**) TvL.

Table 4. Linear range, sensitivities, and correlation coefficients obtained for the calibration curves of the modified electrodes in the determination of ACE.

Bioelectrode	Linear Range (μM)	Sensitivity (μA/μM cm^{-2})	R^2
CP-LacII	66–395	0.058	0.9901
CP-MoS_2-LacII	66–525	0.108	0.9948
CP-TvL	132–395	0.021	0.9901
CP-MoS_2-TvL	66–329	0.015	0.9901

In sensitivity for the LacII electrode, which passed from 0.0586 to 0.1083 μA/μM cm^2, can be attributed to the presence of MoS_2 in the electrode. Consequently, a negative effect of sensitivity could be observed for TvL, which was reduced significantly from 0.0218 to 0.0155 μA/μM cm^2. The sensitivity values obtained may be

It was found that CP-MoS_2-LacII presented a broader linear range of 66–525 μM than TvL, which had a range of 66–329 μM, when both were used in electrodes modified with MoS_2. These results agree with the fact that the linear range of enzymatic biosensors is limited to substrate concentrations well below Km, where the reaction rate is diffusion-limited and grows almost linearly when substrate concentration increases [68]. The almost 2-fold improvement in sensitivity for the LacII electrode, which passed from 0.0586 to 0.1083 μA/μM cm^2, can be attributed to the presence of MoS_2 in the electrode. Consequently, a negative effect of sensitivity could be observed for TvL, which was reduced significantly from 0.0218 to 0.0155 μA/μM cm^2. The sensitivity values obtained may be associated with changes in enzymatic affinity after immobilization since, as shown above, TvL presented a lower affinity with a decreased sensitivity, whereas LacII affinity was not affected by immobilization process, and exhibited an increase in sensitivity.

The limits of detection (LOD) for CP-MoS_2-LacII and CP-MoS_2-TvL were determined by adding a 5 mM acetaminophen solution gradually until a statistically significant change response in current was observed. The obtained values for the modified electrodes were 0.2 μM for CP-MoS_2-LacII and of 2.00 μM for CP-MoS_2-TvL, which are among the lowest reported when compared with other oxidoreductase-based electrochemical biosensors for the detection of acetaminophen, as compared in Table 4. In addition, it is possible to observe that our developed bioelectrodes showed better sensitivity in the detection of ACE, reaching almost twice the value of those reported in Table 5. It is important to mention that the amperometric signals recorded for TvL were noisier than those recorded by the native LacII enzyme; this fact could translate into a much more reliable measurement.

Table 5. Analytical characteristics of some enzyme-based electrochemical biosensors reported for the determination of acetaminophen.

Electrode *	Detection Method	Sample	Linear Range (μM)	Sensitivity (μA/μM cm^2)	LOD (μM)	Ref.
GCPE-PPO	Amp (−0.1 V)	50 M phosphate buffer solution pH 7.4.	Up to70	0.015 μA/μM	7.8	[60]
GCE-HRP @ PAA-BIS	Amp (−0.1 V)	50 mM sodium phosphate buffer pH 7.0 with 100 mM KCl	5.6–331.1	0.069	1.7	[13]
GCE-HRP-PPY SPE-HRP-PPY	Amp (−0.175 V)	0.2 mM H_2O_2 in phosphate buffer pH = 7.4	9.3–83.7 3.1–55.9	- -	6.5 1.52	[69]
GCE-nano PPY-HRP GCE-flat PPY-HRP	Amp (−0.2 V)	Phosphate buffer solution (pH 7.4)	5–60 5–300	0.050 0.002	0.1 4.1	[70]
GCE-clay-PEI-HRP	Amp (0 V)	100 mM phosphate buffer saline (pH 7.4)	5.25–49.5	0.013 μA/μM	0.63	[71]
SPE-CoPC/Tyr	CV	100 m M phosphate-buffer pH 6/100 mM KCl	up to 40	−0.088	0.5	[15]
CPE-EP-PPO	DPV 10 mV/s	100 mM phosphate buffer (pH 6.0)	600–1150	-	5.0	[72]
CPE-PPO	DPV 10 mV/s	100 mM phosphate buffer pH 7.0	5–245	-	3.0	[73]
CP-LacII CP-TvL CP-MoS_2-LacII CP-MoS_2-TvL	Amp −0.1 V	100 mM citric acid/2 M KOH buffer (pH 4)	66–395 132–395 66–525 66–329	0.058 0.021 0.108 0.015	- - 0.2 2.0	Present study
CP-MoS_2-LacII CP-MoS_2-TvL	Amp −0.1 V	Groundwater (50 mM citric acid/2 M KOH)	1–155.1 29.82–155.1	0.017 0.005	0.50 24.88	Present study

* GCPE-: glassy carbon paste electrode. PPO: polyphenol oxidase. GCE: glassy carbon electrode. HRP horseradish peroxidase. PAA-BIS:—polyacrylamide—*N*,*N*-methylenebisacrylamide. PPY: polypyrrole. SPE: screen-printed electrode. PEI: polyethyleneimine. CoPC: polyvinyl alcohol photocrosslinkable polymer. Tyr: tyrosinase. CPE: carbon paste electrode. EP-PPO: eggplant polyphenol oxidase. MWCNT: multiwall carbon nanotubes. PANI: polyaniline. GA: glutaraldehyde. Amp: Amperometry. CAmp: Chronoamperometry. CV: Cyclic Voltammetry. DPV: Differential pulse voltammetry.

Amperometry. CAmp: Chronoamperometry. CV: Cyclic Voltammetry. DPV: Differential p
ammetry.

3.5. Application of Modified Electrodes in the Amperometric Detection of Acetaminophen Groundwater Sample from a City in Northeastern Mexico

With the aim of confirming the validity and feasibility of the biosensor for d
ACE in groundwater, an aliquot of groundwater was preconditioned by adding ci
to reach a concentration of 50 mM, then adjusting pH to 4 with KOH. Then, su
injections of ACE were made to a 5 mL preconditioned groundwater sample. Th
tion of ACE was studied by increasing concentration up to around 150 µM to de
the linear range, sensitivity, and LOD in this water sample used as a model of e
mental importance.

Figure 9 and Table 6 summarize the application of 1 mg/mL modified electrod
TvL and LacII in the detection of ACE in groundwater; this study was performed
concentration of around 150 µM, where typical CECs are found [8,74].

3.5. Application of Modified Electrodes in the Amperometric Detection of Acetaminophen Groundwater Sample from a City in Northeastern Mexico

With the aim of confirming the validity and feasibility of the biosensor for detecting ACE in groundwater, an aliquot of groundwater was preconditioned by adding citric acid to reach a concentration of 50 mM, then adjusting pH to 4 with KOH. Then, successive injections of ACE were made to a 5 mL preconditioned groundwater sample. The detection of ACE was studied by increasing concentration up to around 150 µM to determine the linear range, sensitivity, and LOD in this water sample used as a model of environmental importance.

Figure 9 and Table 6 summarize the application of 1 mg/mL modified electrodes with TvL and LacII in the detection of ACE in groundwater; this study was performed up to a concentration of around 150 µM, where typical CECs are found [8,74].

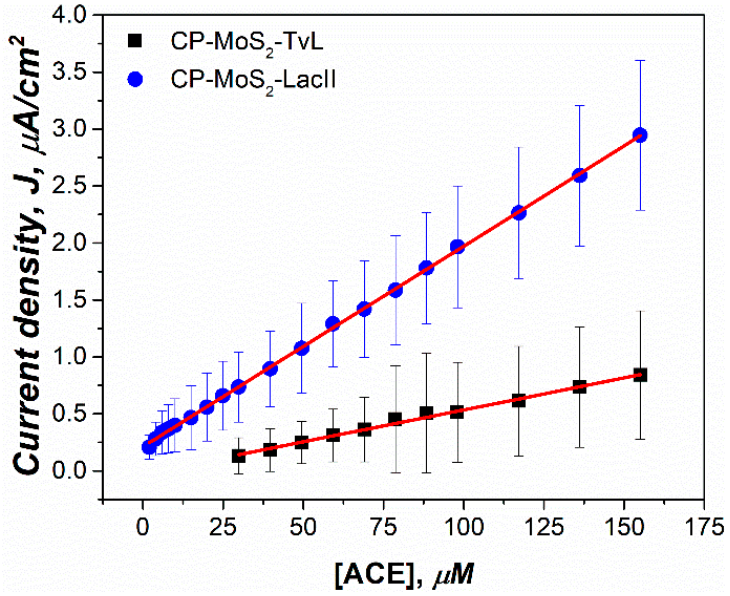

Figure 9. Calibration curves for ACE using the electrodes modified with 1 mg/mL of MoS2-Lac and MoS2-TvL both in groundwater (5 mL) preconditioned with 0.05 M citric acid and adjusted to pH 4 with 2M KOH.

Table 6. Linear range, sensitivities, and correlation coefficients obtained for the calibration curves for the modified electrodes in the determination of ACE in groundwater samples.

Electrode	Linear Range (µM)	Linear Range (µg/L)	Sensitivity (nA/µM·cm²)	R^2	LOD (µM)	LOD (µg/L)
CP-MoS_2-Lac	1–155	151.13–23,436.1	177	0.9992	0.50	75.57
CP-MoS_2-TvL	29.82–155	4507.84–23,436.1	5.6	0.9933	24.88	3760.27

LacII presented a wider linear range from 1 to 155 µM compared to TvL, which had a linear range of 29.82–155 µM. In terms of linearity, LacII also presented a better R^2 value of 0.9992 than the TvL (0.9933). As is also shown in Table 6, LOD for Lac II was lower than that for TvL, which was an expected result since, on the one hand, it is known th
has presented an enhanced resistance to common inhibitors such as major ions
Ca^{2+}, Mg^{2+}, Cl^-, SO_4^{2-}, NO^{3-}, which are normally found in groundwater, and, on t
hand, LacII did not show significant affinity change after the immobilization proc
thermore, the sensitivity of LacII was shown to be around 3-fold higher when co
to TvL, confirming that the native laccase enzyme is a better candidate for use in p
applications for ACE detection in water samples of environmental importance
groundwater.

LacII presented a wider linear range from 1 to 155 µM compared to TvL, which had a linear range of 29.82–155 µM. In terms of linearity, LacII also presented a better R^2 value of 0.9992 than the TvL (0.9933). As is also shown in Table 6, LOD for Lac II was lower than that for TvL, which was an expected result since, on the one hand, it is known that LacII has presented enhanced resistance to common inhibitors such as major ions K^+, Ca^{2+}, Mg^{2+}, Cl^-, SO_4^{2-}, NO^{3-}, which are normally found in groundwater, and, on the other hand, LacII did not show significant affinity change after the immobilization process. Furthermore, the sensitivity of LacII was shown to be around 3-fold higher when compared to TvL, confirming that the native laccase enzyme is a better candidate for use in practical applications for ACE detection in water samples of environmental importance such as groundwater.

From these results, it was possible to observe that the use of native laccase LacII for the fabrication of a modified electrode in the development of a laccase-based electrochemical

biosensor can be a powerful element for the determination of any noticeable increase in the guidance value for ACE of 200 µg/L, which can be an indicator of pollution by this drug. Moreover, laccase-based amperometric biosensors have the advantage of being of easy usage, fast, and with good performance and selectivity, which may be convenient for the detection of these emerging pollutants [75].

4. Conclusions

The use of MoS_2 as a two-dimensional material for the modification of carbon paper electrodes coupled with the immobilization of laccase enzymes allowed the development of a novel bioelectrode for use in the development of a laccase-based amperometric biosensor. The resulting bioelectrode showed good analytical performance in the determination of ACE in citric acid buffer, providing a sensitivity of 108.3 nA/µM∗cm^2 and an LOD of 0.2 µM, which are among the lower values reported for this oxidoreductase-based biosensor. It was also demonstrated that MoS_2 allowed an increase in sensitivity. Furthermore, the difference in the nature of laccase enzymes was investigated, presenting a very important effect for the development of novel bioelectrodes; hence, it is of utmost importance to investigate enzymes with improved detection yields. For example, of the two isoforms of the laccase enzyme from the white-rot fungi, *Pycnoporus sanguineus* CS43 (LacI and LacII) and the commercial laccase (*Trametes versicolor*), better results were achieved for LacII native laccase.

The bioelectrode application in the determination of ACE in groundwater samples was successfully carried out, with LacII showing a good performance against naturally found inhibitors (major ions). This achieved an LOD of 0.5 µM and a linear range of 1–98.04 µM equivalent to 151.13–14,819.9 µg/L. The properties of this developed bioelectrode can be effectively used to develop a monitor tool for any significant increase in guidance values emitted by environmental organisms defined at 200 µg/L to study water pollution by this pharmaceutical. In a field in which few studies have been carried out, this work contributes new findings in the application of these types of electrochemical sensors in environmental samples [60].

Supplementary Materials: The following supporting information can be downloaded at: https://www.mdpi.com/article/10.3390/s23104633/s1, Figure S1: CVs of developed bioelectrodes in the absence of ACE; Figure S2: Representative SEM images of the as obtained MoS_2 nanostructured material; Figure S3: Cyclic voltammograms of modified electrodes using MoS_2-R and MoO_3 in the absence of immobilized enzymes and of ACE; Figure S4: Enzyme leaking test. Refs. [41,45,52] are cited in Supplementary Materials.

Author Contributions: Conceptualization, N.O.-S. and S.D.M.; investigation, M.H.-D., R.G.-M. and K.L.; validation, S.D.M. and K.L.; writing—original draft preparation, R.G.-M., N.O.-S., M.H.-D. and I.A.-H.; writing—review and editing, R.G.-M., N.O.-S., M.H.-D. and I.A.-H.; visualization, K.L. and A.G.-G., supervision: N.O.-S. and S.D.M.; funding acquisition, N.O.-S. All authors have read and agreed to the published version of the manuscript.

Funding: This research was funded by Consejo Nacional de Ciencia y Tecnología (CONACyT) for scholarship #400714, scholarship #855128, and CONACYT grant #PN-2016-4320.

Institutional Review Board Statement: Not applicable.

Informed Consent Statement: Not applicable.

Data Availability Statement: Data available on request.

Acknowledgments: Special thanks to Nayely Pineda Aguilar for the technical support at CIMAV. Raul Garcia-Morales kindly thanks DGAPA-UNAM for his postdoctoral fellowship.

Conflicts of Interest: The authors declare no conflict of interest.

References

1. Butkovskyi, A.; Leal, L.H.; Zeeman, G.; Rijnaarts, H.H.M. Micropollutants in Source Separated Wastewater Streams and Recovered Resources of Source Separated Sanitation. *Environ. Res.* **2017**, *156*, 434–442. [CrossRef]
2. Sousa, J.C.G.; Ribeiro, A.R.; Barbosa, M.O.; Pereira, M.F.R.; Silva, A.M.T. A Review on Environmental Monitoring of Water Organic Pollutants Identified by EU Guidelines. *J. Hazard. Mater.* **2018**, *344*, 146–162. [CrossRef] [PubMed]
3. Gibson, R.; Becerril-Bravo, E.; Silva-Castro, V.; Jiménez, B. Determination of Acidic Pharmaceuticals and Potential Endocrine Disrupting Compounds in Wastewaters and Spring Waters by Selective Elution and Analysis by Gas Chromatography-Mass Spectrometry. *J. Chromatogr. A* **2007**, *1169*, 31–39. [CrossRef] [PubMed]
4. Nunes, B.; Pinto, G.; Martins, L.; Gonçalves, F.; Antunes, S.C. Biochemical and Standard Toxic Effects of Acetaminophen on the Macrophyte Species *Lemna minor* and *Lemna gibba*. *Environ. Sci. Pollut. Res.* **2014**, *21*, 10815–10822. [CrossRef] [PubMed]
5. Anekar, A.A.; Cascella, M. WHO Analgesic Ladder. Available online: https://www.ncbi.nlm.nih.gov/books/NBK554435/ (accessed on 12 October 2022).
6. Yoon, E.; Babar, A.; Choudhary, M.; Kutner, M.; Pyrsopoulos, N. Acetaminophen-Induced Hepatotoxicity: A Comprehensive Update. *J. Clin. Transl. Hepatol.* **2016**, *4*, 131. [CrossRef] [PubMed]
7. Cao, F.; Zhang, M.; Yuan, S.; Feng, J.; Wang, Q.; Wang, W.; Hu, Z. Transformation of Acetaminophen during Water Chlorination Treatment: Kinetics and Transformation Products Identification. *Environ. Sci. Pollut. Res.* **2016**, *23*, 12303–12311. [CrossRef]
8. aus der Beek, T.; Weber, F.A.; Bergmann, A.; Hickmann, S.; Ebert, I.; Hein, A.; Küster, A. Pharmaceuticals in the Environment-Global Occurrences and Perspectives. *Environ. Toxicol. Chem.* **2016**, *35*, 823–835. [CrossRef]
9. Montaseri, H.; Forbes, P.B.C. Analytical Techniques for the Determination of Acetaminophen: A Review. *TrAC-Trends Anal. Chem.* **2018**, *108*, 122–134. [CrossRef]
10. Anthérieu, S.; Le Guillou, D.; Coulouarn, C.; Begriche, K.; Trak-Smayra, V.; Martinais, S.; Porceddu, M.; Robin, M.-A.; Fromenty, B. Chronic Exposure to Low Doses of Pharmaceuticals Disturbs the Hepatic Expression of Circadian Genes in Lean and Obese Mice. *Toxicol. Appl. Pharmacol.* **2014**, *276*, 63–72. [CrossRef]
11. Togola, A.; Budzinski, H. Multi-Residue Analysis of Pharmaceutical Compounds in Aqueous Samples. *J. Chromatogr. A* **2008**, *1177*, 150–158. [CrossRef]
12. Environmental Health Division. *Acetaminophen in Drinking Water*; Environ. Heal. Minnesota Department of Health: Saint Paul, MN, USA, 2014. Available online: www.health.state.mn.us/eh (accessed on 4 May 2023).
13. González-Sánchez, M.I.; Rubio-Retama, J.; López-Cabarcos, E.; Valero, E. Development of an Acetaminophen Amperometric Biosensor Based on Peroxidase Entrapped in Polyacrylamide Microgels. *Biosens. Bioelectron.* **2011**, *26*, 1883–1889. [CrossRef] [PubMed]
14. Thévenot, D.R.; Toth, K.; Durst, R.A.; Wilson, G.S. Electrochemical Biosensors: Recommended Definitions and Classification. *Biosens. Bioelectron.* **2001**, *16*, 121–131. [CrossRef] [PubMed]
15. Calas-Blanchard, C.; Istamboulié, G.; Bontoux, M.; Plantard, G.; Goetz, V.; Noguer, T. Biosensor-Based Real-Time Monitoring of Paracetamol Photocatalytic Degradation. *Chemosphere* **2015**, *131*, 124–129. [CrossRef] [PubMed]
16. Ronkainen, N.J.; Halsall, H.B.; Heineman, W.R. Electrochemical Biosensors. *Chem. Soc. Rev.* **2010**, *39*, 1747. [CrossRef]
17. Barsan, M.M.; Emilia Ghica, M.; Brett, C.M.A. Electrochemical Biosensors. In *Portable Biosensing of Food Toxicants and Environmental Pollutants*; CRC Press, Taylor & Francis Group: Boca Raton, FL, USA, 2013; Volume 39, pp. 33–69. [CrossRef]
18. Zhu, C.; Yang, G.; Li, H.; Du, D.; Lin, Y. Electrochemical Sensors and Biosensors Based on Nanomaterials and Nanostructures. *Anal. Chem.* **2015**, *87*, 230–249. [CrossRef] [PubMed]
19. Perumal, V.; Hashim, U. Advances in Biosensors: Principle, Architecture and Applications. *J. Appl. Biomed.* **2014**, *12*, 1–15. [CrossRef]
20. Mayer, A.M.; Staples, R.C. Laccase: New Functions for an Old Enzyme. *ChemInform* **2002**, *33*, 256. [CrossRef]
21. Yaropolov, A.I.; Skorobogat'ko, O.V.; Vartanov, S.S.; Varfolomeyev, S.D. Laccase—Properties, Catalytic Mechanism, and Applicability. *Appl. Biochem. Biotechnol.* **1994**, *49*, 257–280. [CrossRef]
22. Madhavi, V.; Lele, S.S. Laccase: Properties and Applications. *BioResources* **2009**, *4*, 1694–1717.
23. Rodríguez-Delgado, M.M.; Alemán-Nava, G.S.; Rodríguez-Delgado, J.M.; Dieck-Assad, G.; Martínez-Chapa, S.O.; Barceló, D.; Parra, R. Laccase-Based Biosensors for Detection of Phenolic Compounds. *TrAC-Trends Anal. Chem.* **2015**, *74*, 21–45. [CrossRef]
24. Ramírez-Cavazos, L.I.; Junghanns, C.; Ornelas-Soto, N.; Cárdenas-Chávez, D.L.; Hernández-Luna, C.; Demarche, P.; Enaud, E.; García-Morales, R.; Agathos, S.N.; Parra, R. Purification and Characterization of Two Thermostable Laccases from Pycnoporus Sanguineus and Potential Role in Degradation of Endocrine Disrupting Chemicals. *J. Mol. Catal. B Enzym.* **2014**, *108*, 32–42. [CrossRef]
25. Holmberg, S.; Rodriguez-Delgado, M.; Milton, R.D.; Ornelas-Soto, N.; Minteer, S.D.; Parra, R.; Madou, M.J. Bioelectrochemical Study of Thermostable *Pycnoporus sanguineus* CS43 Laccase Bioelectrodes Based on Pyrolytic Carbon Nanofibers for Bioelectrocatalytic O_2 Reduction. *ACS Catal.* **2015**, *5*, 7507–7518. [CrossRef]
26. Kolev, S.K.; Aleksandrov, H.A.; Atanasov, V.A.; Popov, V.N.; Milenov, T.I. Interaction of Graphene with Out-of-Plane Aromatic Hydrocarbons. *J. Phys. Chem. C* **2019**, *123*, 21448–21456. [CrossRef]
27. Huang, K.J.; Liu, Y.J.; Liu, Y.M.; Wang, L.L. Molybdenum Disulfide Nanoflower-Chitosan-Au Nanoparticles Composites Based Electrochemical Sensing Platform for Bisphenol a Determination. *J. Hazard. Mater.* **2014**, *276*, 207–215. [CrossRef] [PubMed]

28. Bollella, P.; Fusco, G.; Tortolini, C.; Sanzò, G.; Favero, G.; Gorton, L.; Antiochia, R. Beyond Graphene: Electrochemical Sensors and Biosensors for Biomarkers Detection. *Biosens. Bioelectron.* **2017**, *89*, 152–166. [CrossRef]
29. Shavanova, K.; Bakakina, Y.; Burkova, I.; Shtepliuk, I.; Viter, R.; Ubelis, A.; Beni, V.; Starodub, N.; Yakimova, R.; Khranovskyy, V. Application of 2D Non-Graphene Materials and 2D Oxide Nanostructures for Biosensing Technology. *Sensors* **2016**, *16*, 223. [CrossRef]
30. Wang, Y.H.; Huang, K.J.; Wu, X. Recent Advances in Transition-Metal Dichalcogenides Based Electrochemical Biosensors: A Review. *Biosens. Bioelectron.* **2017**, *97*, 305–316. [CrossRef]
31. Zhang, H. Ultrathin Two-Dimensional Nanomaterials. *ACS Nano* **2015**, *9*, 9451–9469. [CrossRef]
32. Li, H.; Yin, Z.; He, Q.; Li, H.; Huang, X.; Lu, G.; Fam, D.W.H.; Tok, A.I.Y.; Zhang, Q.; Zhang, H. Fabrication of Single- and Multilayer MoS_2 Film-Based Field-Effect Transistors for Sensing NO at Room Temperature. *Small* **2012**, *8*, 63–67. [CrossRef]
33. Pramoda, K.; Moses, K.; Maitra, U.; Rao, C.N.R. Superior Performance of a MoS_2 -RGO Composite and a Borocarbonitride in the Electrochemical Detection of Dopamine, Uric Acid and Adenine. *Electroanalysis* **2015**, *27*, 1892–1898. [CrossRef]
34. Mani, V.; Govindasamy, M.; Chen, S.M.; Karthik, R.; Huang, S.T. Determination of Dopamine Using a Glassy Carbon Electrode Modified with a Graphene and Carbon Nanotube Hybrid Decorated with Molybdenum Disulfide Flowers. *Microchim. Acta* **2016**, *183*, 2267–2275. [CrossRef]
35. Jeong, J.M.; Yang, M.H.; Kim, D.S.; Lee, T.J.; Choi, B.G.; Kim, D.H. High Performance Electrochemical Glucose Sensor Based on Three-Dimensional MoS_2/Graphene Aerogel. *J. Colloid Interface Sci.* **2017**, *506*, 379–385. [CrossRef] [PubMed]
36. Nan, F.; Wang, X.; Jiao, K.; Ge, T.; Zhao, J.; Yang, T. A Label-Free Ultrasensitive Electrochemical DNA Sensor Based on Thin-Layer MoS_2 Nanosheets with High Electrochemical Activity. *Biosens. Bioelectron.* **2014**, *64*, 386–391. [CrossRef]
37. Hickey, D.P.; Lim, K.; Cai, R.; Patterson, A.R.; Yuan, M.; Sahin, S.; Abdellaoui, S.; Minteer, S.D. Pyrene Hydrogel for Promoting Direct Bioelectrochemistry: ATP-Independent Electroenzymatic Reduction of N_2. *Chem. Sci.* **2018**, *9*, 5172–5177. [CrossRef]
38. Najmaei, S.; Liu, Z.; Zhou, W.; Zou, X.; Shi, G.; Lei, S.; Yakobson, B.I.; Idrobo, J.-C.; Ajayan, P.M.; Lou, J. Vapor Phase Growth and Grain Boundary Structure of Molybdenum Disulfide Atomic Layers Vapour Phase Growth and Grain Boundary Structure of Molybdenum Disulphide Atomic Layers. *Nat. Mater.* **2013**, *12*, 754–759. [CrossRef]
39. Dominguez-Rovira, M.A.; Garcia-Garcia, A.; Toxqui-Teran, A. Metodo Para La Obtencion de Cintas de Disulfuro de Molibdeno En Fase Gaseosa, a Partir de La Sulfuracion de Trioxido de Molibdeno. Patent Process Number MX-a-2017-016742, 2017.
40. Moore, C.M.; Akers, N.L.; Hill, A.D.; Johnson, Z.C.; Minteer, S.D. Improving the Environment for Immobilized Dehydrogenase Enzymes by Modifying Nafion with Tetraalkylammonium Bromides. *Biomacromolecules* **2004**, *5*, 1241–1247. [CrossRef]
41. Meredith, S.; Xu, S.; Meredith, M.T.; Minteer, S.D. Hydrophobic Salt-Modified Nafion for Enzyme Immobilization and Stabilization. *J. Vis. Exp.* **2012**, *65*, e3949. [CrossRef]
42. Mora, A.; Mahlknecht, J.; Rosales-Lagarde, L.; Hernández-Antonio, A. Assessment of Major Ions and Trace Elements in Groundwater Supplied to the Monterrey Metropolitan Area, Nuevo León, Mexico. *Environ. Monit. Assess.* **2017**, *189*, 394. [CrossRef] [PubMed]
43. Spinelli, D.; Fatarella, E.; Di Michele, A.; Pogni, R. Immobilization of Fungal (*Trametes versicolor*) Laccase onto Amberlite IR-120 H Beads: Optimization and Characterization. *Process Biochem.* **2013**, *48*, 218–223. [CrossRef]
44. Fatarella, E.; Spinelli, D.; Ruzzante, M.; Pogni, R. Nylon 6 Film and Nanofiber Carriers: Preparation and Laccase Immobilization Performance. *J. Mol. Catal. B Enzym.* **2014**, *102*, 41–47. [CrossRef]
45. Batra, B.; Yadav, M.; Pundir, C.S. L-Glutamate Biosensor Based on l-Glutamate Oxidase Immobilized onto ZnO Nanorods/Polypyrrole Modified Pencil Graphite Electrode. *Biochem. Eng. J.* **2016**, *105*, 428–436. [CrossRef]
46. Pereira, A.S.; Tavares, P.; Limão-Vieira, P. *Radiation in Bioanalysis*; Springer: Cham, Switzerland, 2019; ISBN 9783030282462.
47. Qian, X.; Wang, X.; Zhong, J.; Zhi, J.; Heng, F.; Zhang, Y.; Song, S. Effect of Fiber Microstructure Studied by Raman Spectroscopy upon the Mechanical Properties of Carbon Fibers. *J. Raman Spectrosc.* **2019**, *50*, 665–673. [CrossRef]
48. Castellanos-Gomez, A.; Barkelid, M.; Goossens, A.M.; Calado, V.E.; Van Der Zant, H.S.J.; Steele, G.A. Laser-Thinning of MoS_2: On Demand Generation of a Single-Layer Semiconductor. *Nano Lett.* **2012**, *12*, 3187–3192. [CrossRef] [PubMed]
49. Windom, B.C.; Sawyer, W.G.; Hahn, D.W. A Raman Spectroscopic Study of MoS_2 and MoO_3: Applications to Tribological Systems. *Tribol. Lett.* **2011**, *42*, 301–310. [CrossRef]
50. Zeng, J.; Jean, D.I.; Ji, C.; Zou, S. In Situ Surface-Enhanced Raman Spectroscopic Studies of Nafion Adsorption on Au and Pt Electrodes. *Langmuir* **2012**, *28*, 957–964. [CrossRef] [PubMed]
51. Cai, R.; Abdellaoui, S.; Kitt, J.P.; Irvine, C.; Harris, J.M.; Minteer, S.D.; Korzeniewski, C. Confocal Raman Microscopy for the Determination of Protein and Quaternary Ammonium Ion Loadings in Biocatalytic Membranes for Electrochemical Energy Conversion and Storage. *Anal. Chem.* **2017**, *89*, 13290–13298. [CrossRef]
52. Mailley, P.; Cummings, E.A.; Mailley, S.; Cosnier, S.; Eggins, B.R.; McAdams, E. Amperometric Detection of Phenolic Compounds by Polypyrrole-Based Composite Carbon Paste Electrodes. In *Proceedings of the Bioelectrochemistry*; Elsevier: Amsterdam, The Netherlands, 2004; Volume 63, pp. 291–296.
53. Sumayya, A.; Yohannan Panicker, C.; Varghese, H.T.; Harikumar, B. Vibrational Spectroscopic Studies and AB Initio Calculations of L-Glutamic Acid 5-Amide. *Rasayan J. Chem.* **2008**, *1*, 548–555.
54. Baker, M.J.; Hussain, S.R.; Lovergne, L.; Untereiner, V.; Hughes, C.; Lukaszewski, R.A.; Thiéfin, G.; Sockalingum, G.D. Developing and Understanding Biofluid Vibrational Spectroscopy: A Critical Review. *Chem. Soc. Rev.* **2016**, *45*, 1803–1818. [CrossRef]

55. Movasaghi, Z.; Rehman, S.; Rehman, I.U. Raman Spectroscopy of Biological Tissues. *Appl. Spectrosc. Rev.* **2007**, *42*, 493–541. [CrossRef]
56. Yang, S.; Hai, F.I.; Nghiem, L.D.; Price, W.E.; Roddick, F.; Moreira, M.T.; Magram, S.F. Understanding the Factors Controlling the Removal of Trace Organic Contaminants by White-Rot Fungi and Their Lignin Modifying Enzymes: A Critical Review. *Bioresour. Technol.* **2013**, *141*, 97–108. [CrossRef]
57. Donarelli, M.; Ottaviano, L. 2D Materials for Gas Sensing Applications: A Review on Graphene Oxide, MoS2, WS2 and Phosphorene. *Sensors* **2018**, *18*, 3638. [CrossRef]
58. Saraf, M.; Natarajan, K.; Saini, A.K.; Mobin, S.M. Small Biomolecule Sensors Based on an Innovative MoS_2–RGO Heterostructure Modified Electrode Platform: A Binder-Free Approach. *Dalt. Trans.* **2017**, *46*, 15848–15858. [CrossRef]
59. Barua, S.; Dutta, H.S.; Gogoi, S.; Devi, R.; Khan, R. Nanostructured MoS_2-Based Advanced Biosensors: A Review. *ACS Appl. Nano Mater.* **2018**, *1*, 2–25. [CrossRef]
60. Rodríguez, M.C.; Rivas, G.A. Glassy Carbon Paste Electrodes Modified with Polyphenol Oxidase: Analytical Applications. *Anal. Chim. Acta* **2002**, *459*, 43–51. [CrossRef]
61. Economou, A. Enzymatic Biosensors. In *Portable Biosensing of Food Toxicants and Environmental Pollutants*; CRC Press, Taylor & Francis Group: Boca Raton, FL, USA, 2013; pp. 123–160.
62. Janata, J. *Principles of Chemical Sensors*, 2nd ed.; Springer: New York, NY, USA, 2009; ISBN 9780387699301.
63. Mross, S.; Pierrat, S.; Zimmermann, T.; Kraft, M. Microfluidic Enzymatic Biosensing Systems: A Review. *Biosens. Bioelectron.* **2015**, *70*, 376–391. [CrossRef]
64. Milton, R.D.; Wu, F.; Lim, K.; Abdellaoui, S.; Hickey, D.P.; Minteer, S.D. Promiscuous Glucose Oxidase: Electrical Energy Conversion of Multiple Polysaccharides Spanning Starch and Dairy Milk. *ACS Catal.* **2015**, *5*, 7218–7225. [CrossRef]
65. Ranjbakhsh, E.; Bordbar, A.K.; Abbasi, M.; Khosropour, A.R.; Shams, E. Enhancement of Stability and Catalytic Activity of Immobilized Lipase on Silica-Coated Modified Magnetite Nanoparticles. *Chem. Eng. J.* **2012**, *179*, 272–276. [CrossRef]
66. De Lima Citolino, L.V.; Braunger, M.L.; Oliveira, V.J.R.; Olivati, C.A. Study of the Nanostructure Effect on Polyalkylthiophene Derivatives Films Using Impedance Spectroscopy. *Mater. Res.* **2017**, *20*, 874–881. [CrossRef]
67. RoyChoudhury, S.; Umasankar, Y.; Hutcheson, J.D.; Lev-Tov, H.A.; Kirsner, R.S.; Bhansali, S. Uricase Based Enzymatic Biosensor for Non-Invasive Detection of Uric Acid by Entrapment in PVA-SbQ Polymer Matrix. *Electroanalysis* **2018**, *30*, 2374–2385. [CrossRef]
68. Banica, F.-G. *Chemical Sensors and Biosensors: Fundamentals and Applications*; John Wiley & Sons Inc.: Hoboken, NJ, USA, 2012; ISBN 0470710667.
69. Cernat, A.; Tertis, M.; Griveau, S.; Bedioui, F.; Sandulescu, R. New Modified Electrodes with HRP Immobilized in Polymeric Films for Paracetamol Analysis. *Farmacia* **2012**, *60*, 1–12.
70. Cernat, A.; Griveau, S.; Richard, C.; Bedioui, F.; Săndulescu, R. Horseradish Peroxidase Nanopatterned Electrodes by Click Chemistry: Application to the Electrochemical Detection of Paracetamol. *Electroanalysis* **2013**, *25*, 1369–1372. [CrossRef]
71. Maghear, A.; Cristea, C.; Marian, A.; Marian, I.O.; Săndulescu, R. A Novel Biosensor for Acetaminophen Detection with Romanian Clays and Conductive Polymeric Films. *Farmacia* **2013**, *61*, 1–11.
72. Garcia, L.F.; Benjamin, S.R.; Antunes, R.S.; Lopes, F.M.; Somerset, V.S.; Gil, E.d.S. Solanum Melongena Polyphenol Oxidase Biosensor for the Electrochemical Analysis of Paracetamol. *Prep. Biochem. Biotechnol.* **2016**, *46*, 850–855. [CrossRef]
73. Antunes, R.S.; Garcia, L.F.; Somerset, V.S.; de Souza Gil, E.; Lopes, F.M. The Use of a Polyphenoloxidase Biosensor Obtained from the Fruit of Jurubeba (*Solanum paniculatum* L.) in the Determination of Paracetamol and Other Phenolic Drugs. *Biosensors* **2018**, *8*, 36. [CrossRef]
74. Brack, W.; Dulio, V.; Slobodnik, J. The NORMAN Network and Its Activities on Emerging Environmental Substances with a Focus on Effect-Directed Analysis of Complex Environmental Contamination. *Environ. Sci. Eur.* **2012**, *24*, 29. [CrossRef]
75. Fernández-Fernández, M.; Sanromán, M.Á.; Moldes, D. Recent Developments and Applications of Immobilized Laccase. *Biotechnol. Adv.* **2013**, *31*, 1808–1825. [CrossRef] [PubMed]